

Proton and Ion Linear Accelerators

3. Basics of Beam Focusing

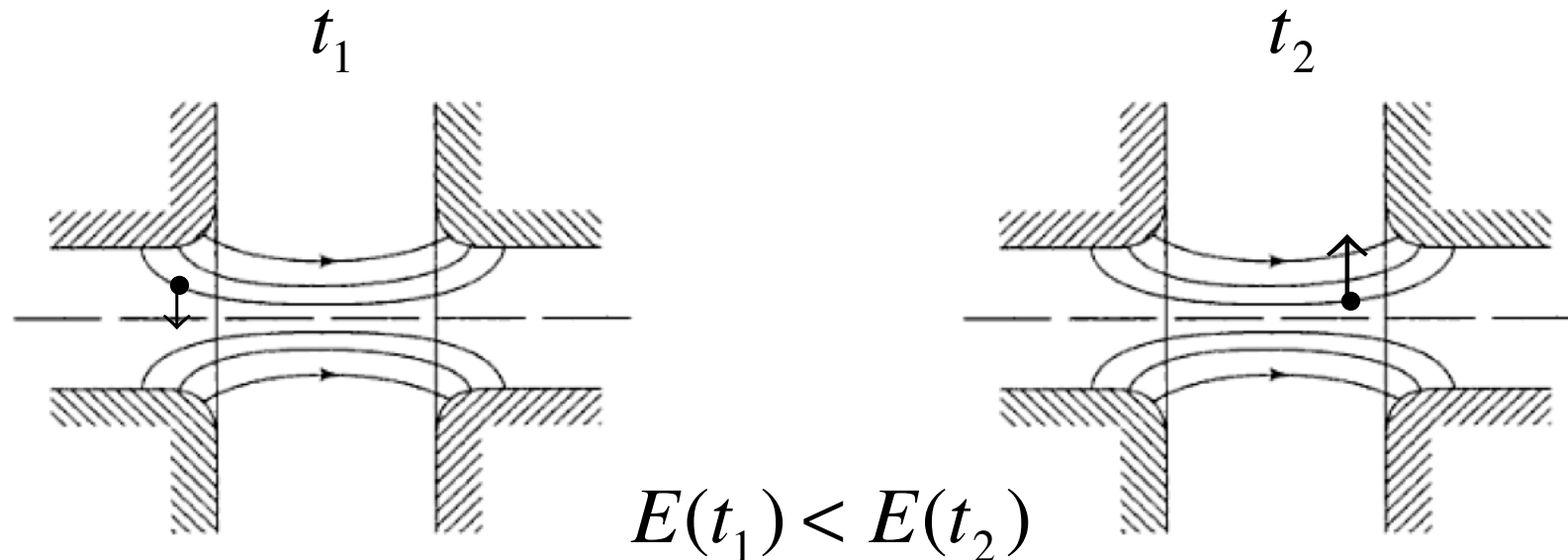
Yuri Batygin

Los Alamos National Laboratory

U.S. Particle Accelerator School

Albuquerque, New Mexico, June 17-28, 2019

RF Defocusing in Particle Accelerator



Electric field lines between the ends drift tubes. If accelerating, the field is focusing at input and defocusing at output. While field level is increasing while particles cross the gap to provide longitudinal beam bunching, the defocusing effect is larger.

RF Defocusing in Particle Accelerator (cont.)

Equation for radial momentum

$$\frac{dp_r}{dt} = q(E_r - \beta c B_\theta)$$

Radial electric field

$$E_r(r) = -\frac{1}{r} \int_0^r \frac{\partial E_z}{\partial z} r' dr' \approx -\frac{1}{2} \frac{\partial E_z}{\partial z} r$$

Azimuthal magnetic field

$$B_\theta = \frac{1}{c^2 r} \int_0^r \frac{\partial E_z}{\partial t} r' dr' \approx \frac{1}{2c^2} \frac{\partial E_z}{\partial t} r$$

Because $E_z = E \cos(\omega t - k_z z)$

$$\frac{\partial E_z}{\partial t} = -v_s \frac{\partial E_z}{\partial z}$$

Equation of radial motion in RF field

$$\frac{d^2 r}{dz^2} = -\frac{q}{2m\gamma^3 v^2} \frac{\partial E_z}{\partial z} r$$

RF Defocusing in Particle Accelerator (cont.)

Assume that particle radius in RF gap
 $r = \text{const}$. Change of slope of particle trajectory at the entrance to RF gap:

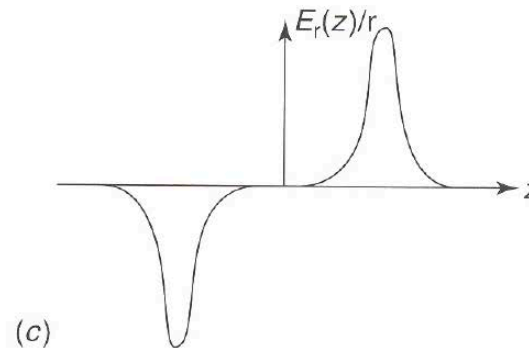
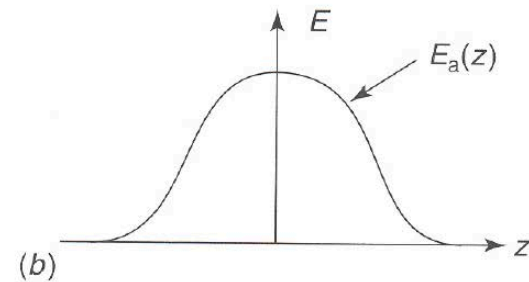
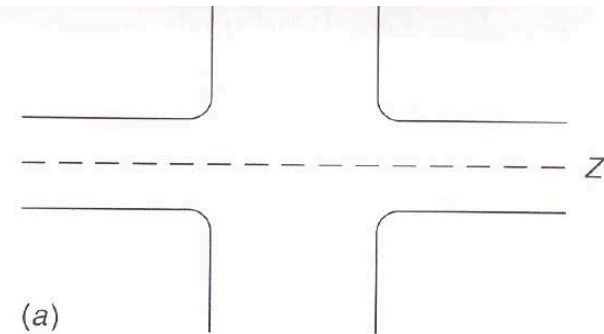
$$\Delta\left(\frac{dr}{dz}\right)_{in} \approx -\frac{q}{2m\gamma^3 v^2} r \int_{-\infty}^{-g/2} \frac{\partial E_z}{\partial z} dz \approx -\frac{qE_{in}}{2m\gamma^3 v_{in}^2} r$$

Change of slope of particle trajectory at the exit of RF gap:

$$\Delta\left(\frac{dr}{dz}\right)_{out} \approx \frac{qE_{out}}{2m\gamma^3 v_{out}^2} r$$

Total change of slope of particle trajectory at RF gap:

$$\Delta\frac{dr}{dz} \approx \frac{qr}{2m\gamma^3} \left(\frac{E_{out}}{v_{out}^2} - \frac{E_{in}}{v_{in}^2} \right)$$



Longitudinal and radial electric field in RF gap.

Y.K. Batygin Basics of Beam Focusing USPAS 2019

RF Defocusing in Particle Accelerator (cont.)

Difference in field $\Delta E_z = E_{out} - E_{in}$

Difference in velocity $\Delta v = v_{out} - v_{in}$

Total change of slope of particle trajectory: defocusing by RF field, but “static” focusing due to change in particle velocity

$$\Delta \frac{dr}{dz} \approx \frac{qE_{in} r}{2m\gamma^3 v_{in}^2} \left(\frac{\Delta E}{E_{in}} - 2 \frac{\Delta v}{v_{in}} \right)$$

Field at the entrance of RF gap $E_{in} = E_g \cos\left(\varphi_s - \frac{\pi g}{\beta\lambda}\right)$

Field at the exit of RF gap $E_{out} = E_g \cos\left(\varphi_s + \frac{\pi g}{\beta\lambda}\right)$

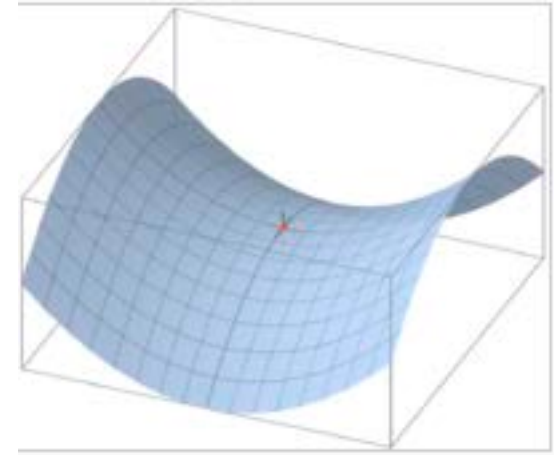
Relative change of RF field $\frac{\Delta E}{E_{in}} \approx 2 \left| \text{tg} \varphi_s \right| \sin\left(\frac{\pi g}{\beta\lambda}\right)$

In order to focus particles in RF gap $\frac{\Delta v}{v_{in}} > \frac{\Delta E}{2E_{in}}$ or $\frac{|\sin \varphi_s|}{\cos^2 \varphi_s} < \frac{qE\lambda}{mc^2 \beta \gamma^3 \sin\left(\frac{\pi g}{\beta\lambda}\right)}$

For proton beam in accelerator with $E = 5$ MV/m, $\lambda = 1$ m, $\beta = 0.04$, $g/\beta\lambda = 0.25$, synchronous phase should be too small: $\varphi_s < 10^\circ$. RF defocusing is dominant effect, which requires additional focusing.

Earnshaw's Theorem

Earnshaw's theorem states that a collection of point charges cannot be maintained in a stable stationary equilibrium configuration solely by the electrostatic interaction of the charges (Samuel Earnshaw, 1842).



Laplace Equation:

$$\frac{\partial^2 U}{\partial x^2} + \frac{\partial^2 U}{\partial y^2} + \frac{\partial^2 U}{\partial z^2} = 0$$

Effective potential created by static field

All second derivatives of potential cannot be positive (at minimum) at the same time.

Grid or Foil Focusing of Charged Particles

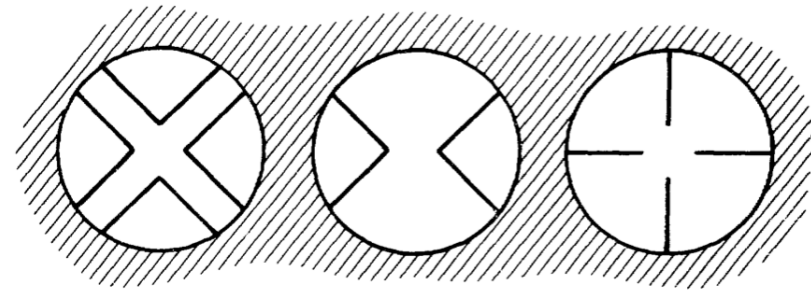
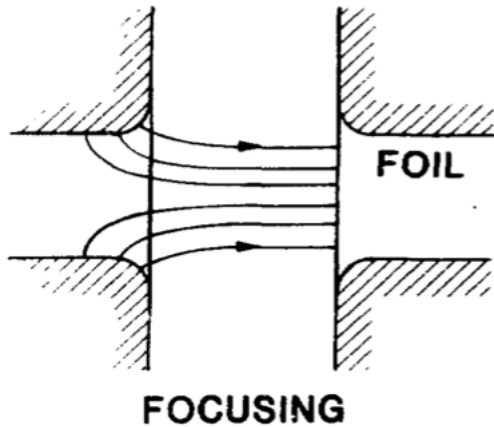
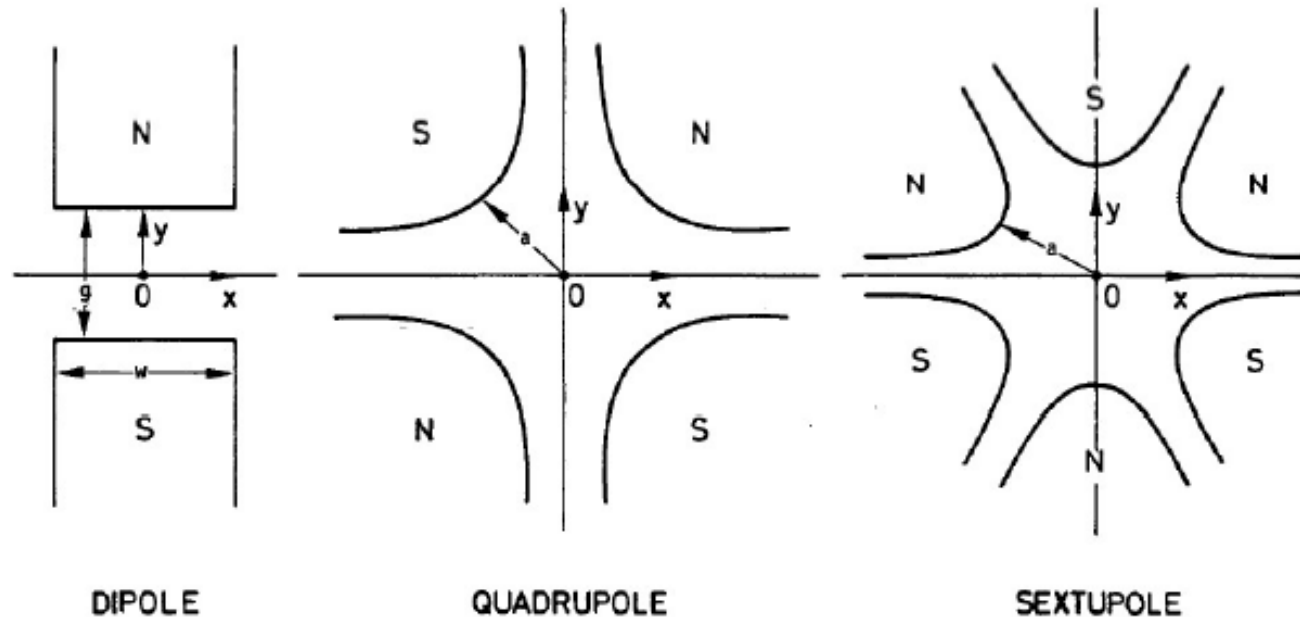


Fig. 7. Various shapes of grids.

Foil or grid focusing—the defocusing effect is suppressed

RF Defocusing effect is suppressed by closing the drift-tube hole at the exit of the gap with a foil thin enough to be crossed by particles. First test: 1947, Alvarez linac

Focusing Elements



Focusing magnets used in accelerator facilities: dipole, quadrupole, sextupole.

Magnetostatic and Electrostatic Fields

Equations describing magnetostatic field are obtained from Maxwell equations assuming $\partial / \partial t = 0$:

$$\text{rot } \vec{H} = 0 \quad \text{div } \vec{B} = 0 \quad \vec{B} = \mu \vec{H}$$

Because $\text{rot}(\text{grad } U_{\text{magn}}) = 0$, the magnetic field can be expressed through magnetic scalar potential, U_{magn} as

$$\vec{B} = -\text{grad } U_{\text{magn}}$$

On the other hand, because $\text{div}(\text{rot } \vec{A}_{\text{magn}}) = 0$, magnetic field can be equally determined using vector potential, \vec{A}_{magn} :

$$\vec{B} = \text{rot } \vec{A}_{\text{magn}}$$

Magnetic scalar potential is convenient to determine ideal pole contour, while vector potential is convenient to determine magnetic field shape. Electrostatic field is expressed through electrostatic potential:

$$\vec{E} = -\text{grad } U_{\text{el}}$$

Laplace Equation for Electrostatic and Magnetic Fields

Because $\text{div}(\text{grad}U) = \nabla^2 U$, both magnetic and electrostatic multipole fields are derived from Laplace equation with appropriate boundary conditions:

$$\nabla^2 U = 0$$

where U stands for U_{magn} or U_{el} . On the other hand, because of equity

$$\text{rot}(\text{rot} \vec{A}_{\text{magn}}) = \text{grad}(\text{div} \vec{A}_{\text{magn}}) - \nabla^2 \vec{A}_{\text{magn}}$$

and taking additional condition $\text{div} \vec{A}_{\text{magn}} = 0$, magnetic field can be expressed through components of vector – potential:

$$\nabla^2 \vec{A}_{\text{magn}} = 0$$

Transverse components of magnetic multipoles can be expressed through z - component of vector potential A_z . Because $(\nabla^2 \vec{A})_z = \nabla^2 A_z$, formally, both magnetic and electrostatic multipole fields are derived from Laplace equation

$$\frac{1}{r} \frac{\partial \Pi}{\partial r} + \frac{\partial^2 \Pi}{\partial r^2} + \frac{1}{r^2} \frac{\partial^2 \Pi}{\partial \theta^2} + \frac{\partial^2 \Pi}{\partial z^2} = 0$$

where $\Pi(r, \theta, z)$ stands for either z - component of vector-potential, $A_{z\text{magn}}$, or scalar potentials U_{magn} , U_{el} .

Solution of Laplace Equation

General solution of 3-dimensional Laplace equation in cylindrical coordinates

$$\begin{aligned} \Pi(r, \theta, z) &= \sum_{m=0}^{\infty} \sum_{n=0}^{\infty} \frac{(-1)^n m!}{4^n n!(m+n)!} r^{m+2n} (\Theta_m^{(2n)} \cos m\theta + \Psi_m^{(2n)} \sin m\theta) \\ &= \Theta_o - \frac{1}{4} r^2 \Theta_o'' + \frac{1}{64} r^4 \Theta_o^{(4)} - \dots \\ &\quad + (\Theta_1 - \frac{1}{8} r^2 \Theta_1'') r \cos \theta + (\Psi_1 - \frac{1}{8} r^2 \Psi_1'') r \sin \theta \\ &\quad + (\Theta_2 - \frac{1}{12} r^2 \Theta_2'') r^2 \cos 2\theta + (\Psi_2 - \frac{1}{12} r^2 \Psi_2'') r^2 \sin 2\theta + \dots \end{aligned}$$

$m = 0$ for axial-symmetric field

$m = 1$ for dipole

$m = 2$ for a quadrupole

$m = 3$ for sextupole,

$m = 4$ for octupole,

$m = 5$ for decapole

$m = 6$ for dodecapole,

Multipole Fields

Number of poles to excite the multipole lens of the order m is

$$N_{poles} = 2m$$

In most of cases, it is possible to substitute actual z-dependence of the field by “step” function. For such representation, solution of Laplace equation is

$$\Pi(r, \theta) = \sum_{m=0}^{\infty} r^m (\Theta_m \cos m\theta + \Psi_m \sin m\theta)$$

Solutions for magnetic field can be represented as a combination of multipoles with field:

$$A_z = -\frac{G_m}{m} r^m \cos m\theta \quad U_{magn} = -\frac{G_m}{m} r^m \sin m\theta$$

where G_m is the strength of the multipole of order m and $B(r_o)$ is the absolute value of magnetic field at certain radius r_o .

$$G_m = \frac{B(r_o)}{r_o^{m-1}} = \frac{\sqrt{B_{rm}^2(r_o) + B_{\theta m}^2(r_o)}}{r_o^{m-1}}$$

Field components:

$$B_{rm} = -\frac{\partial U_{magn}}{\partial r} = \frac{1}{r} \frac{\partial A_z}{\partial \theta} = G_m r^{m-1} \sin m\theta$$

$$B_{\theta m} = -\frac{1}{r} \frac{\partial U_{magn}}{\partial \theta} = -\frac{\partial A_z}{\partial r} = G_m r^{m-1} \cos m\theta$$

Potential of Multipoles

Magnetic vector potential $-A_z$ and electrostatic potential U_{el} of “normal” multipole

$$m = 2 \text{ Quadrupole} \quad \frac{G}{2} r^2 \cos 2\theta = \frac{G}{2} (x^2 - y^2)$$

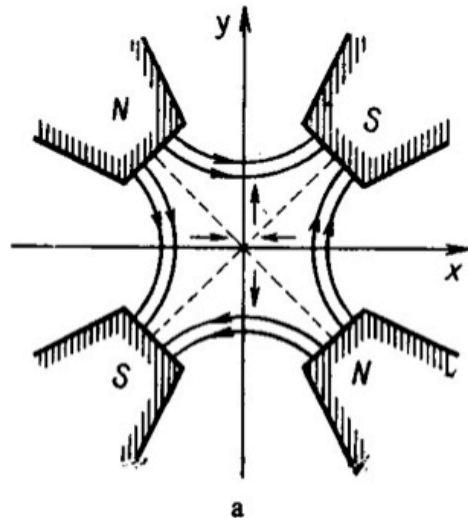
$$m = 3 \text{ Sextupole} \quad \frac{G_3}{3} r^3 \cos 3\theta = \frac{G_3}{3} (x^3 - 3xy^2)$$

$$m = 4 \text{ Octupole} \quad \frac{G_4}{4} r^4 \cos 4\theta = \frac{G_4}{4} (x^4 - 6x^2y^2 + y^4)$$

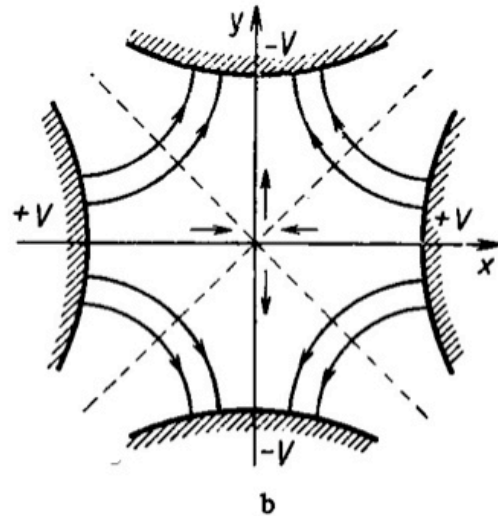
$$m = 5 \text{ Decapole} \quad \frac{G_5}{5} r^5 \cos 5\theta = \frac{G_5}{5} (x^5 - 10x^3y^2 + 5xy^4)$$

$$m = 6 \text{ Dodecapole} \quad \frac{G_6}{6} r^6 \cos 6\theta = \frac{G_6}{6} (x^6 - y^6 - 15x^4y^2 + 15x^2y^4)$$

Quadrupole Focusing



$$B_y = Gx \quad B_x = Gy$$



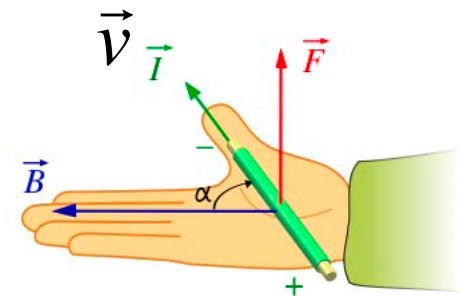
$$E_x = Gx \quad E_y = -Gy$$

(a) Magnetic quadrupole and (b) electric quadrupole.

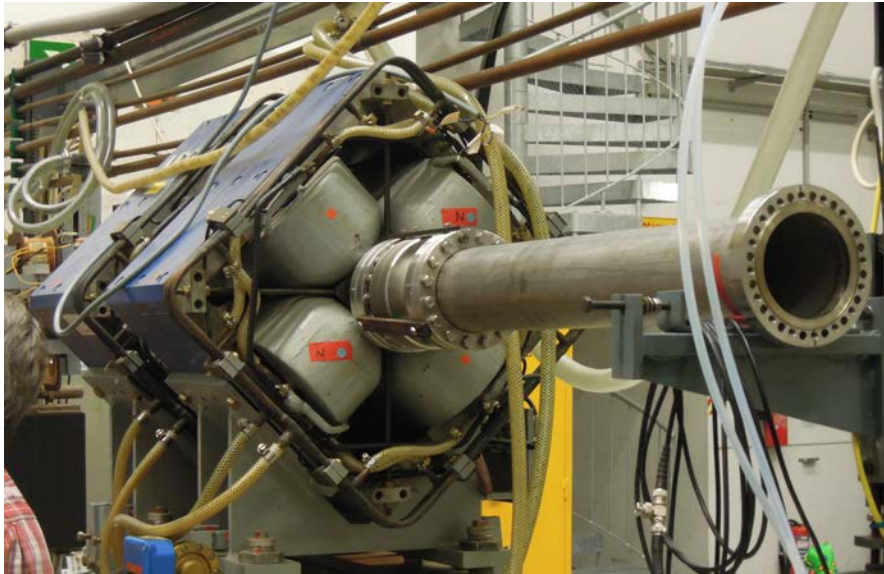
Arrows indicate direction of Lorentz force acting on positively charge particle moving from the screen. Field is proportional to distance from axis, G- gradient of quadrupole field.

Lorentz Force

$$\mathbf{F} = q(\mathbf{E} + \mathbf{v} \times \mathbf{B})$$



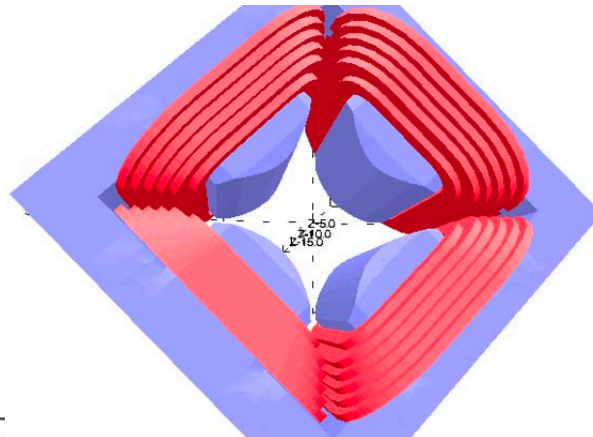
Quadrupole Magnets



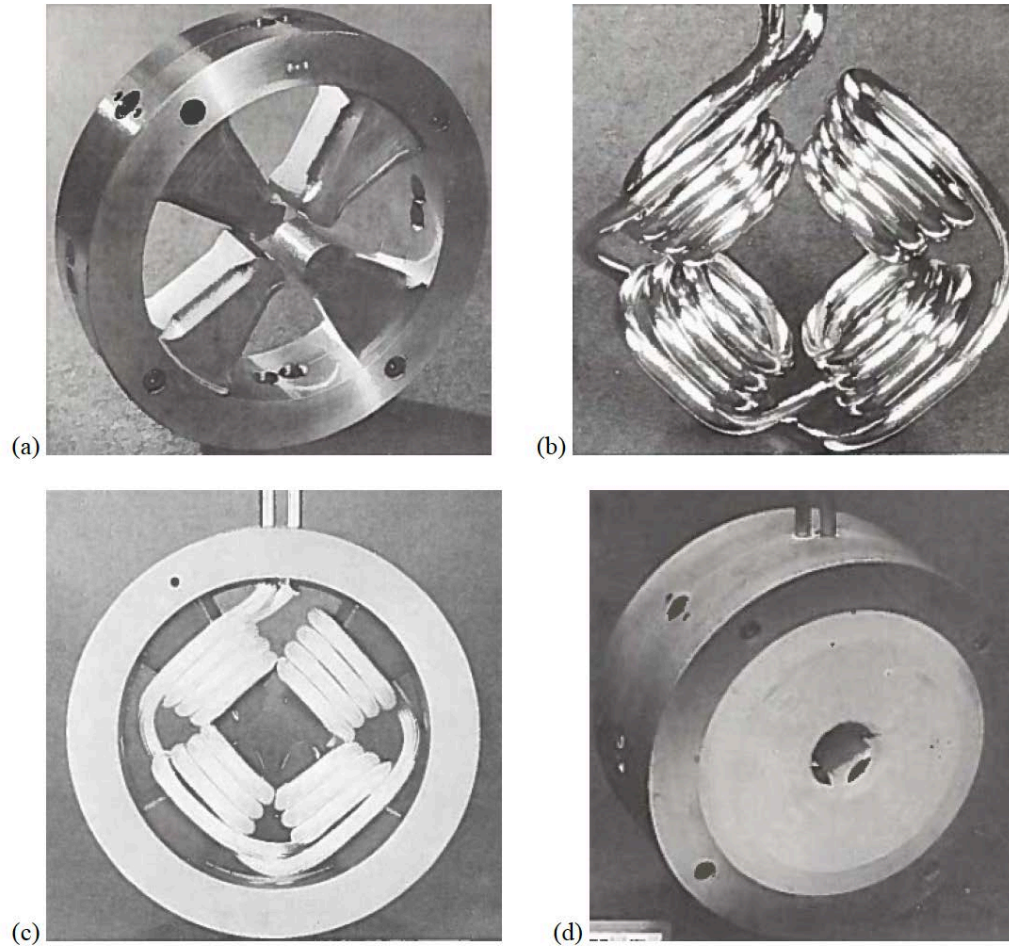
Electromagnetic quadrupole magnet in
Maier-Leibnitz Laboratory, Munich



Electrostatic quadrupole of
High Voltage Engineering
Europa B.V.

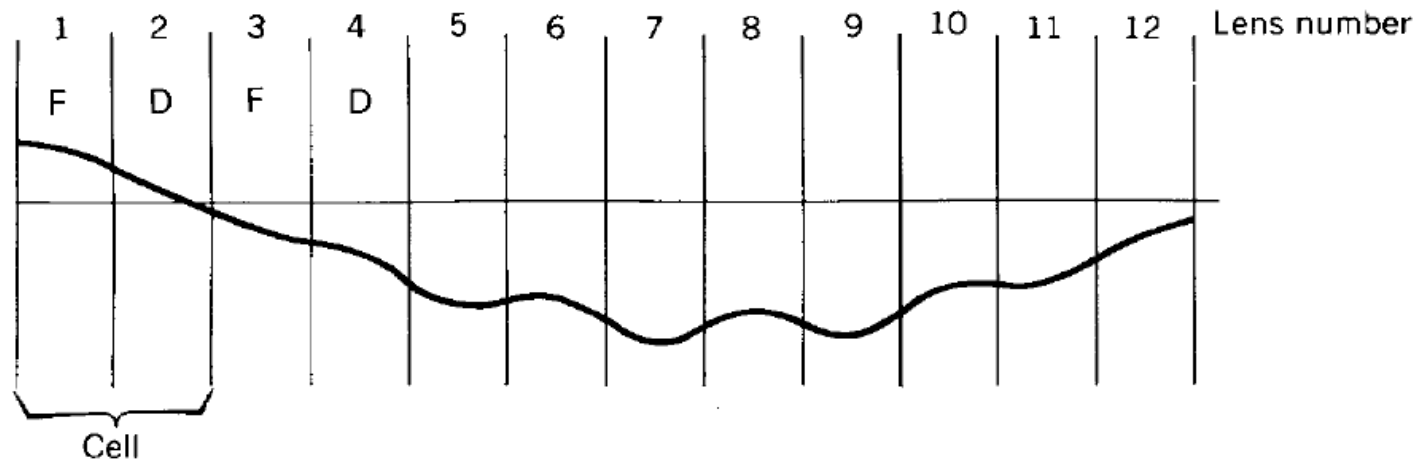
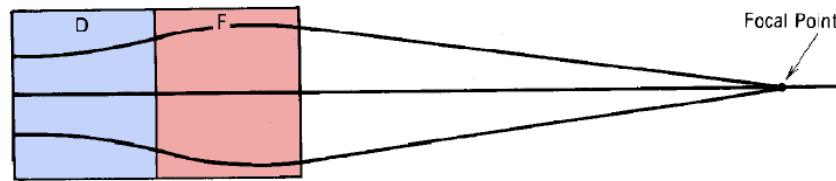
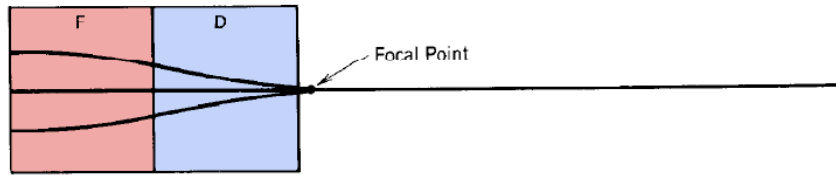


LANL Drift Tube Linac Quadrupole Magnets



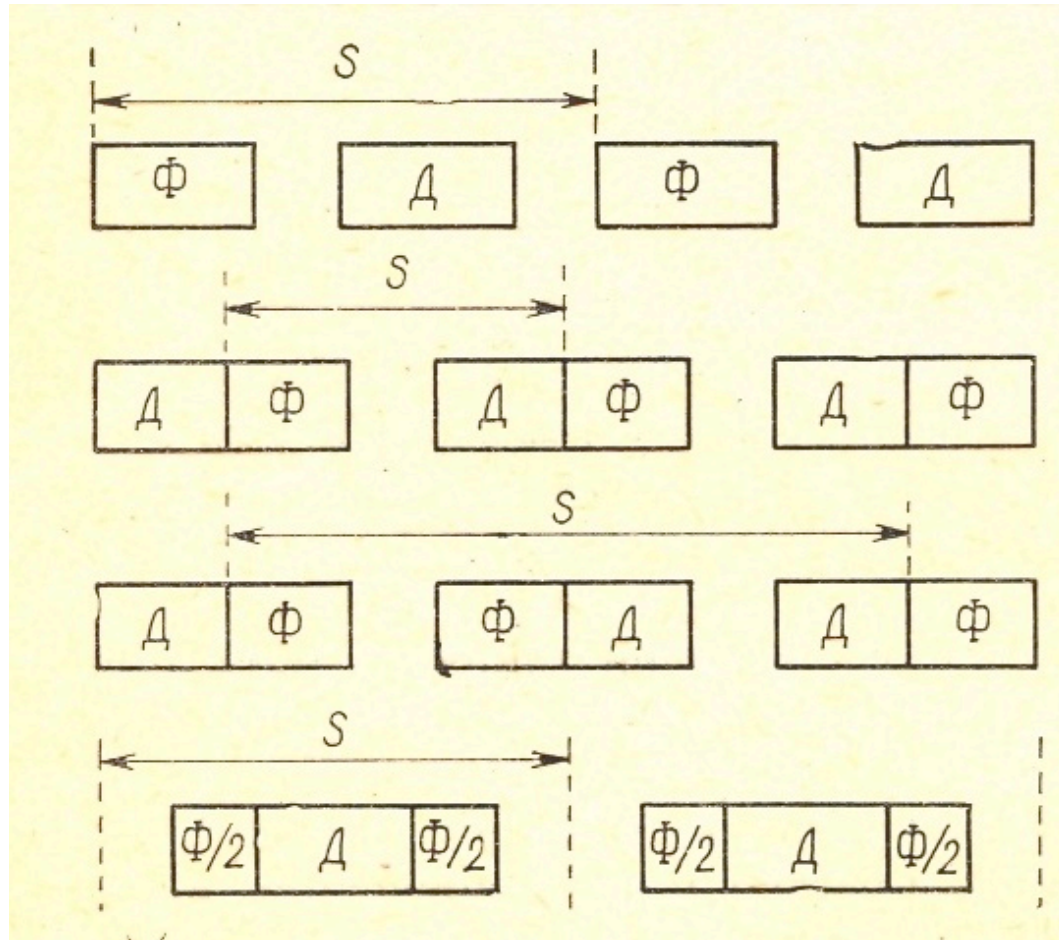
DTL quadrupole details: (a) yoke and pole pieces; (b) current coil; (c) coil assembled with iron; (d) quadrupole fully assembled.

Quadrupole Focusing (cont.)



Focusing properties of combination of quadrupole lenses

Various Types of Focusing Periods



FODO

FOD

FOF-DOD

Triplets

Quadrupole Pole Shapes and Higher Order Harmonics

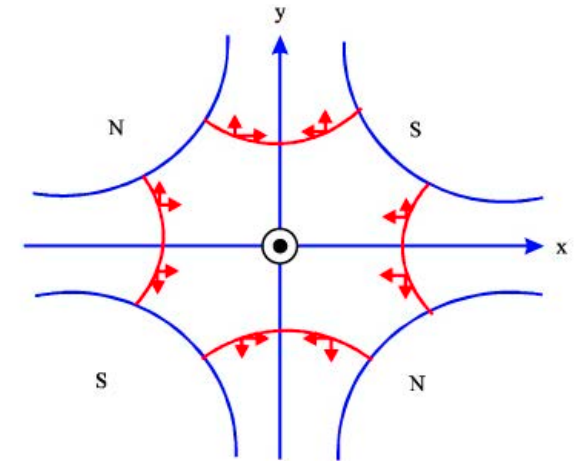
Pole contours are determined by lines of equal values of scalar potentials

$$U_{magn}(r, \theta) = const, \quad U_{el}(r, \theta) = const.$$

Shape of “normal” quadrupole poles are described by infinite hyperbolas:

$$x^2 - y^2 = \pm a^2 \quad \text{for electrostatic quadrupole}$$

$$2xy = \pm a^2 \quad \text{for magnetostatic quadrupole}$$



Actual pole shapes are different from that determined above. Solution of Laplace equation for multipole is anti-symmetric after angle π/m because of separation of neighbor poles with alternative polarity:

$$\Pi(r, \theta) = -\Pi(r, \theta + \frac{\pi}{m})$$

Quadrupole Pole Shapes and Higher Order Harmonics (cont.)

It determines the number of higher harmonics k with respect to fundamental harmonic m :

$$\cos k\left(\theta + \frac{\pi}{m}\right) = -\cos k\theta, \quad \sin k\left(\theta + \frac{\pi}{m}\right) = -\sin k\theta$$

which are satisfied when $\cos\left(k\frac{\pi}{m}\right) = -1$, $\sin\left(k\frac{\pi}{m}\right) = 0$

Both equations are valid for $k = m(1 + 2l)$, $l = 0, 1, 2, 3, \dots$. For example, the field of a quadrupole lens contains the following multipole harmonics:

$$A_z(r, \theta) = -\left(\frac{G}{2}r^2 \cos 2\theta + \frac{G_6}{6}r^6 \cos 6\theta + \frac{G_{10}}{10}r^{10} \cos 10\theta + \dots\right)$$

Multipole Harmonics of Magnetic Field

Multipole harmonics of magnetic field presented in focusing lenses

$m = 1$ Dipole $k = 1, 3, 5, 7, \dots$

$m = 2$ Quadrupole $k = 2, 6, 10, 14, \dots$

$m = 3$ Sextupole $k = 3, 9, 15, 21, 27, \dots$

$m = 4$ Octupole $k = 4, 12, 20, 28, 36, \dots$

$m = 5$ Dodecapole $k = 5, 15, 25, 35, 45, \dots$

$m = 6$ Duodecapole $k = 6, 18, 30, 42, 54, \dots$

Design of Quadrupole Lens

Number of Ampere-Turns per pole

$$NI = 0.44Ga^2$$

P - dissipated power, W

ρ - coil resistance, Ohm cm

l - average length of one turn, cm

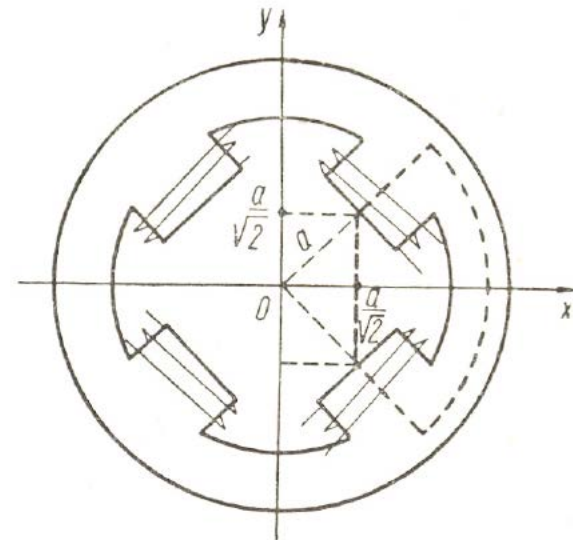
S_o - area of coils

f - ratio of coil area to window area

G - field gradient, Gauss/cm

a - radius of aperture, cm

$$P = 6.1 \frac{\rho l}{S_o f} G^2 a^4$$



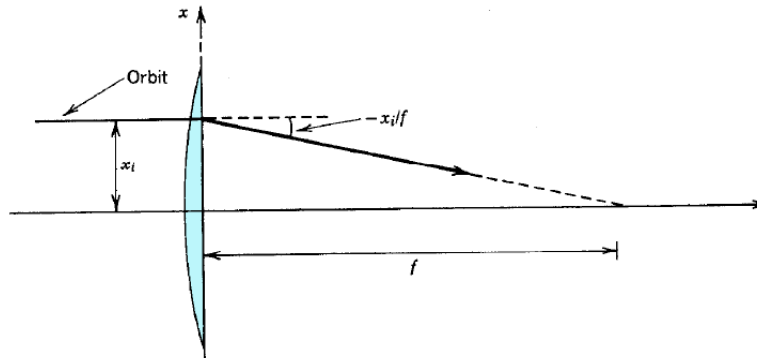
Focal Length of Quadrupole Lens

Equation of motion:
$$\frac{d^2 x}{dz^2} = \frac{qGx}{mc\beta\gamma}$$

Integration of equation of motion along lens assuming constant x

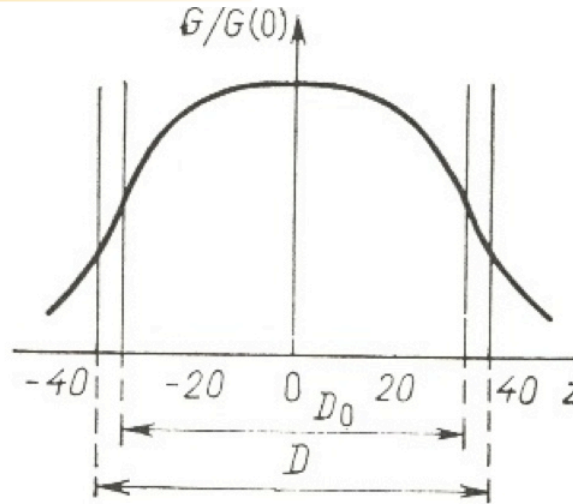
$$\frac{dx}{dz} = \left(\frac{dx}{dz}\right)_o - x \int_{-\infty}^{\infty} \frac{qG}{mc\beta\gamma} dz$$

In the analogy with light optics, we can introduce the focal length of the lens:
$$\frac{1}{f} = \frac{qGD}{m\gamma\beta c}$$



Effect of a thin lens (focal length f) on a particle trajectory initially parallel to the axis (from Humphries, 1999).

Effective Length of the Lens



Variation of gradient along the axis of a quadrupole lens.

We will assume *step function approximation* of the field inside the lens, where actual dependence of field gradient $G(z)$ is substituted by an equivalent lens with constant gradient $G=G(0)$, equal to that in the center of lens. Length of the equivalent lens:

$$D = D_o + R_p$$

where D_o is the length of the real lens, and R_p is the distance from axis to pole tips (radius of the aperture).

Single Particle Dynamics in a Quadrupole Focusing Channel

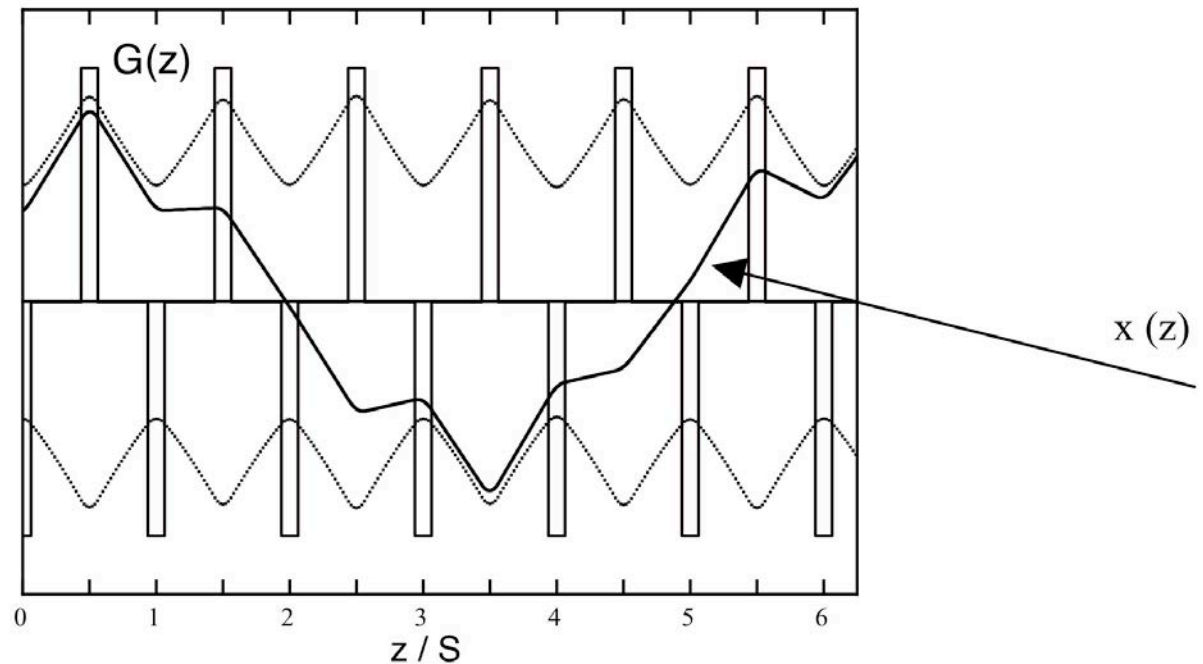
Equation of motion in x- and y- directions (Mathieu-Hill Equations):

$$\frac{d^2 x}{dz^2} + k(z)x = 0$$

$$\frac{d^2 y}{dz^2} - k(z)y = 0$$

where focusing function

$$k(z) = \frac{qG(z)}{mc\beta\gamma}$$



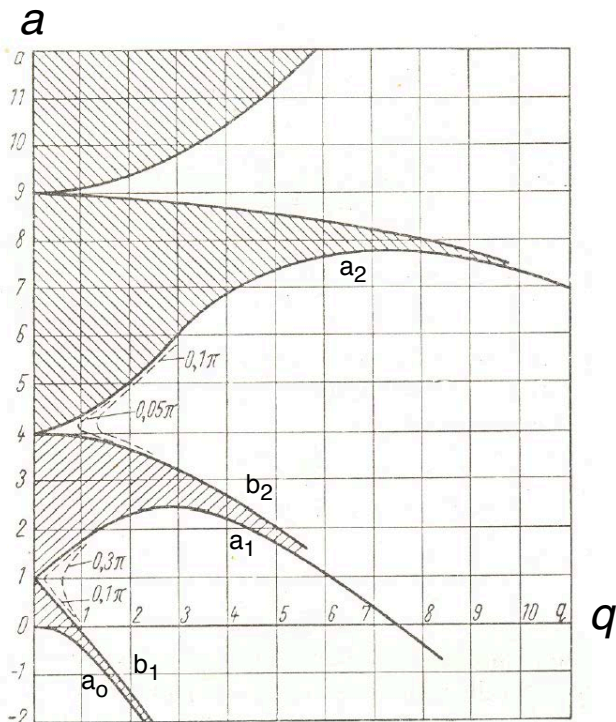
Equivalent gradient of electrostatic lens $G_{el} = \beta c G$

General Form of Mathieu Equation

Mathieu equation

$$\frac{d^2 x}{d\tau^2} + \pi^2 (a - 2q \sin 2\pi\tau)x = 0$$

Unstable solutions are around $a = n^2$, or when average frequency of oscillator is close to half-integer value of that of driving force.



Shaded are stable regions of solutions of Mathie-Hill equation.

First region of parametric instability is $b_1 < a < a_1$,

where:

$$b_1 = 1 - q - \frac{1}{8}q^2 + \frac{1}{64}q^3 - \dots$$

$$a_1 = 1 + q - \frac{1}{8}q^2 - \frac{1}{64}q^3 - \dots$$

The second region of parametric instability is $b_2 < a < a_2$,

where:

$$b_2 = 4 - \frac{1}{12}q^2 + \frac{5}{13824}q^4 - \dots$$

$$a_2 = 4 + \frac{5}{12}q^2 - \frac{763}{13824}q^4 + \dots$$

Amplitude and Phase of Solution

Differential equations with periodic coefficients are called Mathieu - Hill equations. We will be looking for a stable solution in the form:

$$x(z) = \sqrt{\varepsilon_x} \sigma_x(z) \cos(\Phi_x(z) + \Phi_o)$$

where $\sqrt{\varepsilon_x}$ is a constant, $\sigma_x(z)$ is the z - dependent amplitude, and $\Phi_x(z)$ is the z - dependent phase of the solution. Substitution of the expected solution gives:

$$[\sigma_x'' - \sigma_x (\Phi_x')^2 + k\sigma_x] \cos(\Phi_x + \Phi_o) - (\sigma_x \Phi_x'' + 2\sigma_x' \Phi_x') \sin(\Phi_x + \Phi_o) = 0$$

To solve this equation, we can put independently to zero both 'cosine' and 'sine' parts:

$$\sigma_x'' - \sigma_x \Phi_x'^2 + k\sigma_x = 0$$

$$\sigma_x \Phi_x'' + 2\sigma_x' \Phi_x' = 0$$

Amplitude and Phase of Solution (cont.)

Multiplying the second equation by σ_x , it can be written as

$$(\Phi_x' \sigma_x^2)' = 0$$

which gives

$$\Phi_x' \sigma_x^2 = \text{const.}$$

Selecting arbitrary value of constant as 1, finally get for second equation:

$$\Phi_x' = \frac{1}{\sigma_x^2}$$

With that condition, 'cosine' part of equation is written as

$$\sigma_x'' - \frac{1}{\sigma_x^3} + k(z)\sigma_x = 0$$

Courant-Snyder Invariant

Let us determine the physical meaning of the constant ϵ_x . Differentiation of $x(z) = \sqrt{\epsilon_x} \sigma_x(z) \cos \Phi_x(z)$ gives:

$$x' = \sqrt{\epsilon_x} (\sigma_x' \cos \Phi_x - \sigma_x \Phi_x' \sin \Phi_x) = \sqrt{\epsilon_x} (\sigma_x' \cos \Phi_x - \frac{\sin \Phi_x}{\sigma_x}). \quad (2.46)$$

On the other hand, from the original equation it follows, that:

$$\cos \Phi_x = \frac{x}{\sqrt{\epsilon_x} \sigma_x}. \quad (2.47)$$

Substitution gives:

$$x' = \sigma_x' \frac{x}{\sigma_x} - \sqrt{\epsilon_x} \frac{\sin \Phi_x}{\sigma_x}. \quad (2.48)$$

Rearranging of the equation (2.48) results in: $\epsilon_x \sin^2 \Phi_x = (x' \sigma_x - \sigma_x' x)^2$. (2.49)

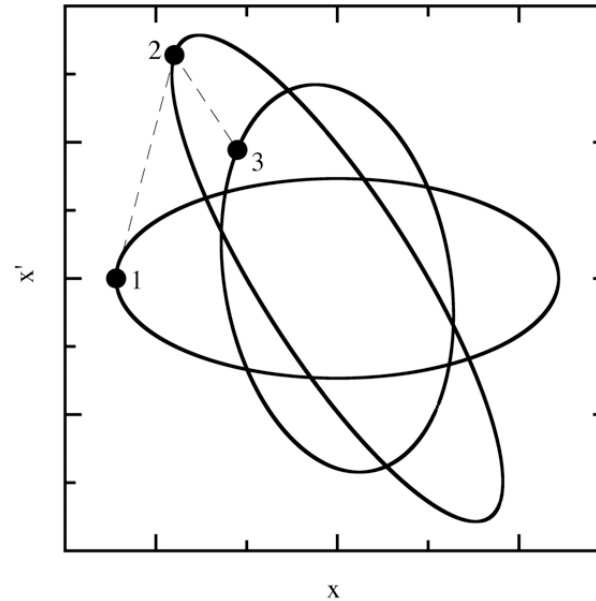
Taking into account Eq. (2.47), let us express the left side of the equation (2.49), $\epsilon_x \sin^2 \Phi_x = \epsilon_x (1 - \cos^2 \Phi_x)$, as

$$\epsilon_x \sin^2 \Phi_x = \epsilon_x - \frac{x^2}{\sigma_x^2}. \quad (2.50)$$

Courant-Snyder Invariant and Beam Emittance

Finally, the following equation is valid:
$$(x' \sigma_x - \sigma_x' x)^2 + \frac{x^2}{\sigma_x^2} = \epsilon_x. \quad (2.51)$$

Equation describes ellipse with constant area, which is called *Courant-Snyder invariant*.



$$\text{Area of Ellipse} = \pi \epsilon_x$$

$$x' = \frac{dx}{dz}$$

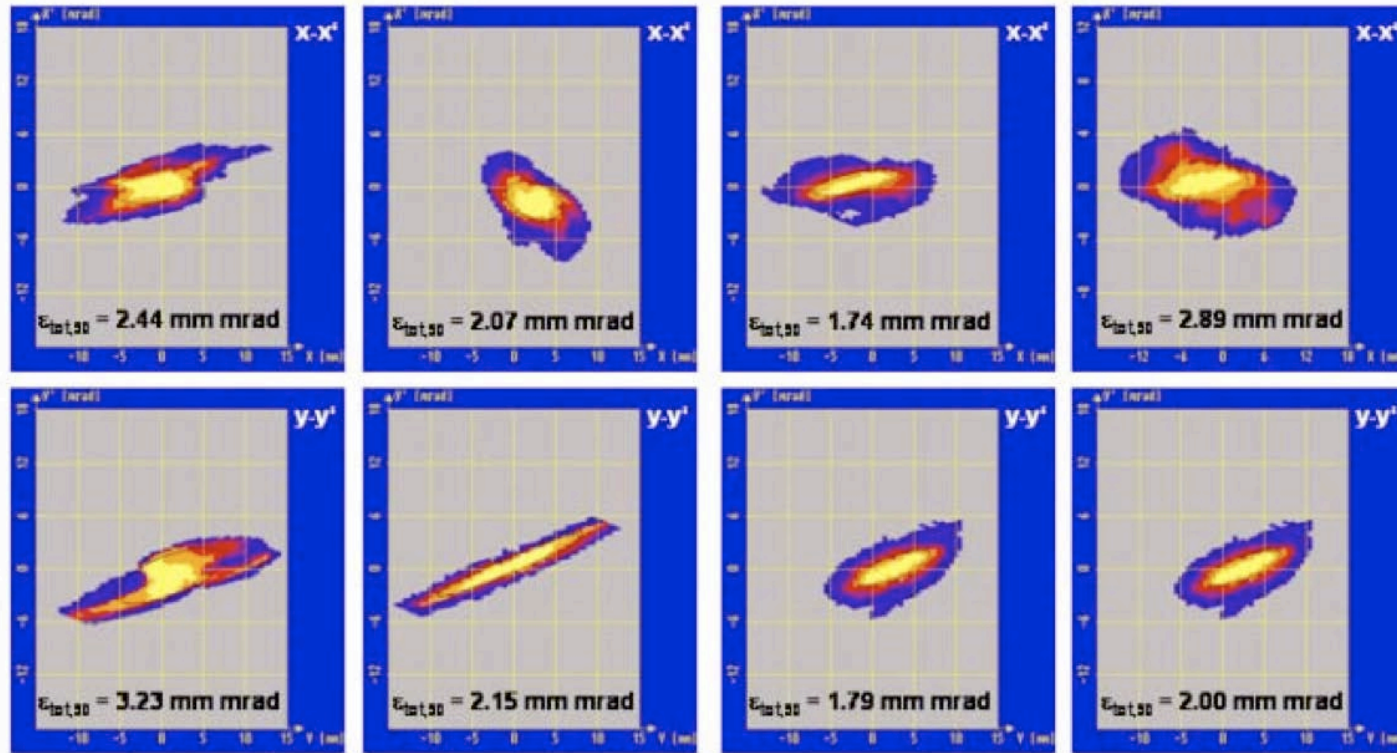
$$\dot{x} = \frac{dx}{dt}$$

Transformation of Courant-Snyder invariant along the channel and subsequent positions of a particle in phase space.

If particle belongs to certain ellipse at the initial moment of time, it will remain on ellipse boundary always. Because it is true for all particles belonging to partial ellipses within largest ellipse comprising all the beam, all particles within largest ellipse remain there. The largest ellipse occupied by particles is associated with **beam emittance**.

Beam Emittance

Beam emittance is the area, occupied by the particles on the phase plane ($x, dx/dz$)



$$\mathfrak{E} = \frac{1}{\pi} \int_{-\infty}^{\infty} \int_{-\infty}^{\infty} dx dx'$$

Results of beam emittance measurements in GSI UNILAC accelerator (W. Bayer et al., Proceedings of PAC07, Albuquerque, New Mexico, p. 1413 (2007)).

Liouville's Theorem

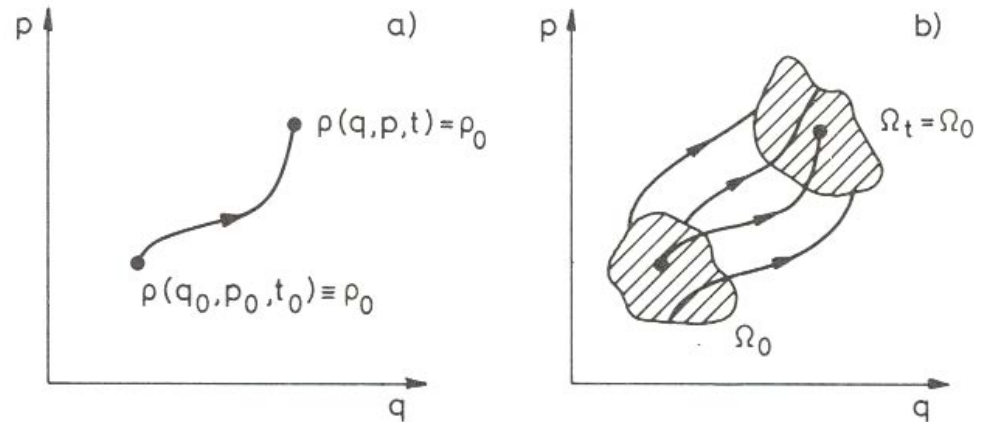
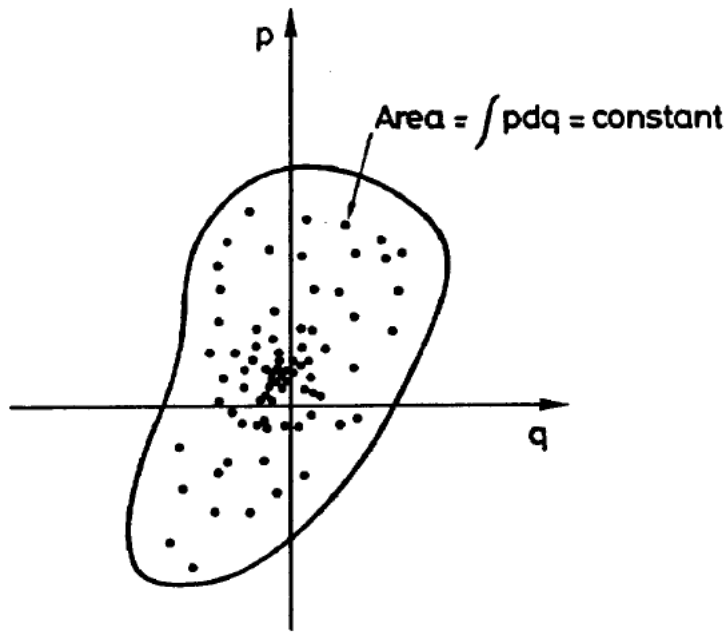


Illustration of conservation of phase space volume

Element of phase space: $dV = dx dy dz dP_x dP_y dP_z$

Phase space density (beam distribution function):

$$f(x, y, z, P_x, P_y, P_z) = \frac{dN}{dx dy dz dP_x dP_y dP_z}$$

Phase space volume occupied by particles is constant.

Liouville's theorem: if the motion of a system of mechanical particles obeys Hamilton's equations, then phase space density remains constant along phase space trajectories and phase space volume occupied by the particles is invariant (Liouville's Equation):

$$\frac{df}{dt} = \frac{\partial f}{\partial t} + \frac{\partial f}{\partial \vec{x}} \frac{d\vec{x}}{dt} + \frac{\partial f}{\partial \vec{P}} \frac{d\vec{P}}{dt} = 0$$

Hamiltonian Dynamics

Hamiltonian of charged particle with charge q and mass m

$$H = c \sqrt{m^2 c^2 + (P_x - qA_x)^2 + (P_y - qA_y)^2 + (P_z - qA_z)^2} + qU$$

x, y, z	position in real space
P_x, P_y, P_z	components of canonical momentum
A_x, A_y, A_z	components of the vector – potential
$U(x,y,z)$	scalar potential of the electromagnetic field

Equations of motion:

$$\frac{d\vec{x}}{dt} = \frac{\partial H}{\partial \vec{P}} \qquad \frac{d\vec{P}}{dt} = - \frac{\partial H}{\partial \vec{x}}$$

Canonical momentum $\vec{P} = (P_x, P_y, P_z)$ and mechanical momentum $\vec{p} = (p_x, p_y, p_z)$ are related:

$$\vec{p} = \vec{P} - q \vec{A}$$

In quadrupoles $\vec{p} = \vec{P}$, while in solenoid $P_x = p_x - qB \frac{y}{2}$ $P_y = p_y + qB \frac{x}{2}$

Liouville's Theorem (Proof)

Consider phase space element $dQdP$.

Number of particles dN inside element is $dN = f(Q,P,t)dQdP$

Change of particle density inside element is equal to divergence of the flux density (*Continuity Equation*)

$$\frac{\partial f}{\partial t} + \text{div}(f \vec{v}) = 0$$

Flux density in Q-direction $f \frac{dQ}{dt}$

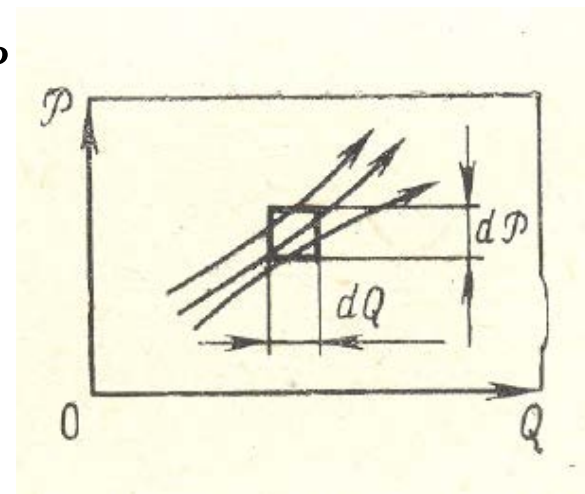
Flux density in P-direction $f \frac{dP}{dt}$

Continuity Equation:
$$\frac{\partial f}{\partial t} = -\frac{\partial}{\partial Q}(f\dot{Q}) - \frac{\partial}{\partial P}(f\dot{P}) = -\frac{\partial f}{\partial Q}\dot{Q} - \frac{\partial f}{\partial P}\dot{P} - f\left[\frac{\partial \dot{Q}}{\partial Q} + \frac{\partial \dot{P}}{\partial P}\right]$$

But because of Hamiltonian equations $\dot{Q} = \frac{\partial H}{\partial P}$ $\dot{P} = -\frac{\partial H}{\partial Q}$ the term in square

brackets is zero and total derivative of distribution function is equal zero (Liouville theorem).

$$\frac{\partial f}{\partial t} + \dot{Q} \frac{\partial f}{\partial Q} + \dot{P} \frac{\partial f}{\partial P} = \frac{df}{dt} = 0$$



On derivation of Liouville theorem.

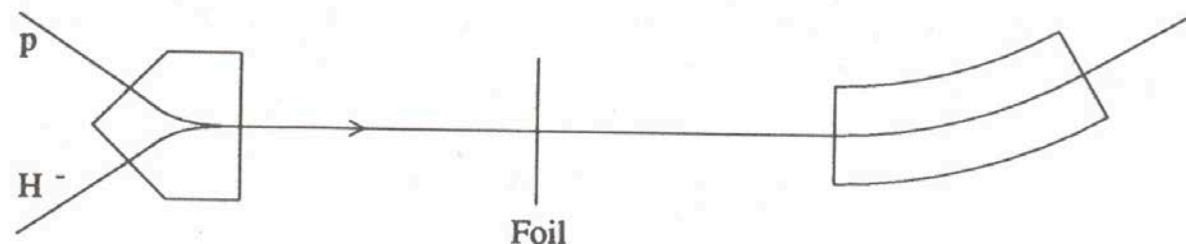
Liouvillian and non-Liouvillian Processes

Liouville theorem is valid for Hamiltonian processes only (where equations of motion are determined by Hamiltonian equations). Liouville's theorem does not allow to insert particles in phase space already occupied by the beam (there are no forces for that).

Liouvillian Processes: Dynamics in any electromagnetic fields without dissipation or scattering.

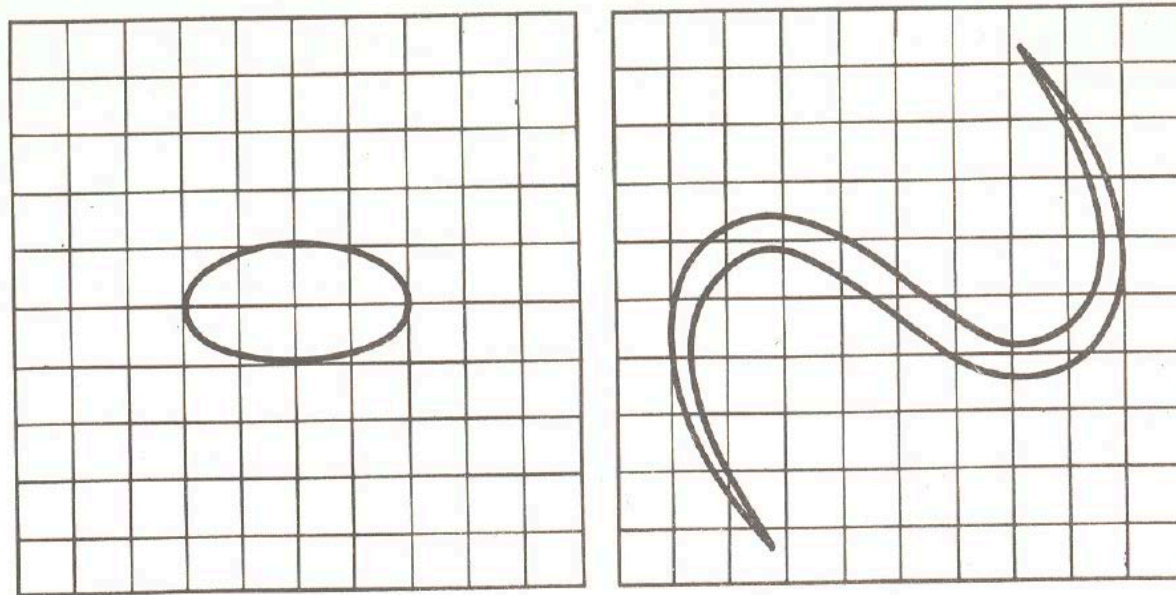
Non-Liouvillian processes: Scattering (foil, residual gas, Coulomb particle-particle), synchrotron radiation.

Example: Two oppositely charged beams can be made to travel along the same trajectory. In the straight section, the beams are passed through a thin foil, which strips the electrons from the H⁻ ions, leaving a single proton beam of higher density in phase space.



Increase of Effective Phase Space Volume

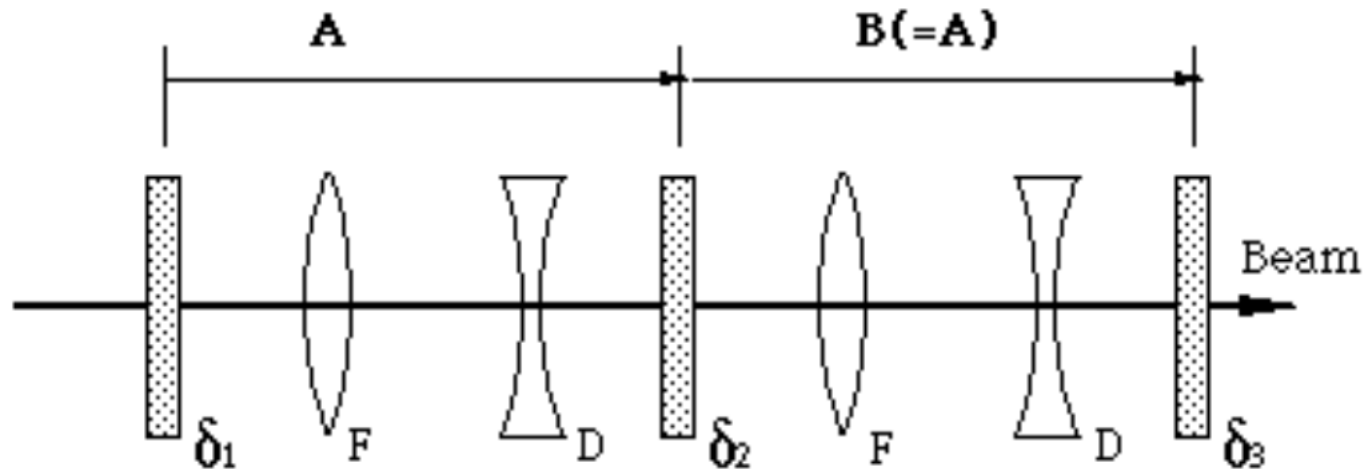
There are processes which do not violate Liouville's theorem, but result in increase of effective phase space volume of the beam. Example: filamentation in phase space.



Two distributions with the same actual areas, but with different effective areas. Left distribution occupies 8 cells, while right distribution occupies 25 cells.

Effect of Coupling on Beam Emittance

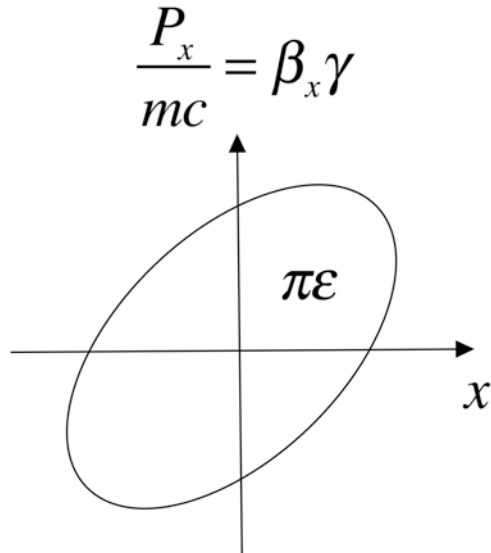
Liouville's theorem is valid in 6-dimensional phase space. Beam emittance is a projection of 6D phase space volume on 2D phase plane. Like any projection, it can be larger or smaller while total 6D phase space volume is conserved. In accelerator technique, emittance exchangers are commonly used:



Insertion of skew quadrupoles δ_1 , δ_2 , δ_3 into regular FODO quadrupole structure to exchange emittances between phase planes (from P.J.Bryant, CERN 1994-001).

Normalized and Un-Normalized Emittance

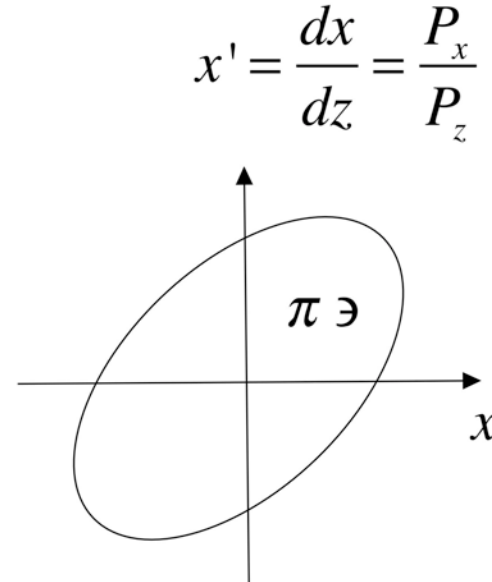
Normalized (energy-independent) emittance, ε



$$\varepsilon = \beta_z \gamma \varepsilon$$

Un-normalized (energy-dependent) emittance

$$\varepsilon \sim \frac{1}{\beta_z \gamma}$$

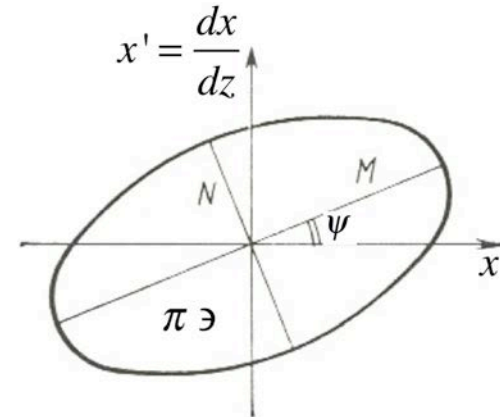


Twiss Parameters and Beam Emittance

The area of an ellipse with semi-axes M and N is $\pi M N$.

The general ellipse equation $\gamma x^2 + 2 \alpha x x' + \beta x'^2 = \varepsilon$

Parameters α, β, γ are called Twiss parameters and ellipse area is $\pi \varepsilon$.

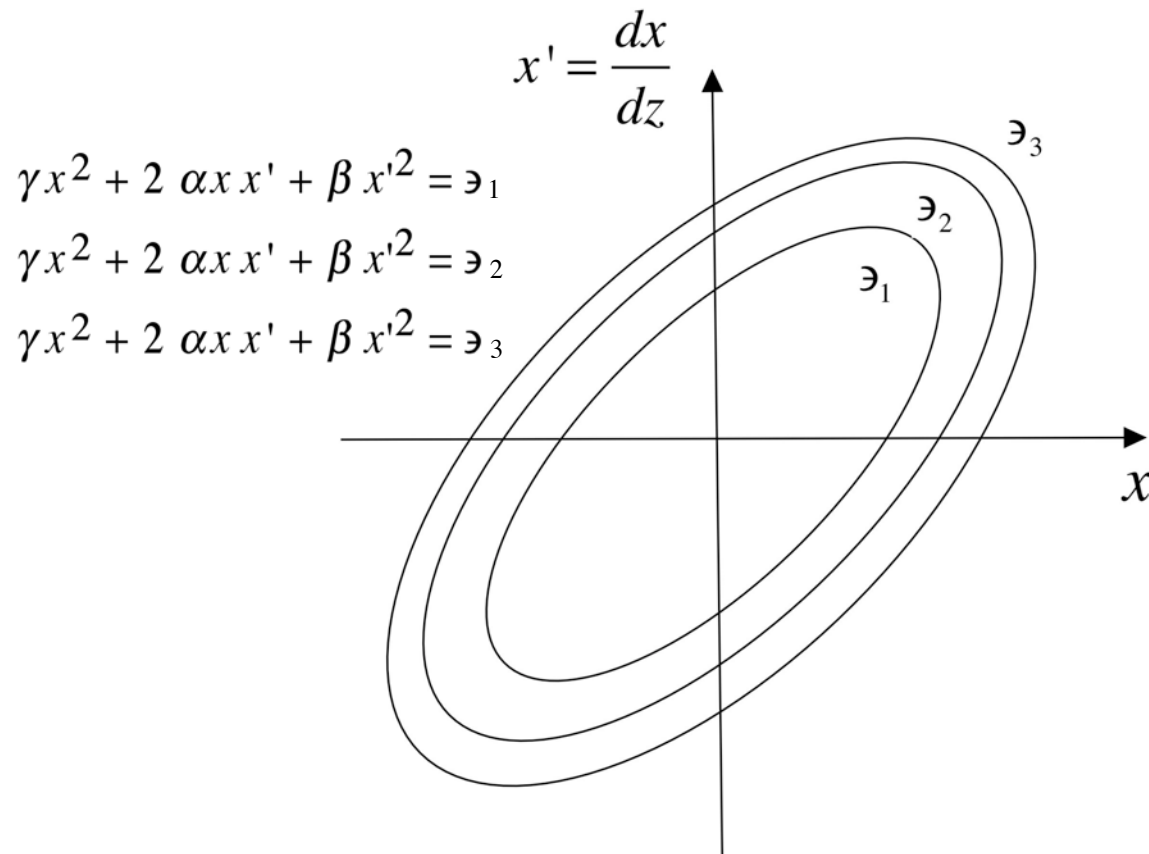


Emittance units: $\pi \cdot m \cdot \text{radian}$ ($\pi \cdot \text{cm} \cdot \text{miloradian}$)

Example : Emittance = $\pi \varepsilon = \pi \cdot M \cdot N = 0.2 \pi \text{ cm mrad}$

Ellipse of the beam at phase plane of transverse oscillations.

Twiss Parameters and Area of Ellipse



Twiss parameters determine family of ellipses, while actual ellipse is determined also by the value of ellipse area.

Twiss parameters:

$$\alpha_1 = \alpha_2 = \alpha_3$$

$$\beta_1 = \beta_2 = \beta_3$$

Area of ellipses:

$$\epsilon_1 < \epsilon_2 < \epsilon_3$$

Ellipse Properties

Let us express the ellipse parameters in terms of the semi-axes M , N and the angle ψ .
In the (\bar{x}, \bar{x}') system of coordinates, the ellipse is upright, and is described by the equation

$$\left(\frac{\bar{x}}{M}\right)^2 + \left(\frac{\bar{x}'}{N}\right)^2 = 1$$

The transformation to this system of coordinates is given by

$$\bar{x} = x \cos\psi + x' \sin\psi$$

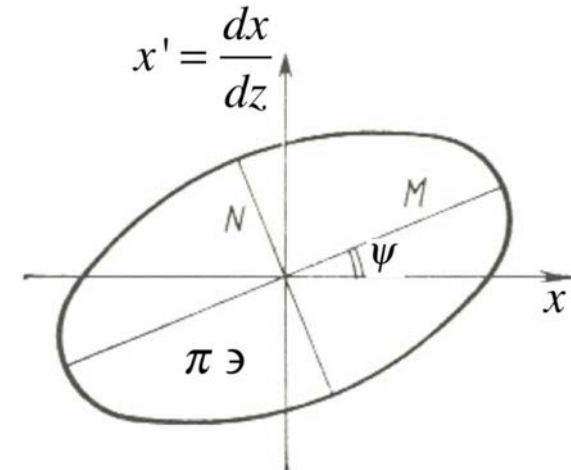
$$\bar{x}' = -x \sin\psi + x' \cos\psi$$

Comparison with previous ellipse equation yields the relationships between Twiss parameters and ellipse parameters:

$$\alpha = \left(\frac{N}{M} - \frac{M}{N}\right) \sin\psi \cos\psi$$

$$\beta = \frac{N}{M} \sin^2\psi + \frac{M}{N} \cos^2\psi$$

$$\gamma = \frac{N}{M} \cos^2\psi + \frac{M}{N} \sin^2\psi$$



Twiss Parameters and Amplitude Function

Compare two ellipses $\gamma x^2 + 2\alpha x x' + \beta x'^2 = \epsilon$ $(x'\sigma - x\sigma')^2 + \left(\frac{x}{\sigma}\right)^2 = \epsilon$

Comparison gives the following relationship between functions $\sigma(z)$, $\sigma'(z)$, and Twiss parameters:

$$\alpha = -\sigma \sigma' \quad \beta = \sigma^2 \quad \gamma = \frac{1}{\sigma^2} + \sigma'^2$$

From equation $\sigma = \sqrt{\beta}$ the equation for amplitude function $\sigma(z)$

$$\sigma_x'' - \frac{1}{\sigma_x^3} + k(z)\sigma_x = 0$$

can be rewritten as

$$\frac{1}{2}\beta_x''\beta_x - \frac{(\beta_x')^2}{4} + k(z)\beta_x^2 = 1$$

Twiss parameters are connected as

$$\alpha(z) = -\frac{\beta'(z)}{2}$$

Beam Envelope

Envelope of the beam, $R_x(z)$, corresponds to the maximum value of $\cos(\Phi_x(z) + \Phi_o) = 1$ in equation $x(z) = \sqrt{\beta_x} \sigma_x(z) \cos(\Phi_x(z) + \Phi_o)$ within the beam:

$$R_x(z) = \max \{x(z)\} = \sqrt{\beta_x} \sigma_x(z). \quad (2.52)$$

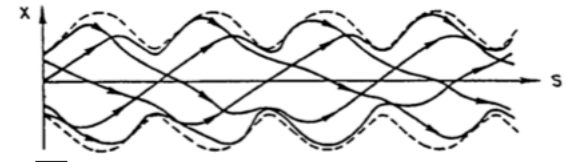
Slope of the beam envelope is, therefore, given by

$$R_x'(z) = \sqrt{\beta_x} \sigma_x'(z). \quad (2.53)$$

Taking into account previously introduced notations

$$\sigma = \sqrt{\beta}$$

$$\sigma' = -\frac{\alpha}{\sqrt{\beta}}$$



beam envelope and slope of beam envelope are given by

$$R_x = \sqrt{\beta_x} \sigma_x \quad \frac{dR_x}{dz} = -\alpha_x \sqrt{\frac{\beta_x}{\beta_x}}$$

Beam Envelopes (cont.)

Substitution of expression for $\sigma_x(z)$

$$\sigma_x(z) = \frac{R_x(z)}{\sqrt{\mathfrak{E}_x}} \quad (2.54)$$

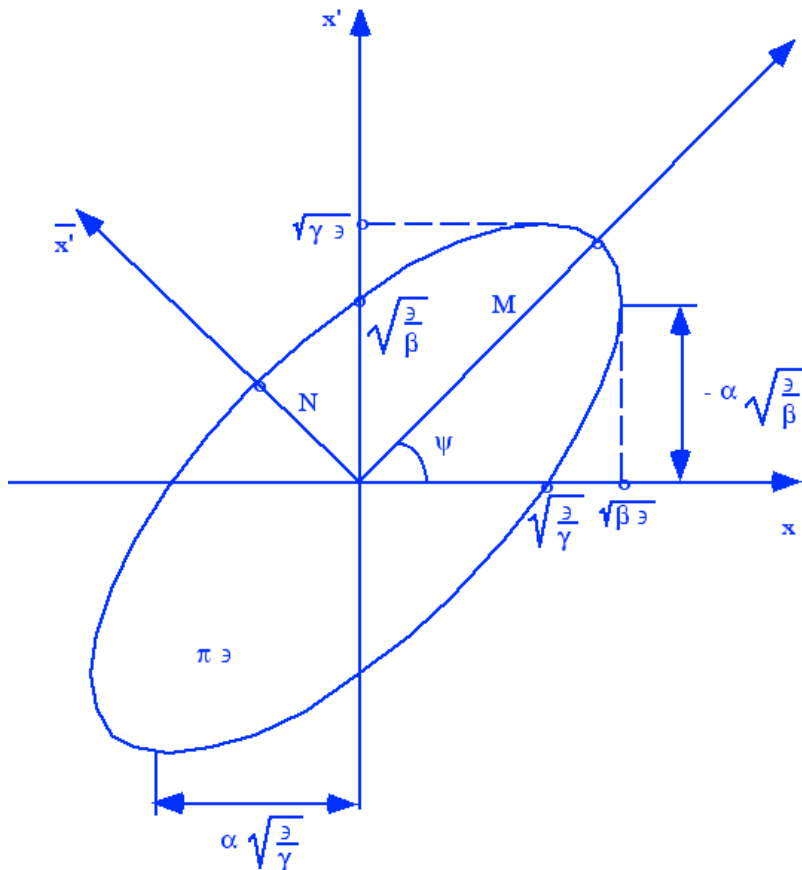
into Eq. (2.43) gives us the equation for beam envelope:

$$R_x'' - \frac{\mathfrak{E}_x^2}{R_x^3} + k(z) R_x = 0. \quad (2.55)$$

Beam envelope equations without space charge forces are:

$$\left\{ \begin{array}{l} R_x'' - \frac{\mathfrak{E}_x^2}{R_x^3} + k_x(z) R_x = 0 \\ R_y'' - \frac{\mathfrak{E}_y^2}{R_y^3} + k_y(z) R_y = 0 \end{array} \right. \quad (2.56)$$

Beam Spot Size and Beam Slope



Beam spot and beam envelope slope can be determined in other way as well. Let us rewrite the ellipse equation as

$$F(x, x') = \gamma x^2 + 2\alpha x x' + \beta x'^2 - \varepsilon = 0$$

We need to find a solution to the equations $\frac{dx}{dx'} = 0$. According to the differentiation rule of an implicit function,

$$\frac{dx}{dx'} = \frac{\frac{dF}{dx}}{\frac{dF}{dx'}} = -\frac{2\alpha x + 2\beta x'}{2\gamma x + 2\alpha x'} = 0$$

which has a solution $x' = -x \alpha / \beta$. Substitution of the obtained value of x' into the ellipse equation gives $x_{max} = \pm \sqrt{\beta \varepsilon}$. The value of $R = x_{max}$ is associated with the envelope size of the beam

$$R = \sqrt{\beta \varepsilon}$$

Differentiation of this equation taking into account that $\alpha(z) = -\frac{\beta'(z)}{2}$,

gives

$$\frac{dR}{dz} = -\alpha \sqrt{\frac{\varepsilon}{\beta}}$$

Floquet Theorem

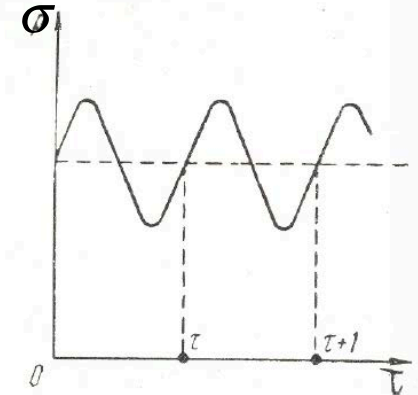
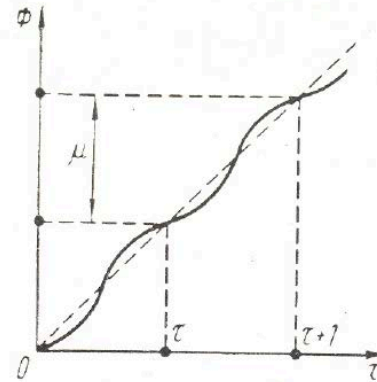
A second-order linear differential equation with periodic coefficients has a solution of the form $e^{\lambda z} \sigma(z)$ where λ is a constant and $\sigma(z)$ a periodic function.

Mathieu - Hill equation $\frac{d^2 x}{dz^2} + k(z) x = 0$

Solution: $x(z) = \sqrt{\sigma_x} \sigma_x(z) \cos(\Phi_x(z) + \Phi_o)$

Equations for amplitude and phase: $\sigma_x'' - \frac{1}{\sigma_x^3} + k(z)\sigma_x = 0$

$$\Phi_x' = \frac{1}{\sigma_x^2}$$



If function $k(z)$ is a periodic function $k(z+S) = k(z)$
 there is an unique periodic solution $\sigma(z+S) = \sigma(z)$.

This solution can be found by adjusting $\sigma(z)$, $\sigma'(z)$ in the way that solution after one period $\sigma(z+S)$, $\sigma'(z+S)$ coincides with $\sigma(z)$, $\sigma'(z)$.

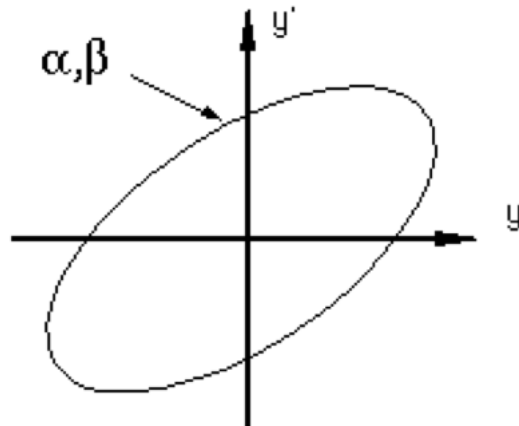
Periodic function $\sigma(z+S) = \sigma(z)$ is called *module of Floquet function*

Corresponding function $\Phi(z)$ is called *phase of Floquet function*

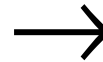
Floquet Ellipse

Beam ellipse:
$$\left(x'\sigma_x - x\sigma_x'\right)^2 + \left(\frac{x}{\sigma_x}\right)^2 = \epsilon_x$$

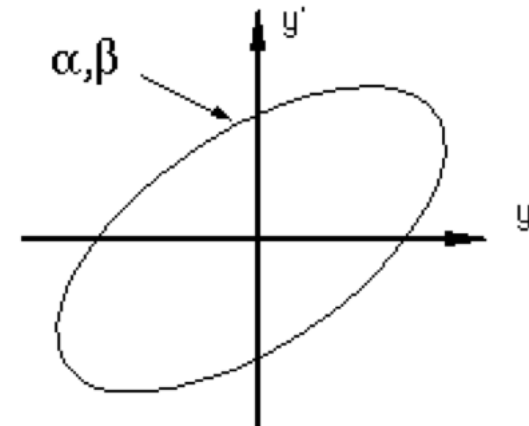
If $\sigma(z+S) = \sigma(z)$, $\sigma'(z+S) = \sigma'(z)$, beam ellipse is transformed into itself after one period.



Input



Focusing period



Output

Floquet ellipse is a unique beam ellipse which transforms into itself after one focusing period.

Beta-Function

Periodic solution of Mathieu – Hill equation is called beta-function of the focusing channel:

$$\beta = \sigma^2$$

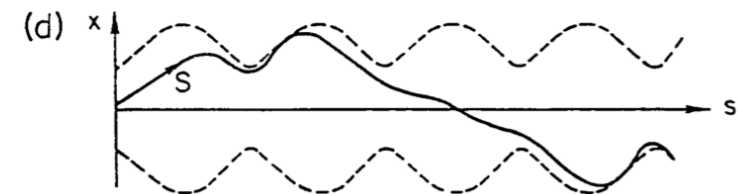
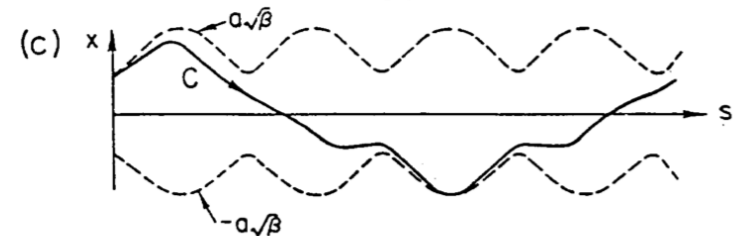
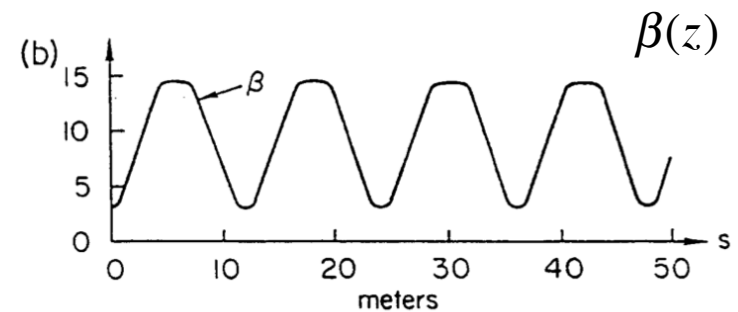
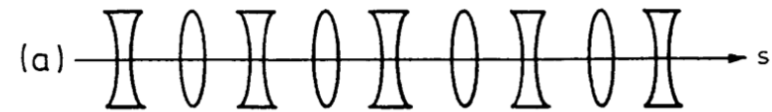
$$\frac{1}{2} \beta'' \beta - \frac{(\beta')^2}{4} + k(z) \beta^2 = 1$$

Beta-function of periodic structure

Twiss parameters:
$$\alpha(z) = -\frac{\beta'(z)}{2}$$

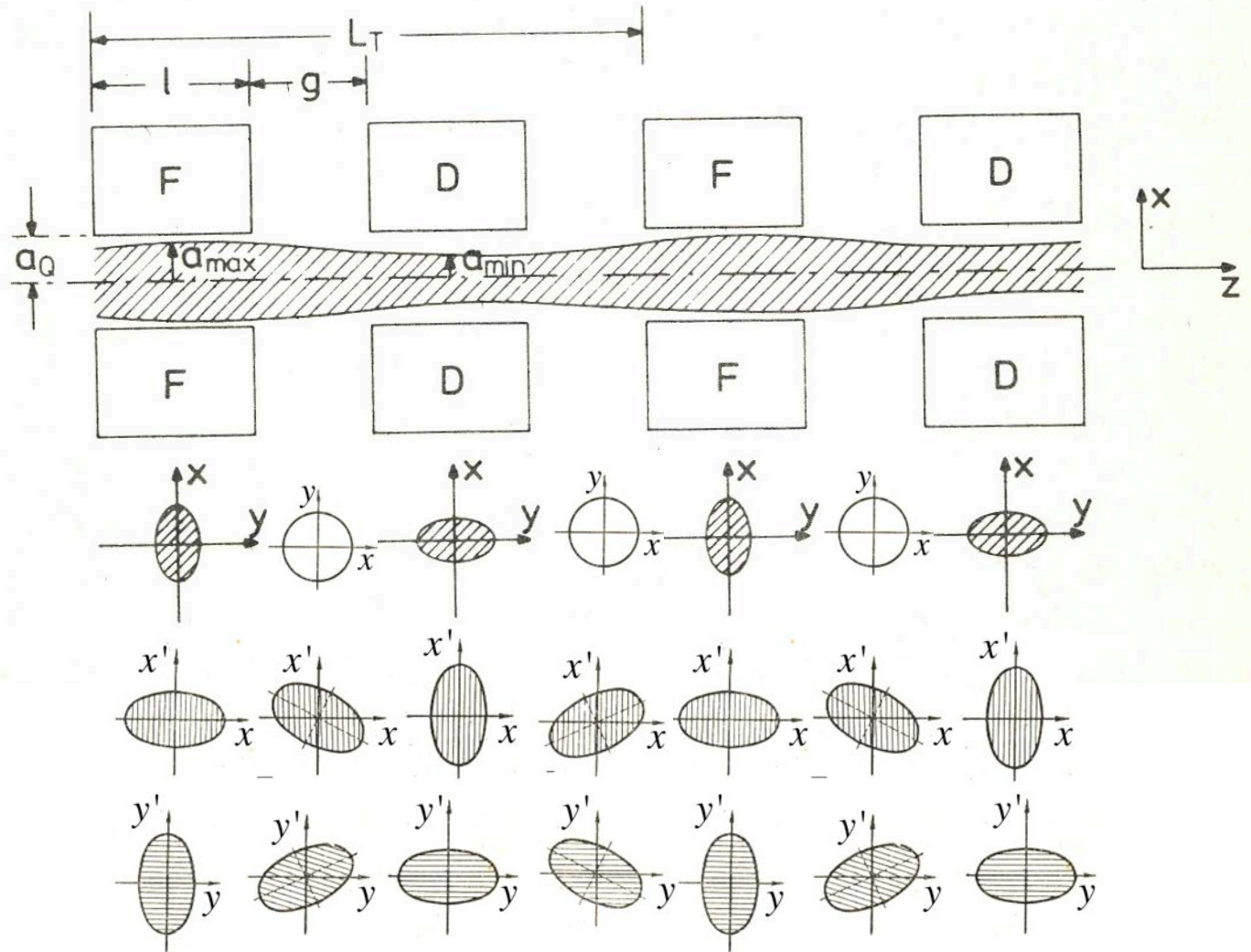
Single-particle trajectories in periodic structure

FODO focusing structure



Matched beam in periodic structure

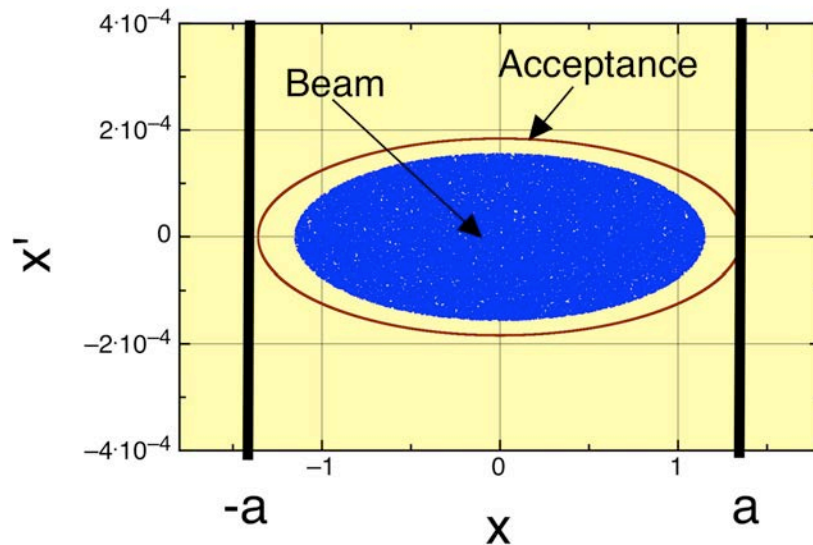
Matched Beam in Periodic Focusing Structure



Transport of a matched beam in a quadrupole channel. Matched beam ellipses repeat into themselves after each focusing period

Acceptance of Periodic Focusing Structure

Focusing Quadrupole

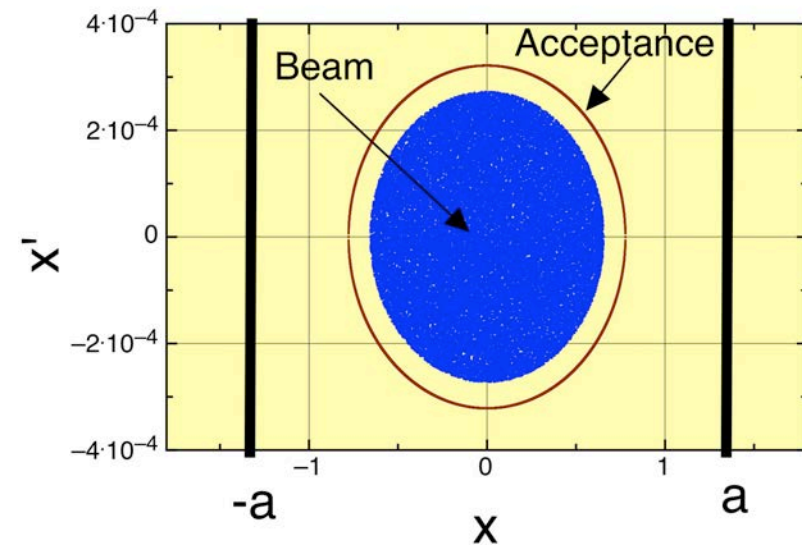


Beam radius

Maximal beam radius $R = a$

Acceptance of periodic focusing channel A is the largest Floquet ellipse limited by the aperture of the structure a .

Defocusing Quadrupole

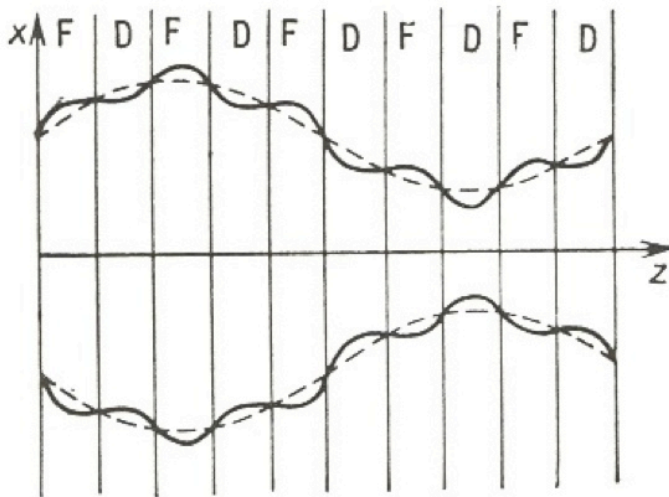


$$R(z) = \sqrt{\epsilon \beta(z)}$$

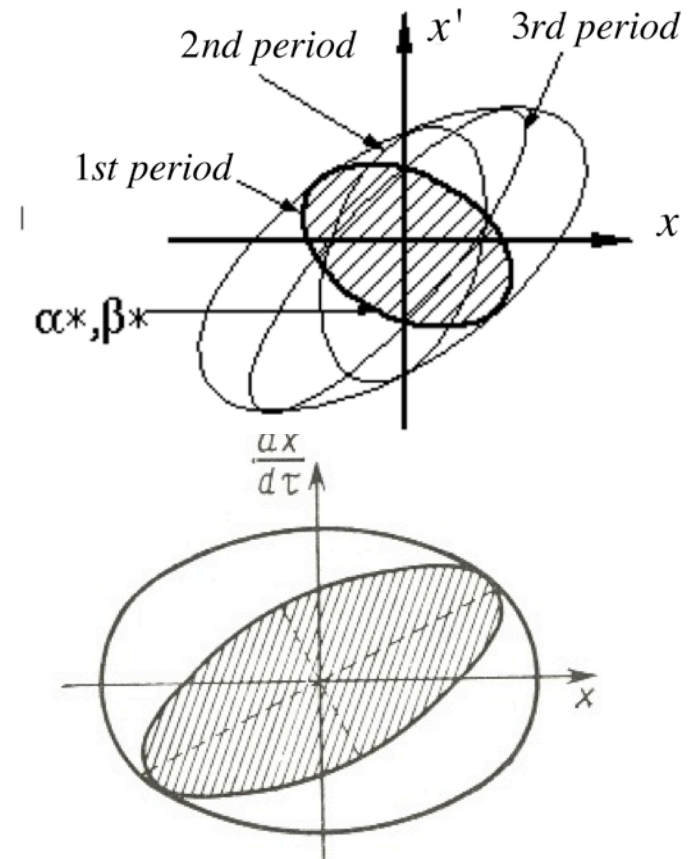
$$a = \sqrt{A \beta_{\max}}$$

$$A = \frac{a^2}{\beta_{\max}}$$

Mismatched Beam in a Periodic Structure



The envelope of an unmatched beam in a quadrupole channel.



Effective beam emittance.

Matched Beam Focusing



Y.K. Batygin Basics of Beam Focusing USPAS 2019

Matched beam in RF linear accelerator (Courtesy of Sergey Kurennoy).

Instantaneous Frequency of Transverse Oscillations

Instantaneous frequency of transverse oscillations:

$$\omega_r = \frac{d\Phi_x}{dt}$$

Combining $\Phi_x' = \frac{1}{\sigma_x^2}$ with expression for beam emittance

$\mathfrak{E}_x = R_x^2 / \sigma_x^2$ one can express beam emittance with instantaneous frequency of transverse oscillations:

$$\mathfrak{E}_x = \frac{R_x^2 \omega_r}{\beta c}$$

Emittance is expressed through Twiss parameter

$$\mathfrak{E}_x = R_x^2 / \beta_x$$

Instantaneous frequency of transverse oscillation and Twiss parameter β are connected as:

$$\omega_r = \frac{v_z}{\beta_x}$$

Instantaneous frequency of transverse oscillations has a minimum value in focusing lens and maximum value in defocusing one.

Matrix Method for Particle Trajectories

Let us divide focusing structure by elements, where equation of motion are individual linear differential equations with constant coefficients (drift space, quadruple lens). Solution at each element can be written as linear combination of initial conditions:

$$x_1 = m_{11}x_o + m_{12}x'_o$$

$$x'_1 = m_{21}x_o + m_{22}x'_o$$

or in matrix form

$$\begin{pmatrix} x_1 \\ x'_1 \end{pmatrix} = M_1 \begin{pmatrix} x_o \\ x'_o \end{pmatrix}$$

Matrix of two subsequent elements:

$$\begin{pmatrix} x_2 \\ x'_2 \end{pmatrix} = M_2 \begin{pmatrix} x_1 \\ x'_1 \end{pmatrix} = M_2 M_1 \begin{pmatrix} x_o \\ x'_o \end{pmatrix}$$

Matrix of sequence of elements is a product of that of each element

$$M = M_n \cdot M_{n-1} \cdot \dots \cdot M_2 \cdot M_1$$

Inverse matrix:

$$\begin{pmatrix} x_o \\ x'_o \end{pmatrix} = \frac{1}{(m_{11}m_{22} - m_{12}m_{21})} \begin{pmatrix} m_{22} & -m_{12} \\ -m_{21} & m_{11} \end{pmatrix} \begin{pmatrix} x_1 \\ x'_1 \end{pmatrix}$$

Matrix Method for Particle Trajectories (cont.)

Particle trajectory at arbitrary point can be expressed as a function of initial conditions

$$\begin{pmatrix} x \\ x' \end{pmatrix} = \begin{pmatrix} m_{11} & m_{12} \\ m_{21} & m_{22} \end{pmatrix} \begin{pmatrix} x_o \\ x'_o \end{pmatrix}$$

$$x = m_{11}x_o + m_{12}x'_o$$

$$x = \frac{\partial x}{\partial x_o}x_o + \frac{\partial x}{\partial x'_o}x'_o$$

$$x' = m_{21}x_o + m_{22}x'_o$$

$$x' = \frac{\partial x'}{\partial x_o}x_o + \frac{\partial x'}{\partial x'_o}x'_o$$

$$M = \begin{vmatrix} \frac{\partial x}{\partial x_o} & \frac{\partial x}{\partial x'_o} \\ \frac{\partial x'}{\partial x_o} & \frac{\partial x'}{\partial x'_o} \end{vmatrix}$$

Matrix elements can be written as

$$m_{11} = \frac{\partial x}{\partial x_o} \quad m_{12} = \frac{\partial x}{\partial x'_o} \quad m_{21} = \frac{\partial x'}{\partial x_o} \quad m_{22} = \frac{\partial x'}{\partial x'_o}$$

$$dx dx' = \det \begin{vmatrix} \frac{\partial x}{\partial x_o} & \frac{\partial x}{\partial x'_o} \\ \frac{\partial x'}{\partial x_o} & \frac{\partial x'}{\partial x'_o} \end{vmatrix} dx_o dx'_o$$

Determinant of matrix coincides with Jacobian:

Because of Liouville's theorem, phase space element is transformed as $dx dx' = dx_o dx'_o$, and, therefore, determinant of matrix M is equal to unity:

$$\det M = 1$$

Transformation of Beam Ellipse Through Arbitrary Channel

$$\begin{pmatrix} y \\ y' \end{pmatrix}_s = \begin{pmatrix} C & S \\ C' & S' \end{pmatrix} \begin{pmatrix} y \\ y' \end{pmatrix}_0$$

By inserting the inverse trajectory transformation

$$\begin{pmatrix} y_0 \\ y'_0 \end{pmatrix} = \begin{pmatrix} S' & -S \\ -C' & C \end{pmatrix} \begin{pmatrix} y \\ y' \end{pmatrix}$$

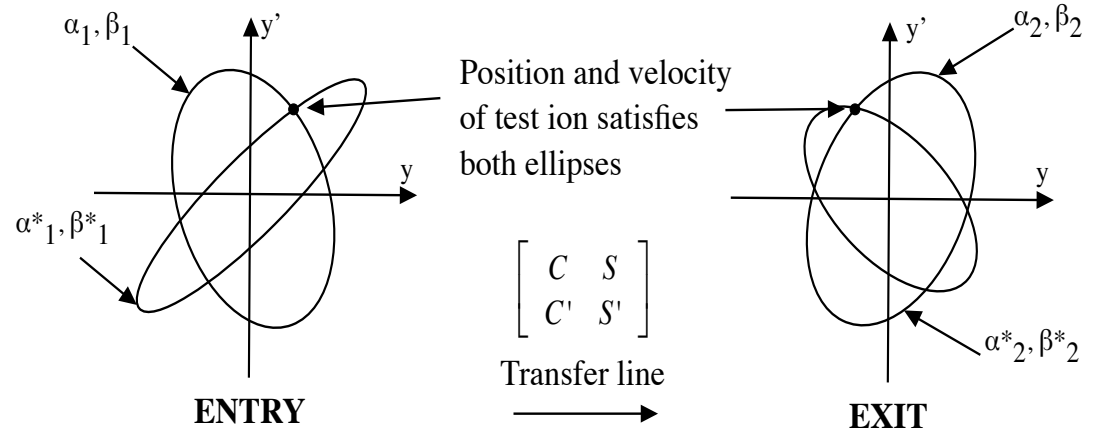
into the ellipse equation, we have at point s_0

$$\begin{aligned} & y_0 y_0'^2 + 2\alpha_0 y_0 y_0' + \beta_0 y_0'^2 \\ &= y_0 (S'y - Sy')^2 + 2\alpha_0 (S'y - Sy')(-C'y + Cy') + \beta_0 (-C'y + Cy')^2 \\ &= \underbrace{(C'^2 \beta_0 - 2C'S'\alpha_0 + S'^2 y_0)}_{\gamma} y^2 + 2 \underbrace{(-CC'\beta_0 + (S'C + SC')\alpha_0 - SS'y_0)}_{\alpha} yy' + \underbrace{(C^2 \beta_0 - 2CS\alpha_0 + S^2 y_0)}_{\beta} y'^2 \\ &= \gamma y^2 + 2\alpha yy' + \beta y'^2 \end{aligned}$$

Thus β , $\alpha = -\frac{1}{2}\beta'$, and $\gamma = \frac{1+\alpha^2}{\beta}$ can be calculated from the principal

trajectories C, S by the linear 3x3 transformation:

$$\begin{pmatrix} \beta \\ \alpha \\ \gamma \end{pmatrix} = \begin{pmatrix} C^2 & -2CS & S^2 \\ -CC' & CS' + SC' & -SS' \\ C'^2 & -2C'S' & S'^2 \end{pmatrix} \begin{pmatrix} \beta_0 \\ \alpha_0 \\ \gamma_0 \end{pmatrix}$$



Transformation of Particle Trajectory Through Arbitrary Channel

Transformation of particle trajectory through arbitrary channel

$$x(z) = \sqrt{\beta_x} \sigma_x(z) \cos(\Phi_x(z) + \Phi_o)$$

$$x'(z) = \sqrt{\beta_x} \left[\sigma'_x(z) \cos(\Phi_x(z) + \Phi_o) - \frac{\sin(\Phi_x(z) + \Phi_o)}{\sigma_x} \right]$$

Initial conditions ($z = 0$):

$$x_o = \sqrt{\beta_x} \sigma_o \cos \Phi_o$$

$$x'_o = \sqrt{\beta_x} \left(\sigma'_o \cos \Phi_o - \frac{\sin \Phi_o}{\sigma_o} \right)$$

Particle transformation through the channel

$$x = x_o \left(\frac{\sigma_x}{\sigma_o} \cos \Phi_x - \sigma_x \sigma'_o \sin \Phi_x \right) + x'_o \sigma_x \sigma_o \sin \Phi_x$$

$$x' = x_o \left[\cos \Phi_x \left(\frac{\sigma'_x}{\sigma_o} - \frac{\sigma'_o}{\sigma_x} \right) - \sin \Phi_x \left(\sigma'_x \sigma'_o + \frac{1}{\sigma_x \sigma_o} \right) \right] + x'_o \left(\frac{\sigma_o}{\sigma_x} \cos \Phi_x + \sigma'_x \sigma_o \sin \Phi_x \right)$$

Or, in matrix form with $\sigma = \sqrt{\beta}$, $\sigma' = -\alpha / \sqrt{\beta}$:

$$\begin{pmatrix} x \\ x' \end{pmatrix} = \begin{pmatrix} \sqrt{\frac{\beta_x(z)}{\beta_o}} (\cos \Phi_x + \alpha_o \sin \Phi_x) & \sqrt{\beta_o \beta_x(z)} \sin \Phi_x \\ -\frac{\cos \Phi_x (\alpha_x(z) - \alpha_o) + \sin \Phi_x (1 + \alpha_o \alpha_x(z))}{\sqrt{\beta_o \beta_x(z)}} & \sqrt{\frac{\beta_o}{\beta_x(z)}} (\cos \Phi_x - \alpha_o \sin \Phi_x) \end{pmatrix} \begin{pmatrix} x_o \\ x'_o \end{pmatrix}$$

Transformation of Particle Trajectory Through *Periodic Channel*

For periodic solution in periodic channel:

$$\beta_x(S) = \beta_o \quad \alpha_x(S) = \alpha_o$$

Transformation matrix through periodic channel (*Twiss matrix*):

$$M = \begin{pmatrix} \cos \mu_o + \alpha_x \sin \mu_o & \beta_x \sin \mu_o \\ -\frac{1 + \alpha_x^2}{\beta_x^2} \sin \mu_o & \cos \mu_o - \alpha_x \sin \mu_o \end{pmatrix}$$

Phase advance of transverse oscillations per period of structure

$$\mu_o = \Phi_x(S)$$

The value of μ_o can be found from transformation matrix as a half sum of diagonal elements

$$\cos \mu_o = \frac{m_{11} + m_{22}}{2} \quad -1 \leq \cos \mu_o \leq 1$$

Stability criteria:

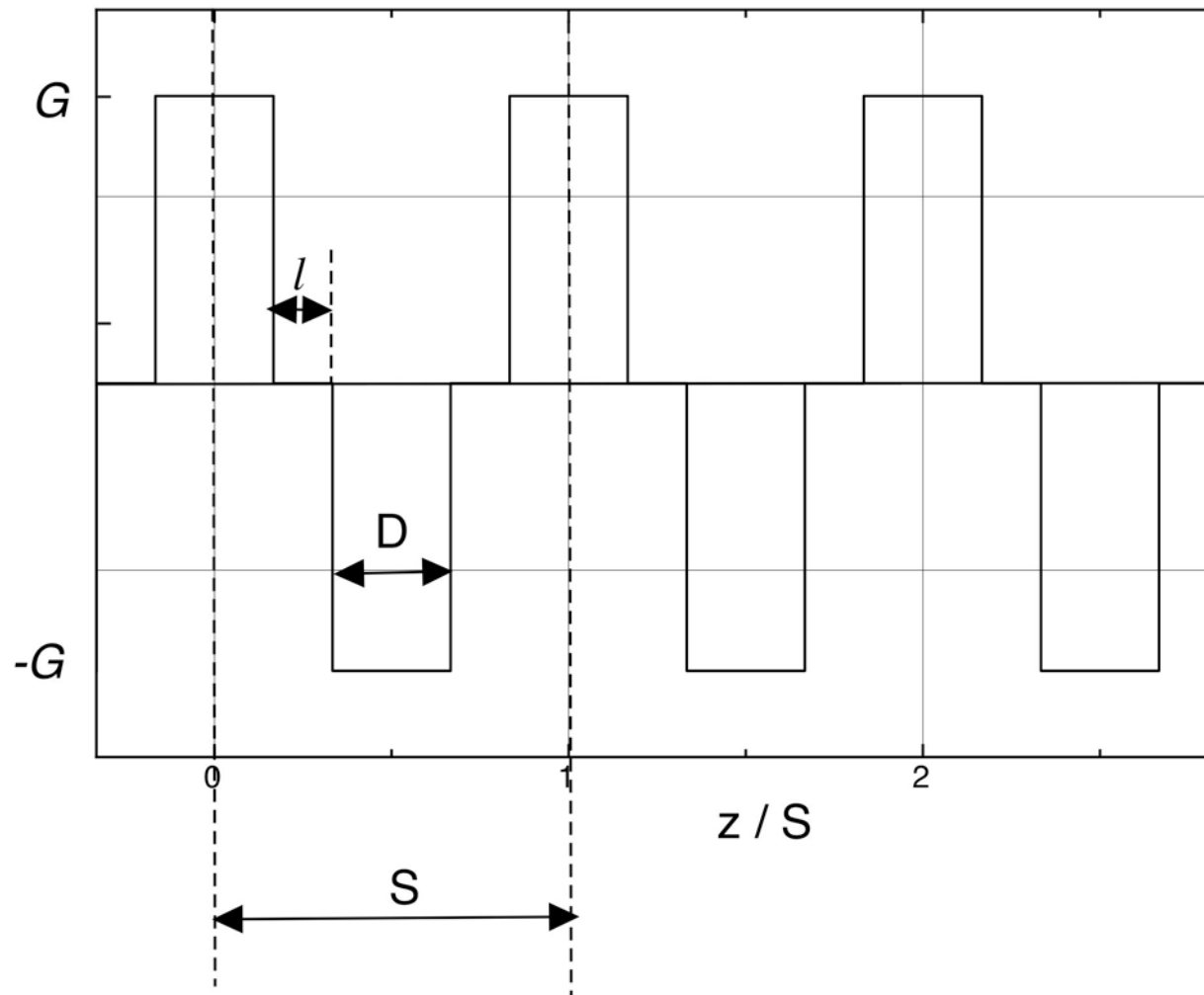
$$m_{11} + m_{22} \leq 2$$

Twiss parameters of matched beam:

$$\beta_x = \frac{m_{12}}{\sin \mu_o}$$

$$\alpha_x = \frac{m_{11} - m_{22}}{2 \sin \mu_o}$$

FODO Quadrupole Focusing Channel



Period of FODO channel $S=2D+2l$

Single-Particle Matrix in a Quadrupole Focusing Channel

In quadrupole lens, the Mathieu – Hill equation is transformed into equation with constant coefficients k :

$$\frac{d^2 x}{dz^2} + kx = 0 \quad \frac{d^2 y}{dz^2} - ky = 0 \quad k = \frac{qG}{m\gamma\beta c}$$

Solution of equations of motion in quadrupole lense:

$$x = x_o \cos(z\sqrt{k}) + \frac{x'_o}{\sqrt{k}} \sin(z\sqrt{k})$$

$$x' = -x_o \sqrt{k} \sin(z\sqrt{k}) + x'_o \cos(z\sqrt{k})$$

$$y = y_o \cosh(z\sqrt{k}) + \frac{y'_o}{\sqrt{k}} \sinh(z\sqrt{k})$$

$$y' = y_o \sqrt{k} \sinh(z\sqrt{k}) + y'_o \cosh(z\sqrt{k})$$

$\cos(i\varphi) = \cosh(\varphi)$
$\sin(i\varphi) = i \sinh(\varphi)$

Single-Particle Matrix in a Quadrupole Focusing Channel

Transformation of particle coordinate and slope of particle trajectory through the quadrupole of the length of D , can be written as a matrix:

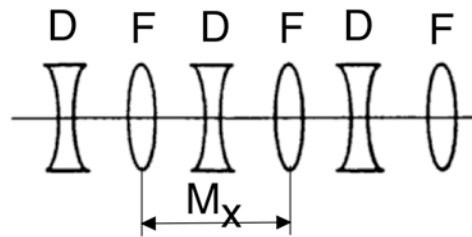
$$\begin{pmatrix} x \\ x' \end{pmatrix} = M_F \begin{pmatrix} x_o \\ x'_o \end{pmatrix} \quad M_F = \begin{pmatrix} \cos(D\sqrt{k}) & \frac{1}{\sqrt{k}} \sin(D\sqrt{k}) \\ -\sqrt{k} \sin(D\sqrt{k}) & \cos(D\sqrt{k}) \end{pmatrix}$$

$$\begin{pmatrix} y \\ y' \end{pmatrix} = M_D \begin{pmatrix} y_o \\ y'_o \end{pmatrix} \quad M_D = \begin{pmatrix} \cosh(D\sqrt{k}) & \frac{1}{\sqrt{k}} \sinh(D\sqrt{k}) \\ \sqrt{k} \sinh(D\sqrt{k}) & \cosh(D\sqrt{k}) \end{pmatrix}$$

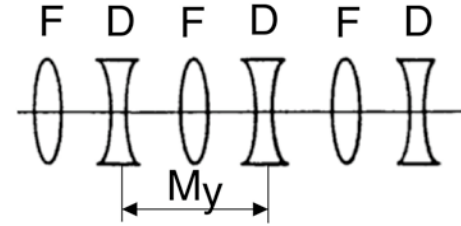
Between lenses particle perform drift at the distance l : $M_o = \begin{pmatrix} 1 & l \\ 0 & 1 \end{pmatrix}$

Matrix of FODO Cell

Matrix of one period of such structure



$$M_x = M_{\frac{F}{2}} M_O M_D M_O M_{\frac{F}{2}}$$



$$M_y = M_{\frac{D}{2}} M_O M_F M_O M_{\frac{D}{2}}$$

Elements of resulting x- matrix of one period

$$m_{11} = \cosh \chi (\cos \chi - l\sqrt{k} \sin \chi) + \sinh \chi (l\sqrt{k} \cos \chi - \frac{kl^2}{2} \sin \chi)$$

$$m_{12} = \cosh \chi \left(\frac{\sin \chi}{\sqrt{k}} + 2l \cos^2 \frac{\chi}{2} \right) + \sinh \chi \left(\frac{1}{\sqrt{k}} + l \sin \chi + l^2 \sqrt{k} \cos^2 \frac{\chi}{2} \right)$$

$$m_{21} = \cosh \chi \left(2lk \sin^2 \frac{\chi}{2} - \sqrt{k} \sin \chi \right) + \sinh \chi \left(\sqrt{k} + k^{3/2} l^2 \sin^2 \frac{\chi}{2} - lk \sin \chi \right)$$

$$m_{22} = \cosh \chi (\cos \chi - l\sqrt{k} \sin \chi) + \sinh \chi (l\sqrt{k} \cos \chi - \frac{kl^2}{2} \sin \chi)$$

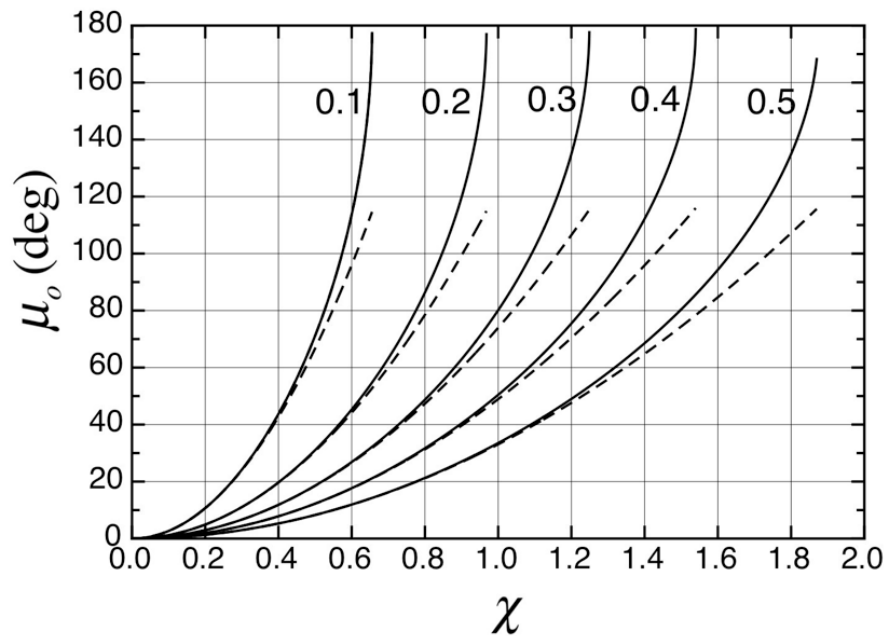
where quadrupole lens rigidity

$$\chi = D\sqrt{k} = D \sqrt{\frac{qG}{m\gamma\beta c}}$$

Phase Advance Per Period in FODO Channel

Using $\cos \mu_o = \frac{m_{11} + m_{22}}{2}$

$$\cos \mu_o = \cosh \chi (\cos \chi - l\sqrt{k} \sin \chi) + \sinh \chi (l\sqrt{k} \cos \chi - \frac{kl^2}{2} \sin \chi)$$



Using approximations

$$\sin \chi = \chi - \frac{\chi^3}{6} + \frac{\chi^5}{120}$$

$$\sinh \chi = \chi + \frac{\chi^3}{6} + \frac{\chi^5}{120}$$

$$\cos \chi = 1 - \frac{\chi^2}{2} + \frac{\chi^4}{24}$$

$$\cosh \chi = 1 + \frac{\chi^2}{2} + \frac{\chi^4}{24}$$

$$\cos \mu_o \approx 1 - \frac{l^2 \chi^2 k}{2} - \frac{2}{3} l\sqrt{k} \chi^3 - \frac{\chi^4}{6}$$

$$\cos \mu_o \approx 1 - \frac{\mu_o^2}{2}$$

Smooth approximation to FODO phase advance:

$$\mu_o = \frac{S}{2D} \sqrt{1 - \frac{4}{3} \frac{D}{S} \frac{qGD^2}{m\gamma\beta c}}$$

Phase advance per period of FODO focusing channel, as a function of quadrupole lens rigidity: (solid) exact values; (dotted) smooth approximation. Numbers indicate ratio of lens length to period, D/S . **Smooth approximation is valid for $\mu_o \leq 60^\circ$.**

Beta Functions and Acceptance of FODO Channel

Beta-function
$$\beta = \frac{m_{12}}{\sin \mu_o}$$

Expansions
$$\cos \mu_o \approx 1 - \frac{l^2 \chi^2 k}{2} = 1 - 2 \sin^2 \frac{\mu_o}{2} \quad \sin \frac{\mu_o}{2} \approx \pm \frac{l \chi \sqrt{k}}{2} = \pm \frac{l D k}{2}$$

Element m_{12}
$$m_{12} \approx 2l + \frac{(2 + kl^2)\chi}{\sqrt{k}} + \frac{3l\chi^2}{2} \approx S(1 \pm \sin \frac{\mu_o}{2})$$

Maximum and minimum values of beta-function

$$\beta_{\min} = \frac{S(1 - \sin \frac{\mu_o}{2})}{\sin \mu_o}$$

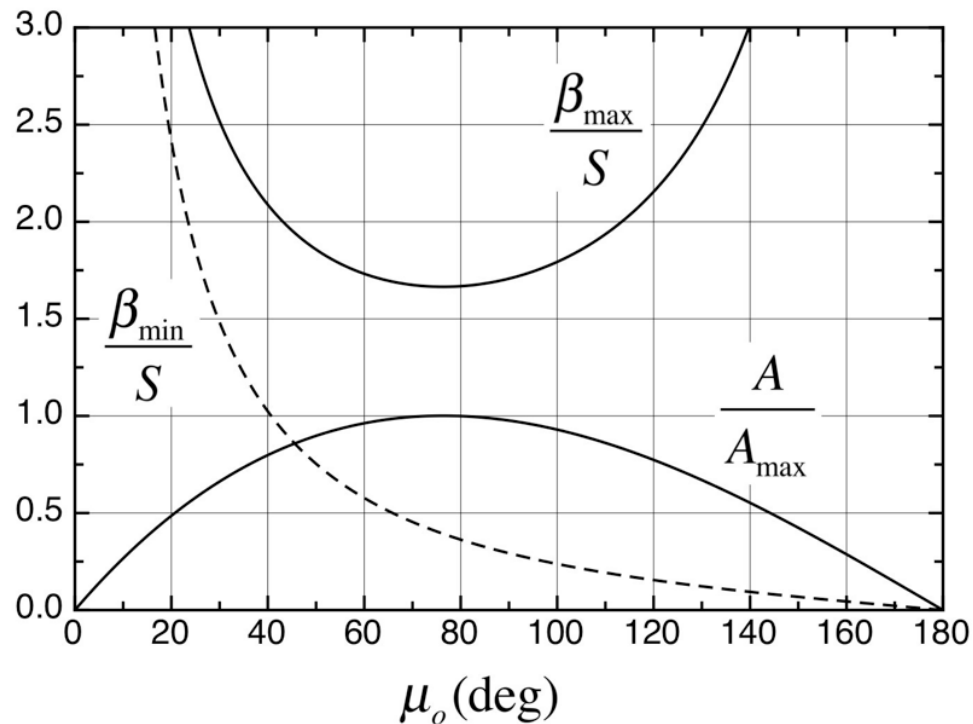
$$\beta_{\max} = \frac{S(1 + \sin \frac{\mu_o}{2})}{\sin \mu_o}$$

Acceptance of FODO channel

$$A = a^2 / \beta_{\max}$$

$$A = \frac{a^2 \sin \mu_o}{S(1 + \sin \frac{\mu_o}{2})}$$

Beta Functions and Acceptance of FODO Channel (cont.)



Acceptance of FODO Channel

$$A = \frac{a^2}{S} \frac{\sin \mu_o}{(1 + \sin \frac{\mu_o}{2})}$$

Optimal value of phase advance, where acceptance reaches it's maximum

$$\frac{\partial A}{\partial \mu_o} = 0 \quad \mu_o = 76.3^\circ$$

Characteristics of FODO focusing channel as functions of phase advance per period of structure.

Maximal FODO acceptance

$$A_{\max} = 0.6 \frac{a^2}{S}$$

Maximal and Minimal Beam Size in FODO Channel

Taking into account expression for beam size $R(z) = \sqrt{\beta(z)}$ and using expressions for β_{max} and β_{min} in FODO channel

Maximal beam size

$$R_{max} = \sqrt{\frac{\beta}{\sin \mu_o} (1 + \sin \frac{\mu_o}{2})} = R_o \sqrt{1 + \sin \frac{\mu_o}{2}}$$

Minimal beam size

$$R_{min} = \sqrt{\frac{\beta}{\sin \mu_o} (1 - \sin \frac{\mu_o}{2})} = R_o \sqrt{1 - \sin \frac{\mu_o}{2}}$$

Average beam size

$$R_o = \sqrt{\frac{\beta}{\sin \mu_o}}$$

Let us express maximal and minimal beam size as

$$R_{max} \approx R_o (1 + v_{max})$$

$$R_{min} \approx R_o (1 - v_{max})$$

Relative variation of beam size

$$v_{max} = \frac{\sqrt{1 + \sin \frac{\mu_o}{2}} - \sqrt{1 - \sin \frac{\mu_o}{2}}}{2}$$

For $\mu_o \leq 60^\circ$

$$v_{max} \approx \frac{1}{2} \sin \frac{\mu_o}{2} \approx \frac{\mu_o}{4}$$

Higher Stability Regions

Consider FD focusing structure. Matrix of of one FD period:

$$M_{\frac{F}{2}} M_D M_{\frac{F}{2}} = \begin{pmatrix} \cos \chi \cosh \chi & \frac{1}{\sqrt{k}} (\cosh \chi \sin \chi + \sinh \chi) \\ \sqrt{k} (-\cosh \chi \sin \chi + \sinh \chi) & \cos \chi \cosh \chi \end{pmatrix}$$

where quadrupole lens rigidity

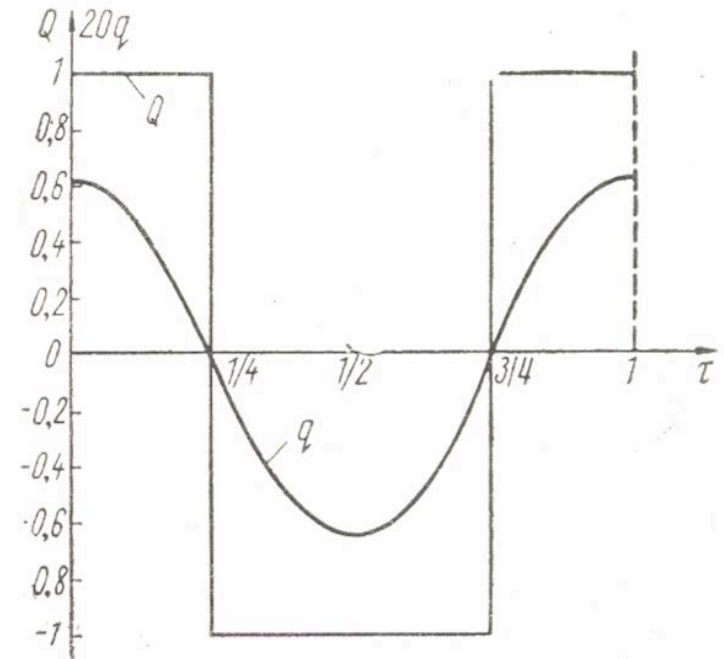
$$\chi = D \sqrt{\frac{qG_o}{m\gamma\beta c}}$$

Phase advance per cell

$$\cos \mu_o = \cos \chi \cosh \chi$$

Condition for stability of transverse oscillations

$$-1 \leq \cos \chi \cosh \chi \leq 1$$



Variation of gradient along FD focusing structure.

Higher Stability Regions (cont.)

The first area of stability $0 \leq \chi \leq 1.873$

Second area of stability $4.694 \leq \chi \leq 4.73$

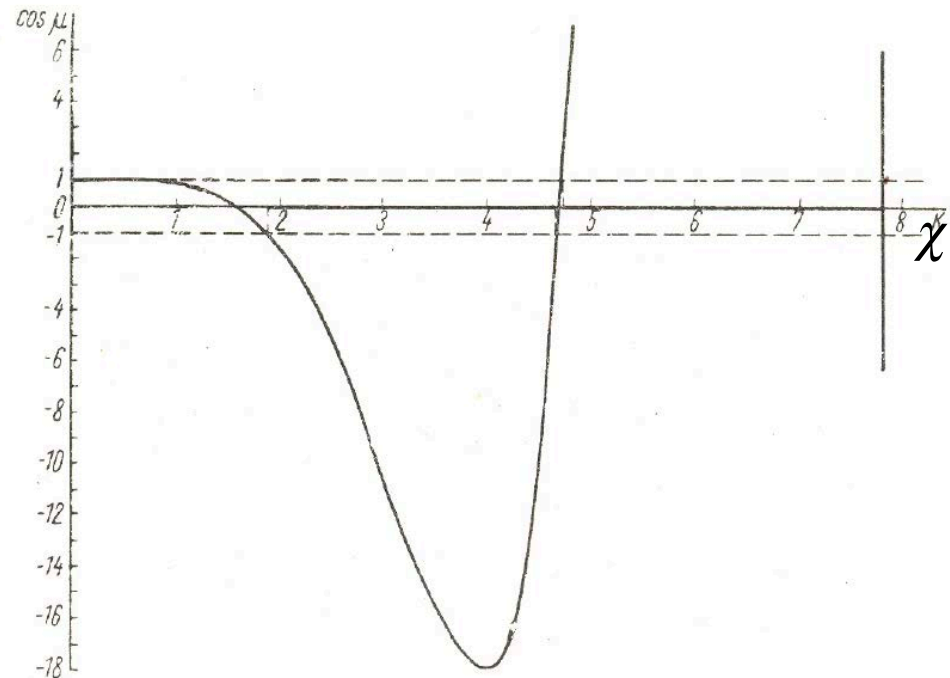
Higher order stability regions are placed around $\cos \chi = 0$, or

$$\chi_n = \frac{\pi}{2}(2n-1), \quad n = 2, 3, 4, \dots$$

Bandwidth of stability regions can be approximately estimated as

$$\Delta\chi_n = \frac{2}{\cosh\left[\frac{\pi}{2}(2n-1)\right]}$$

Stability areas $-1 < \cos \mu_o < 1$ versus quadrupole lens rigidity.



Areas of stability drop quickly with number n . In practice, only first stability area is used for focusing.

Matrix of Thin RF Gap

Change of particle slope in RF gap:

$$\Delta \frac{dr}{dz} \approx \frac{qE_{in}r}{2m\gamma^3 v_{in}^2} \left(\frac{\Delta E}{E_{in}} - 2 \frac{\Delta v}{v_{in}} \right) \approx \frac{qr\Delta E}{2m\gamma^3 v^2}$$

Change of RF field while particle crossing the gap:

$$\Delta E = -2E_g \sin \varphi \sin \frac{\pi g}{\beta \lambda}$$

Transverse matrix of thin RF gap

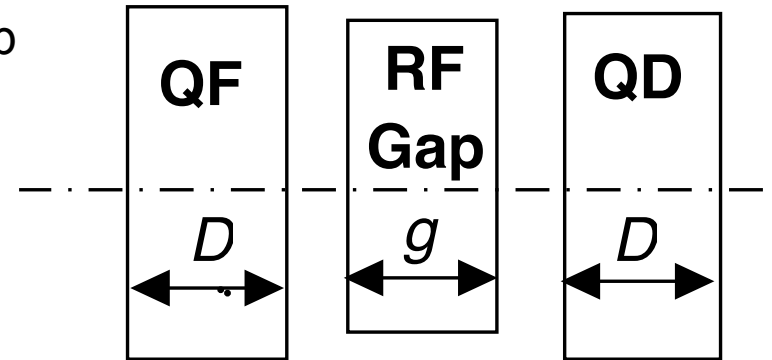
$$\begin{pmatrix} x \\ x' \end{pmatrix} = \begin{pmatrix} 1 & 0 \\ -\frac{qUT\pi \sin \varphi}{mc^2 \beta^3 \gamma^3 \lambda} & 1 \end{pmatrix} \begin{pmatrix} x_o \\ x'_o \end{pmatrix}$$

Focal length f of RF gap is determined by:

$$\frac{1}{f} = -\frac{qUT\pi \sin \varphi}{mc^2 \beta^3 \gamma^3 \lambda}$$

Focusing Structure Including RF Gap

Consider FOD focusing structure including RF gap
(focusing period $S = 2D$, $g \ll D$):



Transfer matrix through focusing period
(neglecting drift spaces between elements):

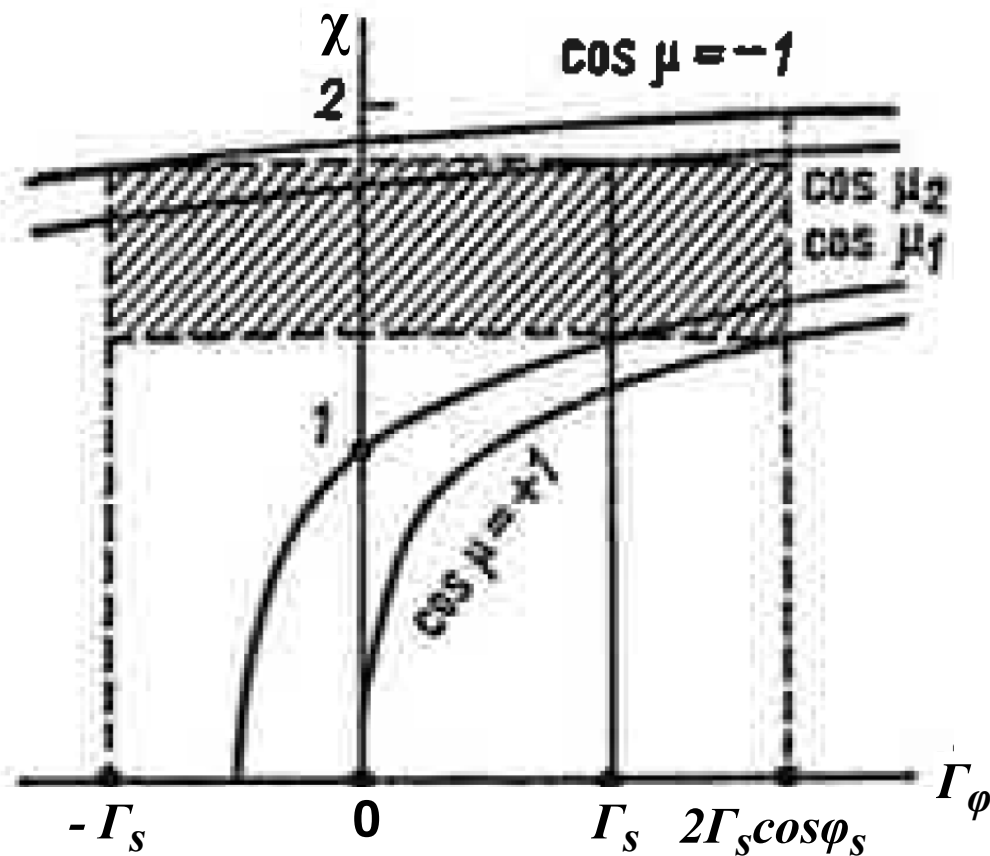
$$\begin{pmatrix} x \\ x' \end{pmatrix} = \begin{pmatrix} \cosh \chi & \frac{1}{\sqrt{k}} \sinh \chi \\ \sqrt{k} \sinh \chi & \cosh \chi \end{pmatrix} \begin{pmatrix} 1 & 0 \\ \frac{1}{f} & 1 \end{pmatrix} \begin{pmatrix} \cos \chi & \frac{1}{\sqrt{k}} \sin \chi \\ -\sqrt{k} \sin \chi & \cos \chi \end{pmatrix} \begin{pmatrix} x_o \\ x'_o \end{pmatrix}$$

Phase advance per period: $\cos \mu = \cos \chi \cosh \chi + \frac{D}{f} \frac{\sin \chi \cosh \chi + \cos \chi \sinh \chi}{2\chi}$

Defocusing factor Γ_φ :

$$\frac{D}{f} = \left(\frac{\pi S \Omega}{\beta \lambda \omega} \right)^2 \frac{\sin \varphi}{|\sin \varphi_s|} = \Gamma_\varphi$$

Smith-Gluckstern Stability Diagram



Transverse stability is provided for area restricted by curves:

$$\cos \mu = -1, \quad \cos \mu = 1$$

Longitudinal stability is provided for phases within separatrix:

$$2\varphi_s < \varphi < -\varphi_s$$

Defocusing factor is varied within

$$-\Gamma_s < \Gamma_\varphi < 2\Gamma_s \cos \varphi_s$$

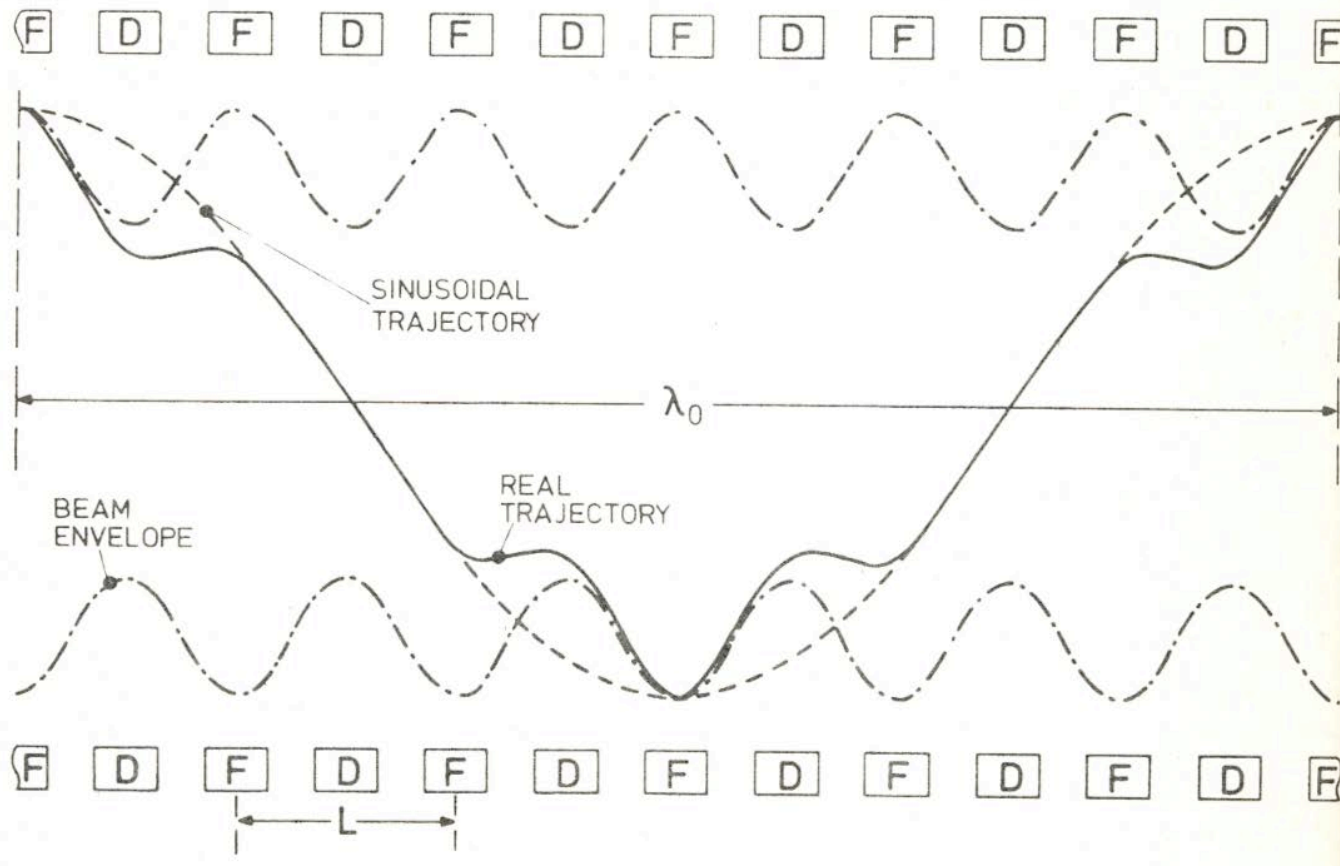
where defocusing factor for synchronous phase

$$\Gamma_s = \left(\frac{\pi S \Omega}{\beta \lambda \omega} \right)^2$$

Stable area is shaded. For synchronous particle:

$$\cos \mu_1 < \cos \mu_s < \cos \mu_2$$

Averaging Method for Particle Trajectory



(Solid line) actual particle trajectory and (dashed line) the sine approximation to that trajectory.

Motion in Fast Oscillating Field (L.Landau, E.Lifshitz, “Mechanics”)

Consider one-dimensional particle motion in the combination of constant field $U(x)$ and fast oscillating field

$$f(x,t) = f_1(x) \cos \omega t + f_2(x) \sin \omega t$$

Fast oscillations means that frequency $\omega \gg \frac{1}{T}$, where T is the time period for particle motion in the constant field U only. Equation of particle motion:

$$m \frac{d^2 x}{dt^2} = -\frac{dU}{dx} + f_1 \cos \omega t + f_2 \sin \omega t$$

Let us express expected solution is a combination of slow variable $X(t)$ and fast oscillation $\xi(t)$:

$$x(t) = X(t) + \xi(t)$$

where $|\xi(t)| \ll |X(t)|$

Fields can be expressed as:

$$U(x) = U(X) + \frac{dU}{dX} \xi$$

$$f(x) = f(X) + \frac{df}{dX} \xi$$

Small Fast Oscillating Term

Substitution of the expected solution into equation of motion gives:

$$m\ddot{X} + m\ddot{\xi} = -\frac{dU}{dX} - \xi \frac{d^2U}{dX^2} + f(X,t) + \xi \frac{df}{dX}$$

For fast oscillating term: $m\ddot{\xi} = f(X,t)$

After integration:

$$\xi = -\frac{f}{m\omega^2}$$

Let us average all terms over time, where averaging means mean value over period $T = \frac{2\pi}{\omega}$

$$\langle g(t) \rangle = \frac{1}{T} \int_0^T g(t) dt$$

$$\langle m\ddot{X} \rangle + \langle m\ddot{\xi} \rangle = -\langle \frac{dU}{dX} \rangle - \langle \xi \frac{d^2U}{dX^2} \rangle + \langle f(X,t) \rangle + \langle \xi \frac{df}{dX} \rangle$$

Average value of $\xi(t)$ at the period of $T = \frac{2\pi}{\omega}$ is zero, while function $X(t)$ is changing slowly during that time. Taking into account that

$$\langle \ddot{X} \rangle \approx \ddot{X} \quad \langle \ddot{\xi} \rangle = 0$$

Effective Potential of Averaged Motion

$$m\ddot{X} = -\frac{dU}{dX} + \left\langle \xi \frac{df}{dX} \right\rangle = -\frac{dU}{dX} - \frac{1}{m\omega^2} \left\langle f \frac{df}{dX} \right\rangle$$

Taking into account that

$$\left\langle f \frac{df}{dX} \right\rangle = \frac{1}{2} \left\langle \frac{df^2}{dX} \right\rangle$$

$$\left\langle \frac{df^2}{dX} \right\rangle = \frac{1}{2} \left(\frac{df_1^2}{dX} + \frac{df_2^2}{dX} \right)$$

equation for slow particle motion is

$$m\ddot{X} = -\frac{dU_{eff}}{dX}$$

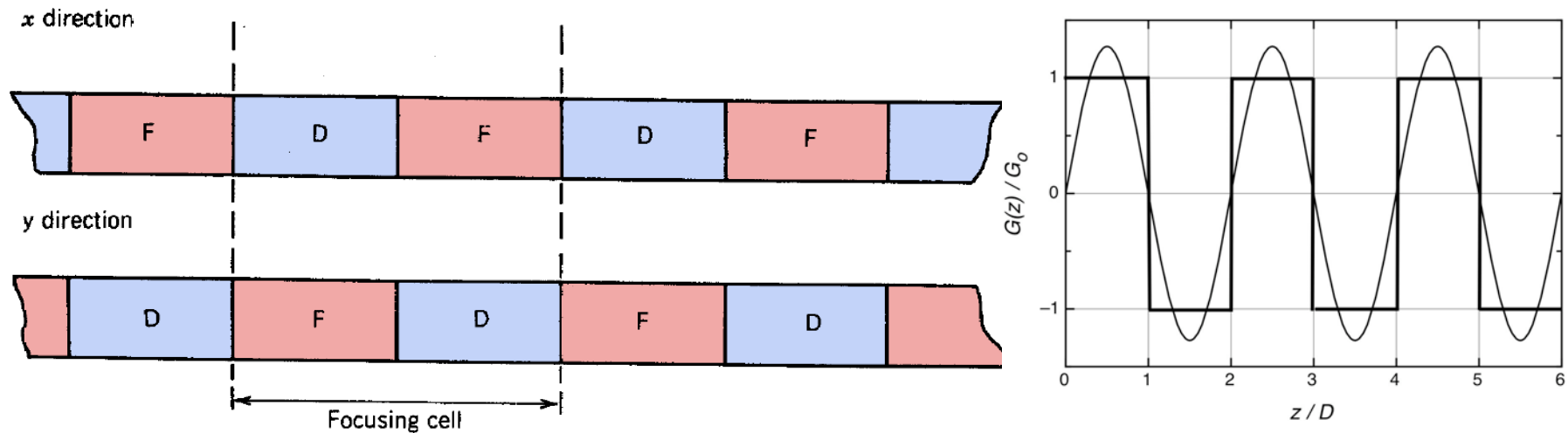
where effective potential is

$$U_{eff} = U + \frac{1}{4m\omega^2} (f_1^2 + f_2^2)$$

Averaging Method for FD Focusing Structure

Consider periodic FD structure of quadrupole lenses with length of $D = S/2$, and field gradient in each lens G_o . In FD structure, focusing-defocusing lenses follow each other without any gap. Let us expand focusing function $G(z)$ in Fourier series:

$$G(z) = \frac{4G_o}{\pi} \left[\sin\left(\frac{\pi z}{D}\right) + \frac{1}{3} \sin\left(\frac{3\pi z}{D}\right) + \frac{1}{5} \sin\left(\frac{5\pi z}{D}\right) + \dots \right]$$



FD focusing structure and approximation of field gradient.

Averaged Particle Trajectory in FD Channel

Let us keep only first term:

$$m \frac{d^2 x}{dt^2} = x \frac{q}{\gamma} \frac{4G_o}{\pi} \beta c \sin\left(\frac{\pi\beta c}{D} t\right)$$

Equation of particle motion in fast oscillating field

$$m \frac{d^2 x}{dt^2} = f_1(x) \sin \omega t$$

$$f_1 = x \frac{q}{\gamma} \frac{4G_o}{\pi} \beta c \quad \omega = \frac{\pi\beta c}{D}$$

can be substituted by slow motion in an effective potential

$$U_{\text{eff}} = \frac{f_1^2}{4m\omega^2} = \frac{4}{m} \left(\frac{q}{\gamma} \frac{G_o D}{\pi^2}\right)^2 X^2$$

Equation for slow particle motion

$$m\ddot{X} = -\frac{dU_{\text{eff}}}{dX}$$

can be written as

$$\frac{d^2 X}{dt^2} + \Omega_r^2 X = 0$$

where frequency of transverse oscillations

$$\Omega_r = \frac{q}{\gamma m} \frac{2\sqrt{2}G_o D}{\pi^2}$$

Phase Advance per FD Period

After substitution $t \rightarrow z$ equation for transverse oscillations is

$$\frac{d^2 X}{dz^2} + \left(\frac{\Omega_r}{\beta c}\right)^2 X = 0$$

Averaged particle trajectory

$$X = X_o \sin\left(\frac{\Omega_r}{\beta c} z + \Phi_{ox}\right)$$

Phase advance of slow oscillations per period S

$$\mu_o = \frac{\Omega_r}{\beta c} S$$

Phase advance of slow oscillations in FD channel per period $S = 2D$

$$\mu_o = \frac{q}{\gamma m} \frac{4\sqrt{2}G_o D^2}{\pi^2 \beta c}$$

Taking into account, that $\frac{4\sqrt{2}}{\pi^2} \approx \frac{1}{\sqrt{3}}$ the phase advance can be written

$$\mu_o = \frac{1}{\sqrt{3}} \frac{qG_o D^2}{m\gamma\beta c}$$

(This result can be obtained exactly if we take all terms in FD expansion)

Compare with matrix method for FODO period with $S = 2D$:

$$\mu_o = \frac{S}{2D} \sqrt{1 - \frac{4}{3} \frac{D}{S} \frac{qG_o D^2}{m\gamma\beta c}} = \frac{1}{\sqrt{3}} \frac{qG_o D^2}{m\gamma\beta c}$$

Averaging method gives the same result for smoothed phase advance as matrix method.

Averaged Particle Dynamics in a Quadrupole Focusing Channel

Equation of motion in x- and y- directions

$$\frac{d^2 x}{dz^2} + k(z)x = 0$$

$$\frac{d^2 y}{dz^2} - k(z)y = 0$$

where focusing function $k(z) = \frac{qG(z)}{mc\beta\gamma}$

are substituted by averaged trajectories

$$\frac{d^2 X}{dz^2} + \left(\frac{\mu_o}{S}\right)^2 X = 0$$

$$\frac{d^2 Y}{dz^2} + \left(\frac{\mu_o}{S}\right)^2 Y = 0$$

Fast oscillating term is substituted as:

$$k(z) = \frac{qG(z)}{mc\beta\gamma} \rightarrow \left(\frac{\mu_o}{S}\right)^2$$

Particle Trajectory in Averaging Method

Equation for fast component: $\xi = -\frac{f}{m\omega^2}$

$$\xi = -x \frac{q}{\gamma m} \frac{4G_o D^2}{\pi^3 \beta c} \sin\left(\frac{\pi \beta c}{D} t\right)$$

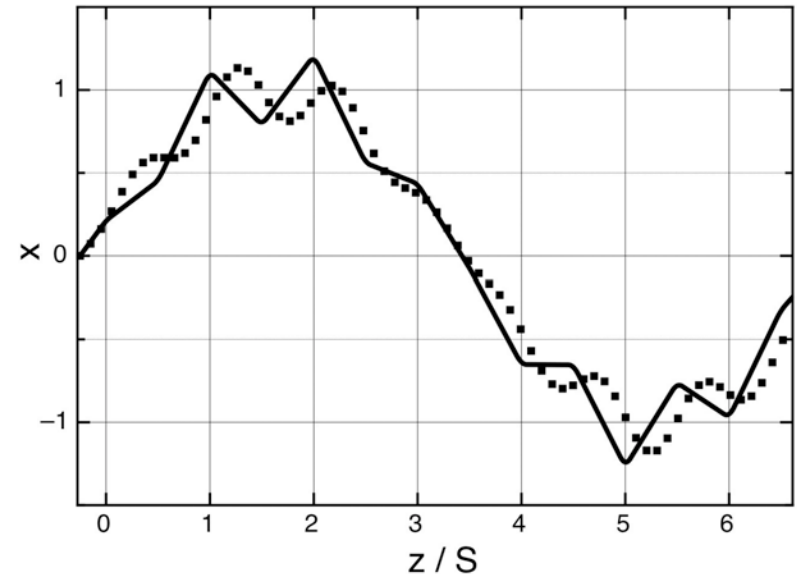
Relative amplitude of small fast oscillations in FD structure:

$$v_{\max} = \frac{\xi_{\max}}{x} = \frac{4\sqrt{3}}{\pi^3} \mu_o = 0.223\mu_o$$

Solution of equation of motion in averaged approximation ($\tau = z / S$) :

$$x = X_o \sin(\mu_o \tau + \Phi_{ox})(1 + v_{\max} \sin 2\pi\tau)$$

$$y = Y_o \sin(\mu_o \tau + \Phi_{oy})(1 - v_{\max} \sin 2\pi\tau)$$



(Solid) particle trajectory in quadrupole channel and (dotted) approximation by averaging method.

Averaging Method for Trajectory in FODO Channel

Fourier expansion of field gradient

$$G(z) = \frac{4G_o}{\pi} \sum_{m=1}^{\infty} \frac{(-1)^{m-1}}{2m-1} \sin\left[(2m-1)\pi \frac{D}{S}\right] \sin\left[2\pi(2m-1)\frac{z}{S}\right]$$

Smoothed phase advance per FODO period (compare with matrix method)

$$\mu_o = \sqrt{2} \frac{qG_o S^2}{\pi^2 m\gamma \beta c} \sqrt{\sum_{m=1}^{\infty} \frac{\sin^2\left[(2m-1)\pi \frac{D}{S}\right]}{(2m-1)^4}}$$

$$\sum_{m=1}^{\infty} \frac{\sin^2\left[(2m-1)\pi \frac{D}{L}\right]}{(2m-1)^4} = \frac{\pi^4}{8} \left(\frac{D}{S}\right)^2 \left(1 - \frac{4}{3} \frac{D}{S}\right)$$

$$\mu_o = \frac{S}{2D} \sqrt{1 - \frac{4}{3} \frac{D}{S}} \frac{qG_o D^2}{m\gamma \beta c}$$

Amplitude of small oscillation term

$$v_{\max} = \frac{2}{\pi^2} \frac{\sin\left(\pi \frac{D}{S}\right)}{\sqrt{1 - \frac{4}{3} \frac{D}{S}}} \frac{\left(\pi \frac{D}{S}\right)}{S} \mu_o \approx \frac{2}{\pi^2} \mu_o = 0.2026 \mu_o$$

for $D \ll S$

Transverse Dynamics Including RF Field

Equation of transverse motion in traveling wave:

$$\frac{dp_r}{dt} = q(E_r - \beta c B_\theta) = -q \frac{E}{\gamma} I_1\left(\frac{k_z r}{\gamma}\right) \sin \varphi$$

For near-axis particles $I_1\left(\frac{k_z r}{\gamma}\right) \approx \frac{k_z r}{2\gamma}$
transverse equation of motion in RF traveling wave

$$\frac{d^2 x}{dt^2} = -\frac{qE\pi \sin \varphi}{m\lambda\beta\gamma^3} x$$

Transverse equation of motion in quadrupole structure and RF traveling wave

$$\frac{d^2 x}{dt^2} = -\left[\frac{q\beta c}{m\gamma} G(z) + \frac{qE\pi \sin \varphi}{m\lambda\beta\gamma^3}\right] x$$

Smooth approximation to transverse motion

$$\frac{d^2 X}{dt^2} = -\Omega_r^2 X - \frac{qE\pi \sin \varphi}{m\lambda\beta\gamma^3} X$$

Frequency of smoothed oscillations

$$\Omega_r = \mu_o \frac{\beta c}{S}$$

Transverse-Longitudinal Coupling

Let us express

$$\sin \varphi = \sin(\varphi_s + \psi) \approx \sin \varphi_s + \psi \cos \varphi_s = \sin \varphi_s (1 + \psi \operatorname{ctg} \varphi_s)$$

Smoothed transverse oscillations in focusing and RF field

$$\frac{d^2 X}{dt^2} + \left[\Omega_r^2 - \frac{\Omega^2}{2} (1 + \psi \operatorname{ctg} \varphi_s) \right] X = 0$$

Frequency of longitudinal oscillations:

$$\Omega^2 = \frac{2\pi}{\lambda} \frac{qE}{m} \frac{|\sin \varphi_s|}{\beta \gamma^3}$$

Non-synchronous particle performs longitudinal oscillations with amplitude Φ and longitudinal frequency Ω :

$$\psi = -\Phi \sin(\Omega t + \psi_o)$$

Transverse equation of motion can be rewritten as

$$\frac{d^2 X}{dt^2} + X \left[\Omega_{rs}^2 - \frac{\Omega^2}{2} \operatorname{ctg} \varphi_s \Phi \sin(\Omega t + \psi_o) \right] = 0$$

Transverse oscillation frequency of synchronous particle

$$\Omega_{rs}^2 = \Omega_r^2 - \frac{\Omega^2}{2}$$

Phase advance of synchronous particle at the period of focusing structure in RF field

$$\mu_s = \mu_o \sqrt{1 - \frac{\mu_{ol}^2}{2\mu_o^2}}$$

Parametric Resonance in RF Field

Selecting $\Omega t = 2\pi\tau$ transverse oscillation in RF field becomes

$$\frac{d^2 X}{d\tau^2} + \pi^2 \left[\left(\frac{2\Omega_{rs}}{\Omega} \right)^2 - 2\Phi |\text{ctg}\varphi_s| \sin 2\pi\tau \right] X = 0$$

Parameters of Mathieu equation

$$a = \left(\frac{2\Omega_{rs}}{\Omega} \right)^2$$

$$q = \Phi |\text{ctg}\varphi_s| \approx \frac{\varphi_s}{\text{tg}\varphi_s}$$

Parametric resonance occurs when $a = n^2$

$$\Omega_{rs} = \frac{n}{2}\Omega, \quad n = 1, 2, 3$$

Regions of parametric instability

$$\frac{\sqrt{b_n}}{2} < \frac{\Omega_{rs}}{\Omega} < \frac{\sqrt{a_n}}{2}$$

where for the first two regions of instability, $n = 1, 2$, the parameters a_n, b_n are

$$a_1 = 1 + q - \frac{q^2}{8} - \frac{q^3}{64} \qquad b_1 = 1 - q - \frac{q^2}{8} + \frac{q^3}{64}$$

$$a_2 = 4 + \frac{5q^2}{12} - \frac{763q^4}{13824} \qquad b_2 = 4 - \frac{q^2}{12} + \frac{5q^4}{13824}$$

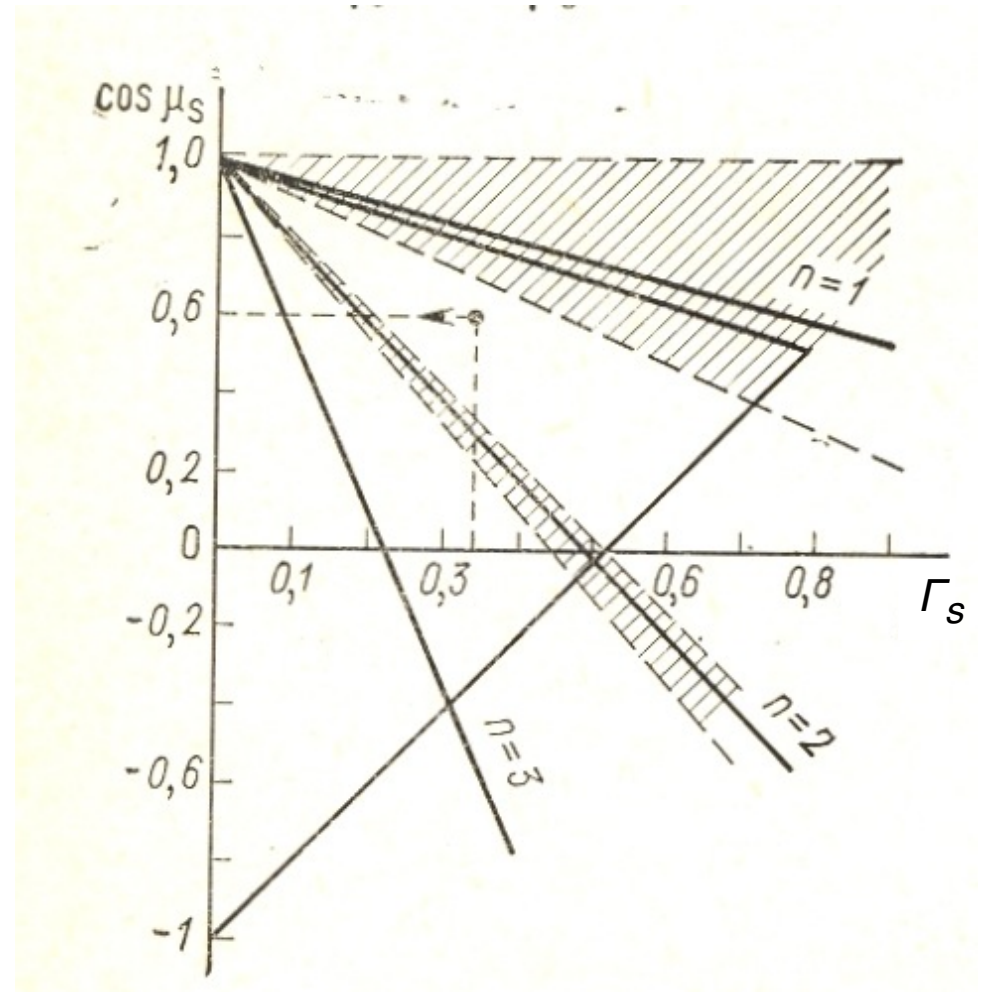
Regions of Parametric Resonance

Phase advance for synchronous particle

in RF field
$$\mu_s = \Omega_{rs} \frac{S}{\beta c}$$

Defocusing factor
$$\Gamma_s = \left(\frac{\pi S \Omega}{\beta \lambda \omega} \right)^2$$

In linac, the transverse oscillation frequency is typically larger than the longitudinal oscillation frequency, and the first parametric resonance instability region is avoided. The potentially dangerous region in this case is the second parametric resonance bandwidth where $n = 2$. Instabilities of higher-order resonance regions are typically unimportant.



Parametric resonance regions.

Experimental Observation of Parametric Resonance

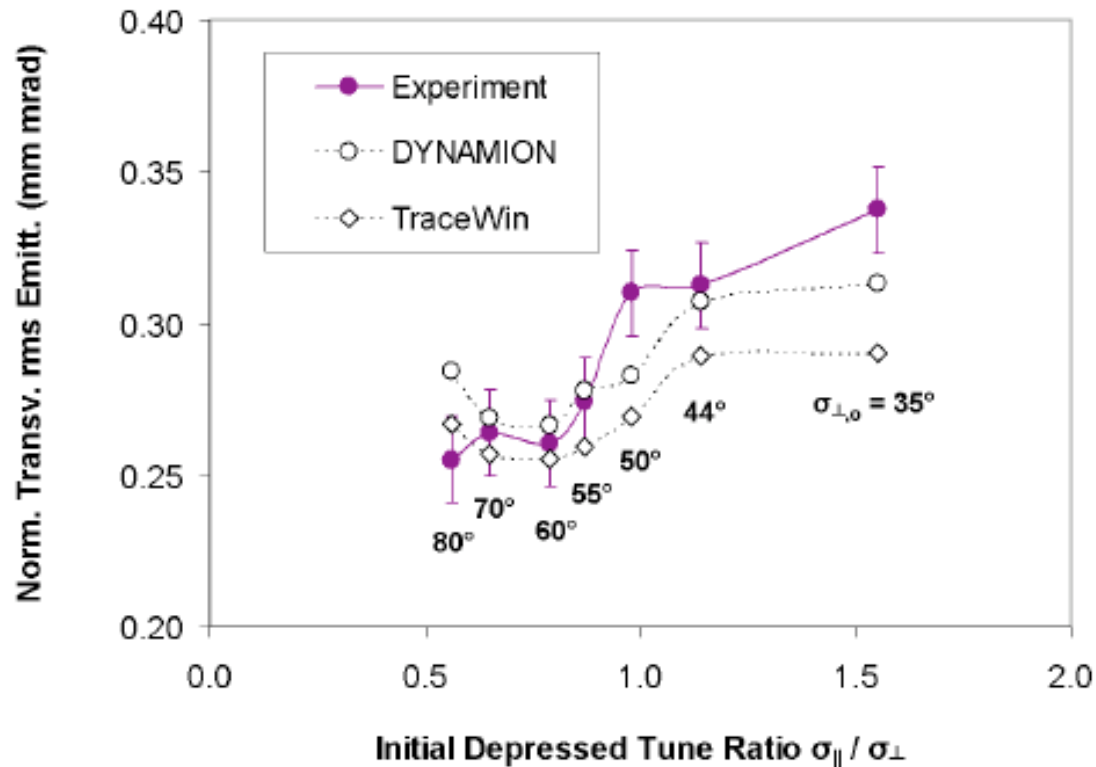
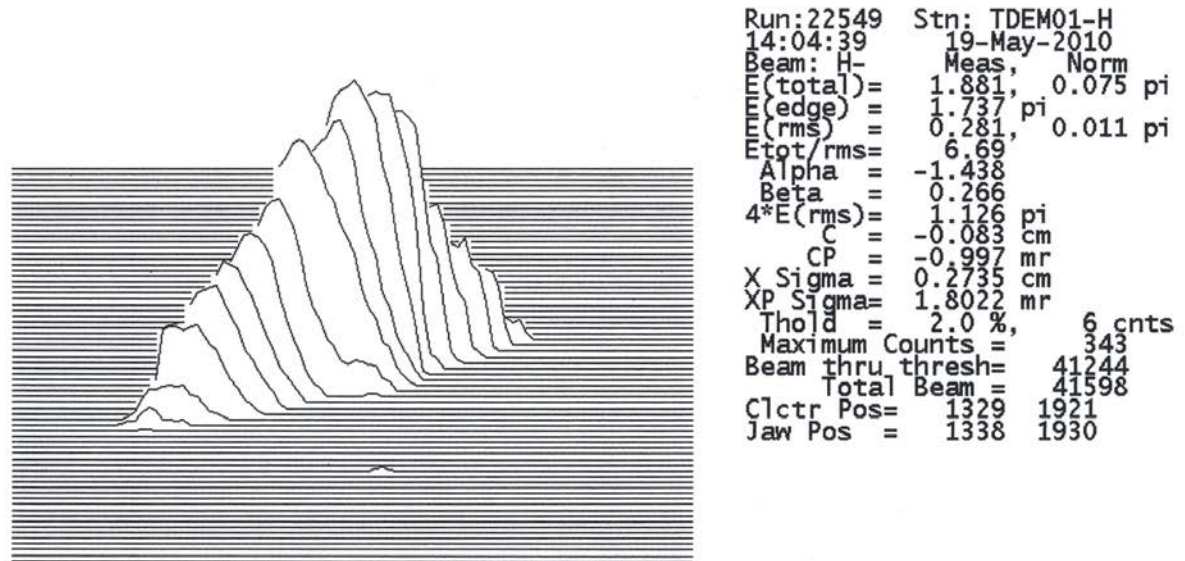
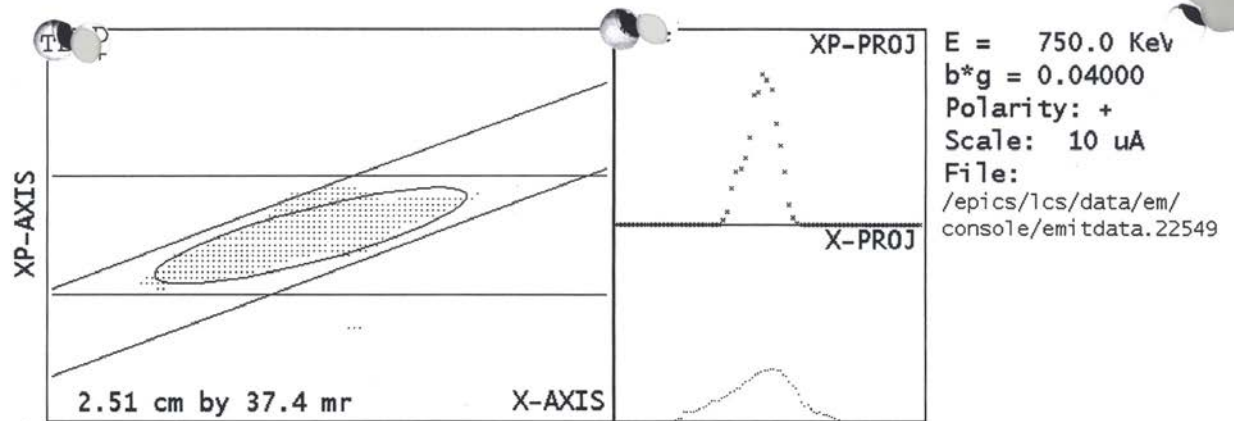


Figure 8: Mean of horizontal and vertical rms emittance at the DTL exit as a function of the initial ratio of depressed longitudinal and transverse phase advance.

Statistical Description of Beams

Realistic beam is characterized by certain distribution in phase space. In order to apply theory to real beams, the concept of moments of distribution function is used.



Realistic beam distribution in phase space.

Statistical Description of Beams (cont.)

Consider a beam with a distribution function $f(\vec{x}, \vec{P}, t)$ and let $g(\vec{x}, \vec{P}, t)$ be an arbitrary function of position, momentum, and time. The average value of the function $g(\vec{x}, \vec{P}, t)$ is defined as:

$$\langle g \rangle = \frac{\int_{-\infty}^{\infty} \int_{-\infty}^{\infty} g(\vec{x}, \vec{P}, t) f(\vec{x}, \vec{P}, t) d\vec{x} d\vec{P}}{\int_{-\infty}^{\infty} \int_{-\infty}^{\infty} f(\vec{x}, \vec{P}, t) d\vec{x} d\vec{P}}$$

The integral in the denominator is just the total number of particles. Now, let us consider some examples of physically significant average values. For $g(\vec{x}, \vec{P}, t) = x$, the average value

$$\langle x \rangle = \bar{x} = \frac{1}{N} \int_{-\infty}^{\infty} \int_{-\infty}^{\infty} x f(\vec{x}, \vec{P}, t) d\vec{x} d\vec{P}$$

gives the center of gravity of the beam in the x -direction.

Moments of Distribution Function

Analogously, for $g(\vec{x}, \vec{P}, t) = (x - \bar{x})^2$, the average value of x^2 is defined as

$$\langle x^2 \rangle = \frac{1}{N} \int_{-\infty}^{\infty} \int_{-\infty}^{\infty} (x - \bar{x})^2 f(\vec{x}, \vec{P}, t) d\vec{x} d\vec{P}$$

and is called the mean-square value of x . Similarly, the mean-square value of transverse canonical momentum P_x is defined as

$$\langle P_x^2 \rangle = \frac{1}{N} \int_{-\infty}^{\infty} \int_{-\infty}^{\infty} (P_x - \bar{P}_x)^2 f(\vec{x}, \vec{P}, t) d\vec{x} d\vec{P}$$

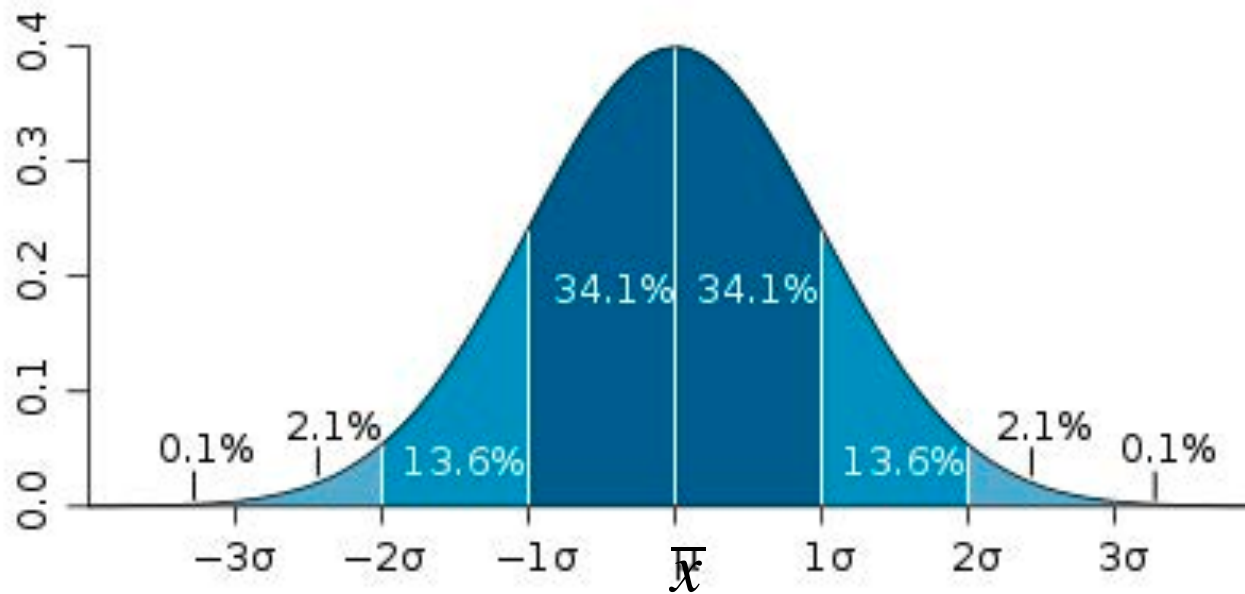
The correlation between variables x and P_x is given by the following expression taking $g(\vec{x}, \vec{P}, t) = (x - \bar{x})(P_x - \bar{P}_x)$:

$$\langle xP_x \rangle = \frac{1}{N} \int_{-\infty}^{\infty} \int_{-\infty}^{\infty} (x - \bar{x})(P_x - \bar{P}_x) f(\vec{x}, \vec{P}, t) d\vec{x} d\vec{P}$$

Gaussian Distribution

$$\frac{dN}{dx} = \frac{1}{\sqrt{2\pi\sigma}} \exp\left[-\frac{(x-\bar{x})^2}{2\sigma^2}\right]$$

$$\sigma = \sqrt{\langle x^2 \rangle}$$



Root-Mean-Square (RMS) Beam Emittance

The following combination of second moments of distribution function is called the root-mean-square beam emittance:

$$\vartheta_{rms} = \sqrt{\langle x^2 \rangle \langle x'^2 \rangle - \langle xx' \rangle^2}$$

and the normalized root-mean-square beam emittance is given by

$$\varepsilon_{rms} = \frac{1}{mc} \sqrt{\langle x^2 \rangle \langle P_x^2 \rangle - \langle xP_x \rangle^2}$$

By the reasons discussed below, beam emittance is adopted as the value, four times large than rms emittance

$$\vartheta = 4 \sqrt{\langle x^2 \rangle \langle x'^2 \rangle - \langle xx' \rangle^2}$$

Distributions with Elliptical Symmetry

The density of particles in phase space, normalized by the total number of particles N , is described by a distribution function $\rho_x(x, x')$, which is an integral of the beam distribution function over the remaining variables:

$$\rho_x(x, x') = \frac{1}{N} \int_{-\infty}^{\infty} \int_{-\infty}^{\infty} \int_{-\infty}^{\infty} \int_{-\infty}^{\infty} f(x, x', y, y', z, z') dy dz dz'$$

It is convenient to consider distributions in phase space with elliptical symmetry:

$$\rho_x(x, x') = \rho_x(\gamma_x x^2 + 2\alpha_x x x' + \beta_x x'^2)$$

Such distributions have particle densities, $\rho_x(x, x')$, that are constant along concentric ellipses

$$r_x^2 = \gamma_x x^2 + 2\alpha_x x x' + \beta_x x'^2$$

but are different from ellipse to ellipse, so one can write $\rho_x(x, x') = \rho_x(r_x^2)$. Namely, equation this describes a family of similar ellipses, which differ from each other by their areas.

Rms Beam Parameters

Using transformation

$$\sigma = \sqrt{\beta} \quad \sigma' = -\frac{\alpha}{\sqrt{\beta}}$$

the ellipse equation can be rewritten as

$$r_x^2 = (x\sigma_x' - x'\sigma_x)^2 + \left(\frac{x}{\sigma_x}\right)^2$$

Let us calculate rms beam parameters and rms beam emittance for an arbitrary function $\rho_x(x, x')$. We begin by changing variables:

$$\begin{cases} \frac{x}{\sigma_x} = r_x \cos\varphi \\ x\sigma_x' - x'\sigma_x = r_x \sin\varphi \end{cases}$$

Now we rewrite it as

$$\begin{cases} x = r_x \sigma_x \cos\varphi \\ x' = r_x \sigma_x' \cos\varphi - \frac{r_x}{\sigma_x} \sin\varphi \end{cases}$$

The absolute value of the Jacobian of transformation gives us the volume transformation factor of the phase space element:

$$dx dx' = (abs \begin{vmatrix} \frac{\partial x}{\partial r_x} & \frac{\partial x}{\partial \varphi} \\ \frac{\partial x'}{\partial r_x} & \frac{\partial x'}{\partial \varphi} \end{vmatrix}) dr_x d\varphi = r_x dr_x d\varphi$$

Rms Beam Parameters (cont.)

Then, the rms values are:

$$\langle x^2 \rangle = \int_0^{2\pi} \int_0^{\infty} (r_x \sigma_x \cos \varphi)^2 \rho_x(r_x^2) r_x dr_x d\varphi$$

$$\langle x'^2 \rangle = \int_0^{2\pi} \int_0^{\infty} \left(r_x \sigma'_x \cos \varphi - \frac{r_x}{\sigma_x} \sin \varphi \right)^2 \rho_x(r_x^2) r_x dr_x d\varphi$$

$$\langle xx' \rangle = \int_0^{2\pi} \int_0^{\infty} r_x \sigma_x \cos \varphi \left(r_x \sigma'_x \cos \varphi - \frac{r_x}{\sigma_x} \sin \varphi \right) \rho_x(r_x^2) r_x dr_x d\varphi$$

Let us take into account previously introduced expressions:

$$\sigma = \sqrt{\beta}$$

$$\sigma' = -\frac{\alpha}{\sqrt{\beta}}$$

$$\beta\gamma - \alpha^2 = 1$$

Rms Beam Ellipse

Calculation of integrals over φ gives:

$$\langle x^2 \rangle = \pi \beta_x \int_0^\infty r_x^3 \rho_x(r_x^2) dr_x$$

$$\langle x'^2 \rangle = \pi \gamma_x \int_0^\infty r_x^3 \rho_x(r_x^2) dr_x$$

$$\langle x x' \rangle = -\pi \alpha_x \int_0^\infty r_x^3 \rho_x(r_x^2) dr_x$$

Therefore, four-rms beam emittance is given by

$$\varepsilon = \pi \int_0^\infty r_x^3 \rho_x(r_x^2) dr_x$$

Twiss parameters

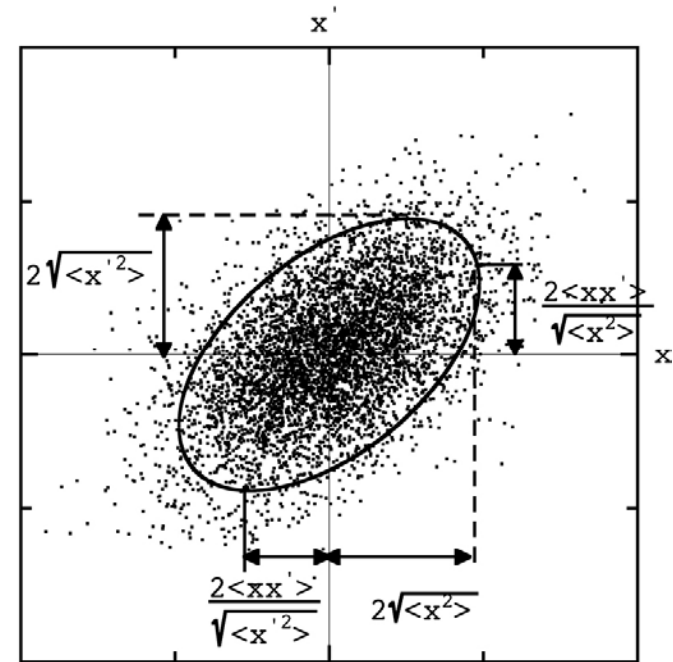
$$\alpha_x = -\frac{\langle x x' \rangle}{\varepsilon_x}$$

$$\beta_x = \frac{\langle x^2 \rangle}{\varepsilon_x}$$

$$\gamma_x = \frac{\langle x'^2 \rangle}{\varepsilon_x}$$

Rms beam ellipse

$$\frac{\langle x'^2 \rangle}{\varepsilon_x} x^2 - 2 \frac{\langle x x' \rangle}{\varepsilon_x} x x' + \frac{\langle x^2 \rangle}{\varepsilon_x} x'^2 = \varepsilon_x$$



Beam distribution and rms ellipse.

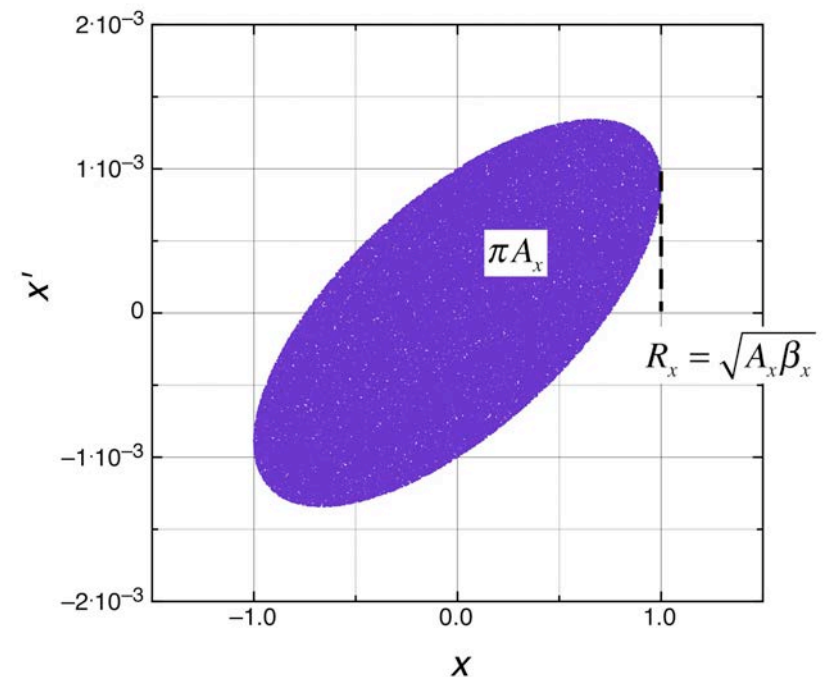
Example: Uniformly Populated Ellipse

Consider an example, where the beam ellipse has an area of πA_x , and is uniformly populated by particles. Particle density is constant inside the ellipse $r_x^2 = A_x$:

$$\rho_x(r_x^2) = \frac{1}{\pi A_x}$$

Calculation of the rms value, $\langle x^2 \rangle$, gives:

$$\langle x^2 \rangle = \pi \beta_x \int_0^{\sqrt{A_x}} r_x^3 \rho_x(r_x^2) dr_x = \frac{A_x \beta_x}{4}$$



Uniformly populated ellipse at phase plane (x, x') .

4-RMS Emittance of Uniformly Populated Ellipse

The beam boundary is given by

$$R_x = \sqrt{A_x \beta_x}$$

Radius of the beam represented as a uniformly populated ellipse is equal to twice the rms beam size:

$$R = 2 \sqrt{\langle x^2 \rangle}$$

Rms beam emittance:

$$\epsilon_x = \frac{4}{A_x} \int_0^{\sqrt{A_x}} r_x^3 dr_x = A_x$$

Therefore, the area of an ellipse, uniformly populated by particles, coincides with the 4 x rms beam emittance. This explains the choice of the coefficient 4 in the definition of rms beam emittance.

Beam with Gaussian Distribution

Particle density in the phase plane (x, x')

$$\rho_x(r_x^2) = \frac{1}{N} \frac{dN}{r_x dr_x d\phi}$$

Fraction of particles within emittance ε

$$\frac{N(\varepsilon)}{N} = \pi \int_0^{\varepsilon} \rho_x(r_x^2) dr_x^2$$

Beam with Gaussian distribution in phase space $\varepsilon_x = \text{rms emittance}$

$$\rho_x(r_x^2) = \frac{1}{2\pi \varepsilon_x} \exp\left(-\frac{r_x^2}{2 \varepsilon_x}\right)$$

Normalization condition

$$\frac{N(\infty)}{N} = \pi \int_0^{\infty} \rho_x(r_x^2) dr_x^2 = 1$$

Fraction of particles within the emittance of a Gaussian beam is:

$$\frac{N(\varepsilon)}{N} = 1 - \exp\left(-\frac{\varepsilon}{2 \varepsilon_x}\right)$$

Fraction of particles within the four-rms emittance of Gaussian beam

$$1 - \exp(-2) \approx 0.865$$

Sigma Matrix of the Beam

It is common to represent beam in 4D phase space (x, x', y, y') as an 4D ellipsoid:

$$a_{11}x^2 + a_{22}x'^2 + a_{33}y^2 + a_{44}y'^2 + 2a_{12}xx' + 2a_{13}xy + 2a_{14}xy' + 2a_{23}x'y + 2a_{24}x'y' + 2a_{34}yy' = 1$$

This equation can be written as $\vec{X}^T \vec{a} \vec{X} = 1$

where the vector of particle position in phase space

$$\vec{X} = \begin{pmatrix} x \\ x' \\ y \\ y' \end{pmatrix}$$

and \vec{a} is 4x4 symmetrical matrix of coefficients, $a_{ij}=a_{ji}$. Let us introduce inverse matrix $\vec{\sigma}^{-1} = \vec{a}$, and rewrite 4D ellipsoid equation as

$$\vec{X}^T \vec{\sigma}^{-1} \vec{X} = 1$$

where introduced sigma-matrix has the form

$$\vec{\sigma} = \begin{pmatrix} \sigma_{11} & \sigma_{12} & \sigma_{13} & \sigma_{14} \\ \sigma_{21} & \sigma_{22} & \sigma_{23} & \sigma_{24} \\ \sigma_{31} & \sigma_{32} & \sigma_{33} & \sigma_{34} \\ \sigma_{41} & \sigma_{42} & \sigma_{43} & \sigma_{44} \end{pmatrix}$$

Explicit Expression for Sigma-Matrix Equation

Explicit expression of equation for sigma-matrix $\vec{X}^T \vec{\sigma}^{-1} \vec{X} = 1$ is (4D beam ellipsoid):

$$\begin{aligned}
 F(x, x', y, y') = & \\
 & -y'^2 \sigma_{11} \sigma_{23}^2 + 2y'y \sigma_{11} \sigma_{23} \sigma_{24} - y^2 \sigma_{11} \sigma_{24}^2 - y'^2 \sigma_{12}^2 \sigma_{33} + y'^2 \sigma_{11} \sigma_{22} \sigma_{33} - 2y'x' \sigma_{11} \sigma_{24} \\
 & \sigma_{33} + 2y'x \sigma_{12} \sigma_{24} \sigma_{33} - x^2 \sigma_{24}^2 \sigma_{33} - \sigma_{14}^2 (y^2 \sigma_{22} + x' (-2y \sigma_{23} + x' \sigma_{33})) + 2y'y \sigma_{12}^2 \\
 & \sigma_{34} - 2y'y \sigma_{11} \sigma_{22} \sigma_{34} + 2y'x' \sigma_{11} \sigma_{23} \sigma_{34} - 2y'x \sigma_{12} \sigma_{23} \sigma_{34} + 2x'y \sigma_{11} \sigma_{24} \sigma_{34} - 2xy \\
 & \sigma_{12} \sigma_{24} \sigma_{34} + 2x^2 \sigma_{23} \sigma_{24} \sigma_{34} - x'^2 \sigma_{11} \sigma_{34}^2 + 2x'x \sigma_{12} \sigma_{34}^2 - x^2 \sigma_{22} \sigma_{34}^2 - 2\sigma_{14} (\sigma_{12} (y'y \\
 & \sigma_{23} - y^2 \sigma_{24} - y'x' \sigma_{33} + x'y \sigma_{34}) + x(-y' \sigma_{23}^2 + (y' \sigma_{22} - x' \sigma_{24}) \sigma_{33} - y \sigma_{22} \sigma_{34} + \sigma_{23} (y \\
 & \sigma_{24} + x' \sigma_{34})) - (y^2 \sigma_{12}^2 - \sigma_{11} (y^2 \sigma_{22} - 2x'y \sigma_{23} + x'^2 \sigma_{33}) + \sigma_{12} (-2xy \sigma_{23} + 2x'x \\
 & \sigma_{33}) + x^2 (\sigma_{23}^2 - \sigma_{22} \sigma_{33})) \sigma_{44} - \sigma_{13}^2 (y'^2 \sigma_{22} + x' (-2y' \sigma_{24} + x' \sigma_{44})) + 2 \sigma_{13} (\sigma_{14} (y' \\
 & y \sigma_{22} + x' (-y' \sigma_{23} - y \sigma_{24} + x' \sigma_{34})) + \sigma_{12} (y'^2 \sigma_{23} - y' (y \sigma_{24} + x' \sigma_{34}) + x' y \sigma_{44}) + x \\
 & (y \sigma_{24}^2 - x' \sigma_{24} \sigma_{34} + \sigma_{23} (-y' \sigma_{24} + x' \sigma_{44}) + \sigma_{22} (y' \sigma_{34} - y \sigma_{44}))) = 1 \quad (5)
 \end{aligned}$$

Projection of 4D Ellipsoid on (x-x')

Projection of ellipsoid on any plane (for example, x, x') is obtained as

$$\frac{\partial F}{\partial y}(x, x', y, y') = 0,$$

$$\frac{\partial F}{\partial y'}(x, x', y, y') = 0$$

and substitution solutions of these equations into equation for ellipsoid.

Actually, for every fixed value of x, the point at the boundary of projection corresponds to max possible value of x':

$$\frac{\partial x'}{\partial y} = 0,$$

$$\frac{\partial x'}{\partial y'} = 0$$

or, according to differentiation of implicit functions,

$$\frac{\partial x'}{\partial y} = -\frac{\frac{\partial F}{\partial y}}{\frac{\partial F}{\partial x'}},$$

$$\frac{\partial x'}{\partial y'} = -\frac{\frac{\partial F}{\partial y'}}{\frac{\partial F}{\partial x'}}.$$

Projection of 4D Ellipsoid on (x-x') (cont.)

$$\frac{\partial F}{\partial y} = -\sigma_{14}^2 (2y\sigma_{22} - 2x'\sigma_{23}) + 2y'\sigma_{11}\sigma_{23}\sigma_{24} - 2y\sigma_{11}\sigma_{24}^2 + 2y'\sigma_{12}^2\sigma_{34} - 2y'\sigma_{11}\sigma_{22}\sigma_{34} + 2x'\sigma_{11}\sigma_{24}\sigma_{34} - 2x\sigma_{12}\sigma_{24}\sigma_{34} - 2\sigma_{14}(\sigma_{12}(y'\sigma_{23} - 2y\sigma_{24} + x'\sigma_{34}) + x(\sigma_{23}\sigma_{24} - \sigma_{22}\sigma_{34})) - (2y\sigma_{12}^2 - 2x\sigma_{12}\sigma_{23} - \sigma_{11}(2y\sigma_{22} - 2x'\sigma_{23}))\sigma_{44} + 2\sigma_{13}(\sigma_{14}(y'\sigma_{22} - x'\sigma_{24}) + \sigma_{12}(-y'\sigma_{24} + x'\sigma_{44}) + x(\sigma_{24}^2 - \sigma_{22}\sigma_{44})) = 0 \quad (9)$$

$$\frac{\partial F}{\partial y'} = -2y'\sigma_{11}\sigma_{23}^2 + 2y\sigma_{11}\sigma_{23}\sigma_{24} - \sigma_{13}^2(2y'\sigma_{22} - 2x'\sigma_{24}) - 2y'\sigma_{12}^2\sigma_{33} + 2y'\sigma_{11}\sigma_{22}\sigma_{33} - 2x'\sigma_{11}\sigma_{24}\sigma_{33} + 2x\sigma_{12}\sigma_{24}\sigma_{33} - 2\sigma_{14}(\sigma_{12}(y\sigma_{23} - x'\sigma_{33}) + x(-\sigma_{23}^2 + \sigma_{22}\sigma_{33})) + 2y\sigma_{12}^2\sigma_{34} - 2y\sigma_{11}\sigma_{22}\sigma_{34} + 2x'\sigma_{11}\sigma_{23}\sigma_{34} - 2x\sigma_{12}\sigma_{23}\sigma_{34} + 2\sigma_{13}(\sigma_{14}(y\sigma_{22} - x'\sigma_{23}) + \sigma_{12}(2y'\sigma_{23} - y\sigma_{24} - x'\sigma_{34}) + x(-\sigma_{23}\sigma_{24} + \sigma_{22}\sigma_{34})) = 0 \quad (10)$$

Solutions:

$$y = -\frac{x'\sigma_{12}\sigma_{13} + x\sigma_{13}\sigma_{22} + x'\sigma_{11}\sigma_{23} - x\sigma_{12}\sigma_{23}}{\sigma_{12}^2 - \sigma_{11}\sigma_{22}}$$

$$y' = -\frac{x'\sigma_{12}\sigma_{14} - x\sigma_{14}\sigma_{22} - x'\sigma_{11}\sigma_{24} + x\sigma_{12}\sigma_{24}}{\sigma_{12}^2 - \sigma_{11}\sigma_{22}}$$

Coefficients of Sigma-Matrix

After substitution solutions to 4D ellipsoid equation, we get projection on (x-x') plane

$$\sigma_{22}x^2 + \sigma_{11}x'^2 - 2\sigma_{12}xx' = \sigma_{11}\sigma_{22} - \sigma_{12}^2$$

This equation determines ellipse on phase plane (x,x'). Comparison with equation for rms beam ellipse, one determines coefficients in sigma – matrix:

$$\sigma_{11} = \langle x^2 \rangle \quad \sigma_{12} = \langle xx' \rangle \quad \sigma_{22} = \langle x'^2 \rangle$$

Right-hand terms determine square of area of ellipse (rms beam emittance):

$$\epsilon_{x_rms}^2 = \sigma_{11}\sigma_{22} - \sigma_{12}^2$$

Analogously, projection on x-y plane

$$\sigma_{33}x^2 + \sigma_{11}y^2 - 2\sigma_{13}xy = \sigma_{11}\sigma_{33} - \sigma_{13}^2$$

where $\sigma_{13} = \langle xy \rangle$

Explicit Expression of Sigma-Matrix

Finally, sigma-matrix is expressed through second order momentums of beam distribution

$$\vec{\sigma} = \begin{pmatrix} \langle x^2 \rangle & \langle xx' \rangle & \langle xy \rangle & \langle xy' \rangle \\ \langle xx' \rangle & \langle x'^2 \rangle & \langle x'y \rangle & \langle x'y' \rangle \\ \langle xy \rangle & \langle x'y \rangle & \langle y^2 \rangle & \langle yy' \rangle \\ \langle xy' \rangle & \langle x'y' \rangle & \langle yy' \rangle & \langle y'^2 \rangle \end{pmatrix}$$

Because of identity $\langle \xi\zeta \rangle = \langle \zeta\xi \rangle$ 10 elements in sigma-matrix are independent. Combinations of coefficients $\sigma_{ii}\sigma_{jj} - \sigma_{ij}^2$ determine area of projections of beam ellipsoid on each plane, and, therefore, must be positive. Coefficients of sigma-matrix must satisfy the following conditions:

$$\sigma_{ii} > 0$$

$$\begin{vmatrix} \sigma_{ii} & \sigma_{ij} \\ \sigma_{ij} & \sigma_{jj} \end{vmatrix} > 0 \quad i = 1, 2, 3, 4; \quad j > i$$

Evolution of Sigma-Matrix

Volume of n-dimensional ellipsoid
where $\Gamma(x)$ is the gamma-function:

$$V_n = \frac{\pi^{n/2}}{\Gamma(1 + \frac{n}{2})} \sqrt{\det \sigma}$$

For different dimensions the volume is $V_2 = \pi \sqrt{\det \sigma}$ $V_4 = \frac{\pi^2}{2} \sqrt{\det \sigma}$ $V_6 = \frac{\pi^3}{6} \sqrt{\det \sigma}$

During beam transport, beam phase space volume experiences rotation in phase space, which can be described as evolution of sigma-matrix between two points of transport channel. Initial phase space volume is determined by initial sigma-matrix:

$$\vec{X}_1^T \vec{\sigma}_1^{-1} \vec{X}_1 = 1$$

while final phase space volume is determined by $\vec{X}_2^T \vec{\sigma}_2^{-1} \vec{X}_2 = 1$

Evolution of single particle between two points is determined by R-matrix: $\vec{X}_2 = \vec{R} \vec{X}_1$

Evolution of sigma matrix is determined by

(K.Brown et al, SLAC-PUB-3381)

$$\vec{\sigma}_2 = \vec{R} \vec{\sigma}_1 \vec{R}^T$$

$$\begin{pmatrix} x_2 \\ x_2' \\ y_2 \\ y_2' \end{pmatrix} = \begin{pmatrix} R_{11} & R_{12} & R_{13} & R_{14} \\ R_{21} & R_{22} & R_{23} & R_{24} \\ R_{31} & R_{32} & R_{33} & R_{34} \\ R_{41} & R_{42} & R_{43} & R_{44} \end{pmatrix} \begin{pmatrix} x_1 \\ x_1' \\ y_1 \\ y_1' \end{pmatrix}$$

Because $\det \vec{R} = 1$, then $\det \vec{\sigma}_2 = \det \vec{\sigma}_1$ which means that phase space volume is conserved (Liouville's theorem).

Evolution of Sigma-Matrix (cont.)

Example: $(x-x')$ beam dynamics can be determined by 2x2 sigma-matrix. In this case

$$\frac{1}{\det \sigma} \begin{vmatrix} x & x' \\ \sigma_{22} & -\sigma_{12} \\ -\sigma_{21} & \sigma_{11} \end{vmatrix} \begin{vmatrix} x \\ x' \end{vmatrix} = 1$$

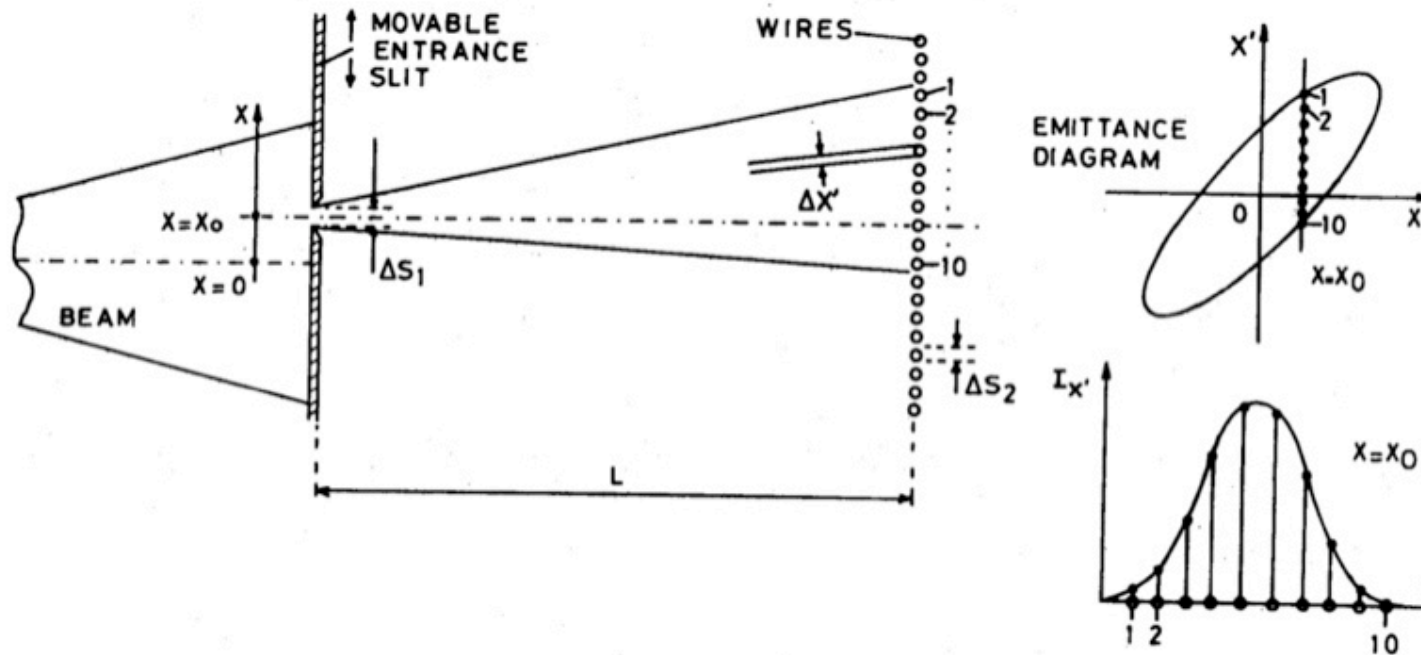
which gives equation for beam ellipse at phase plane (x, x') . Application of equation describing evolution of beam ellipse using single-particles matrix gives:

$$\begin{vmatrix} \langle x^2 \rangle & \langle xx' \rangle \\ \langle xx' \rangle & \langle x'^2 \rangle \end{vmatrix} = \begin{vmatrix} m_{11} & m_{12} \\ m_{21} & m_{22} \end{vmatrix} \begin{vmatrix} \langle x_0^2 \rangle & \langle x_0 x'_0 \rangle \\ \langle x_0 x'_0 \rangle & \langle x'^2_0 \rangle \end{vmatrix} \begin{vmatrix} m_{11} & m_{21} \\ m_{12} & m_{22} \end{vmatrix}$$

which can be written in explicit way as

$$\begin{vmatrix} \langle x^2 \rangle \\ \langle xx' \rangle \\ \langle x'^2 \rangle \end{vmatrix} = \begin{pmatrix} m_{11}^2 & 2m_{11}m_{12} & m_{12}^2 \\ m_{11}m_{21} & m_{21}m_{12} + m_{11}m_{22} & m_{22}m_{12} \\ m_{21}^2 & 2m_{21}m_{22} & m_{22}^2 \end{pmatrix} \begin{vmatrix} \langle x_0^2 \rangle \\ \langle x_0 x'_0 \rangle \\ \langle x'^2_0 \rangle \end{vmatrix}$$

Slit-Collector Beam Emittance Measurement Device

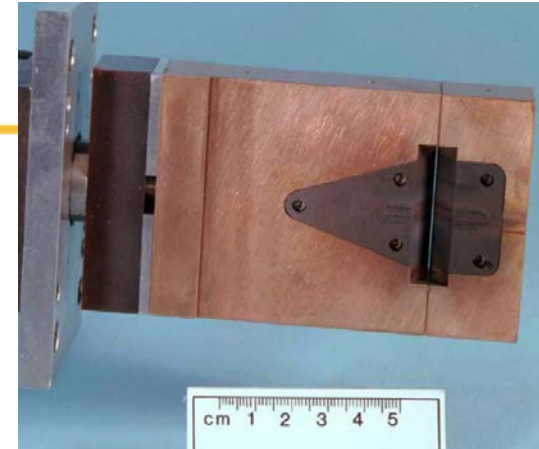


Emittance measuring device.

LANL Slits and Collectors

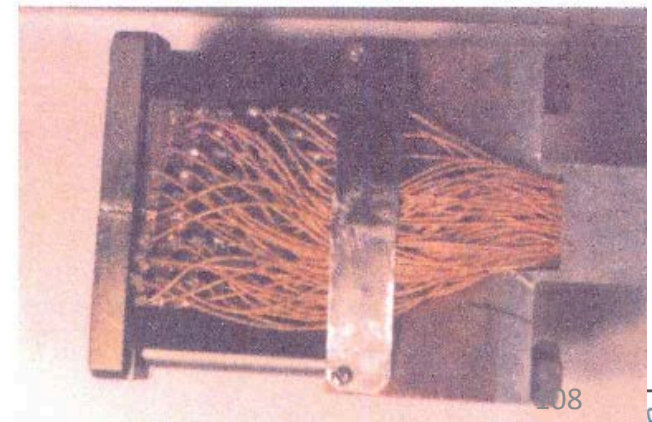
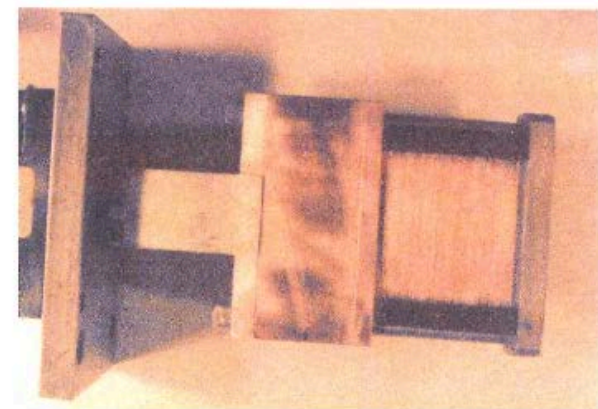
Slit: For energy < 1 MeV: water-cooled graphite with a 0.012" wide slit

For energy 100 MeV: 0.025" wide BeCu slits

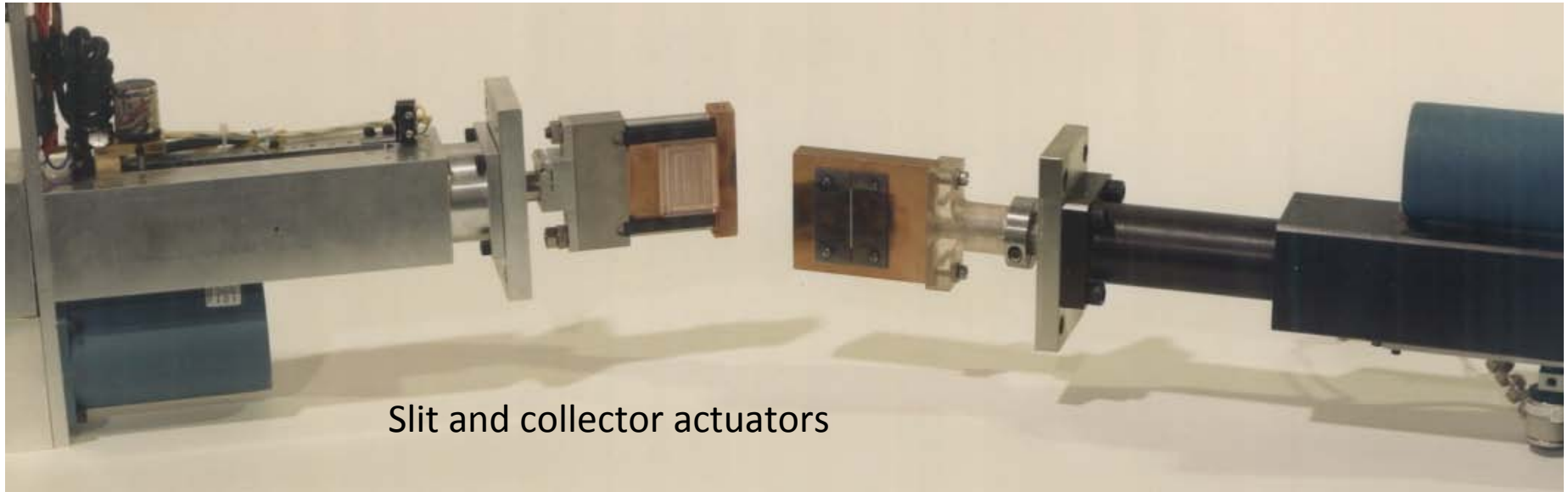


Collector:

- Low energy transport collectors
 - 70 ea. 0.016" thick copper plates.
 - 0.004" mica spacers.
 - 1.625" x 1.625" active area.
 - Take signal off downstream side.
 - Water cooled.
 - Envex (polyamide) used for rad-hard insulating material to hold assembly together.
 - Rad-hard Kapton wires used to bring signals out.
 - Advantages compared to harps: acts as beam stop, 12X more signal.



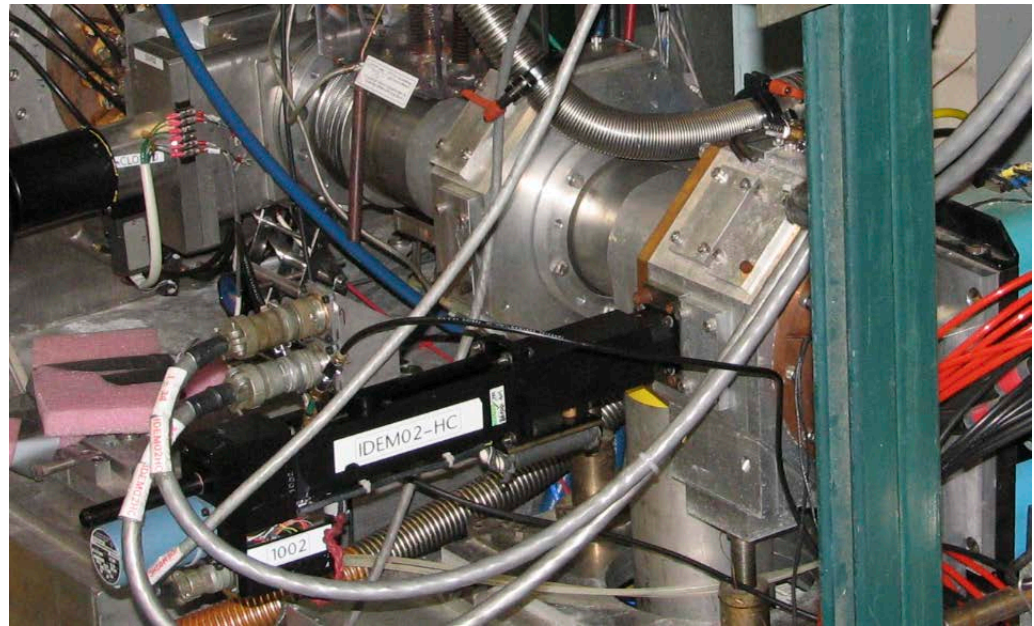
Slit and Collector Actuators



Slit and collector actuators



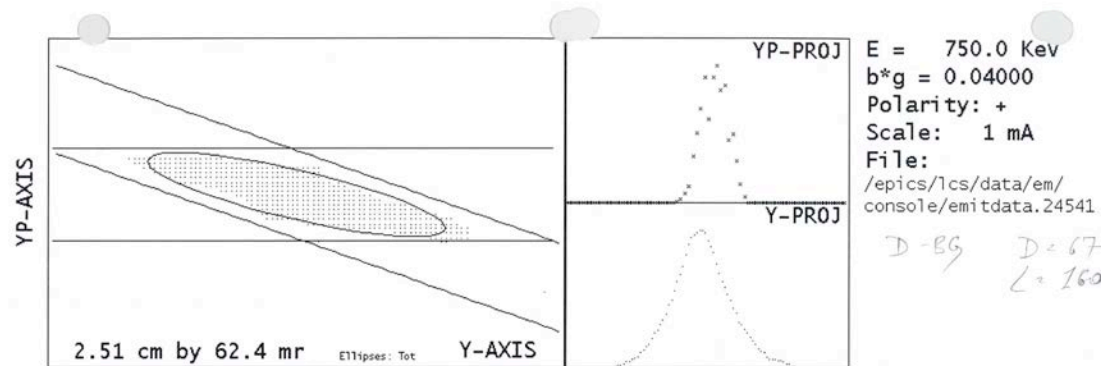
Emittance
measurement
switcher



Collector actuator in beam box

Emittance Scan and Equivalent 4-RMS Beam Ellipse

Result of measurement are two-dimensional function of intensity distribution at phase plane $I_i(x, x')$

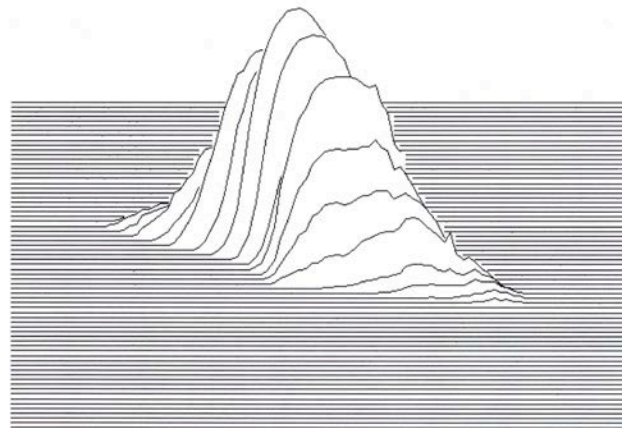


Rms beam parameters

$$\langle x^2 \rangle = \frac{1}{I} \sum_{i=1}^N (x_i - \bar{x})^2 I_i(x, x')$$

$$\langle x'^2 \rangle = \frac{1}{I} \sum_{i=1}^N (x'_i - \bar{x}')^2 I_i(x, x')$$

$$\langle xx' \rangle = \frac{1}{I} \sum_{i=1}^N (x - \bar{x})(x'_i - \bar{x}') I_i(x, x')$$



```

Run: 24541   Stn: TBEM01-V
02:45:13   09-Sep-2013
Beam: H-    Meas, Norm
I (total) = 3.635, 0.145 pi
I (edge) = 3.354 pi
E (rms) = 0.474, 0.019 pi
Etot/rms = 7.66
Alpha = 1.337
Beta = 0.150
4*E (rms) = 1.897 pi
C = -0.046 cm
CP = 1.674 mr
X Sigma = 0.2670 cm
XP Sigma = 2.9664 mr
Thold = 2.0 %, 14 cnts
Maximum Counts = 745
Beam thru thresh = 101149
Total Beam = 102966
Slit Pos = 1160 1375
Clctr Pos = 1262 1820
Slit Rate = 91, Nom. =
Clctr Rate = 238, Nom. = 227
E(ea) = 5.811, 0.232 pi
E(ea)/E(rms) = 12.252
    
```

Four-rms beam emittance: $\varepsilon = 4\sqrt{\langle x^2 \rangle \langle x'^2 \rangle - \langle xx' \rangle^2}$

Twiss rms parameters: $\alpha = -4 \frac{\langle xx' \rangle}{\varepsilon}$ $\beta = 4 \frac{\langle x^2 \rangle}{\varepsilon}$ $\gamma = 4 \frac{\langle x'^2 \rangle}{\varepsilon}$

Rms beam ellipse

$$\gamma x^2 + 2\alpha xx' + \beta x'^2 = \varepsilon$$

Allison Scanner

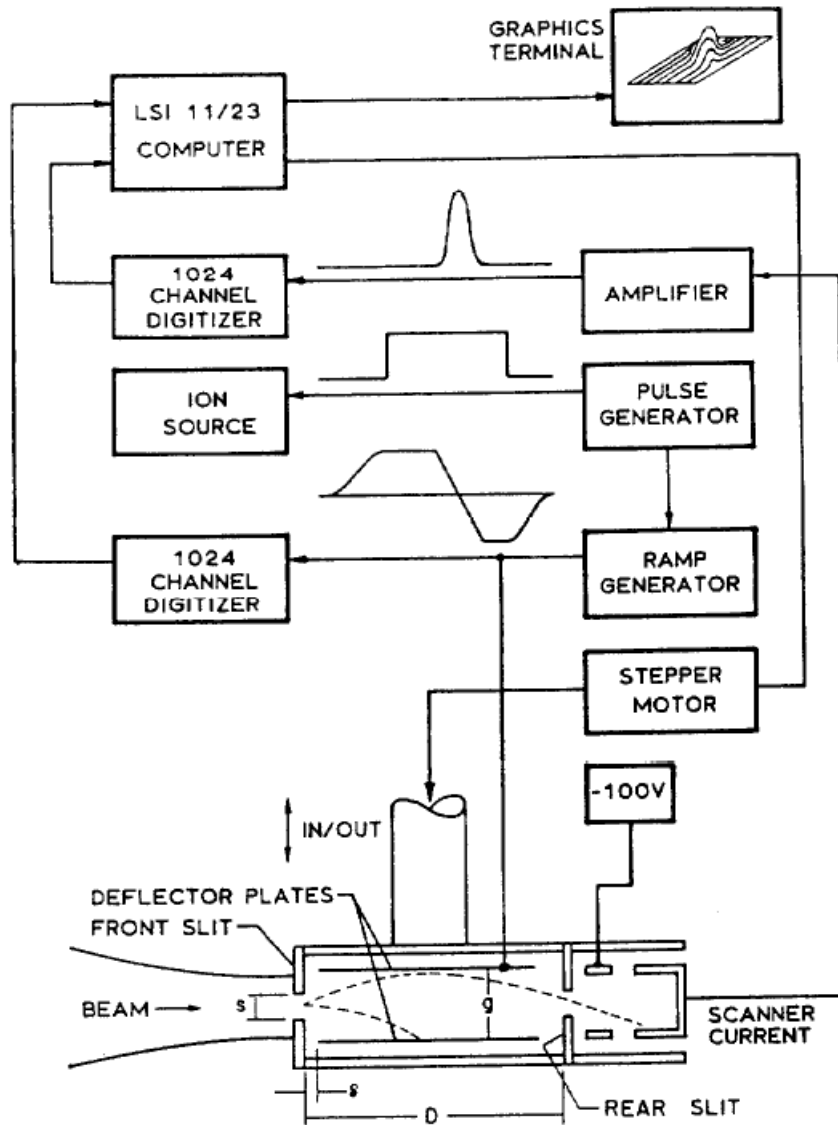


Fig. 1. Schematic of electric-sweep emittance scanner.

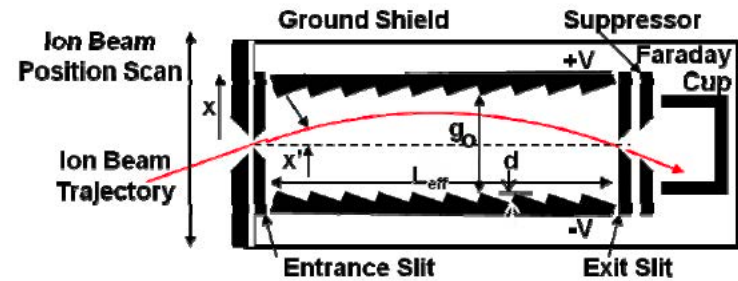
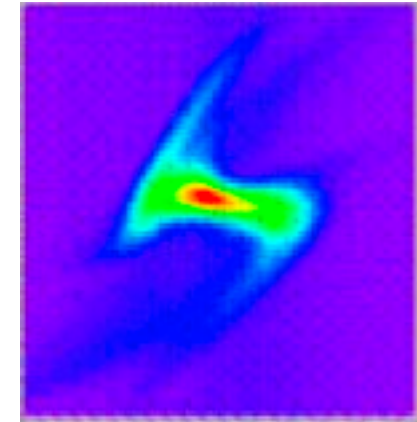
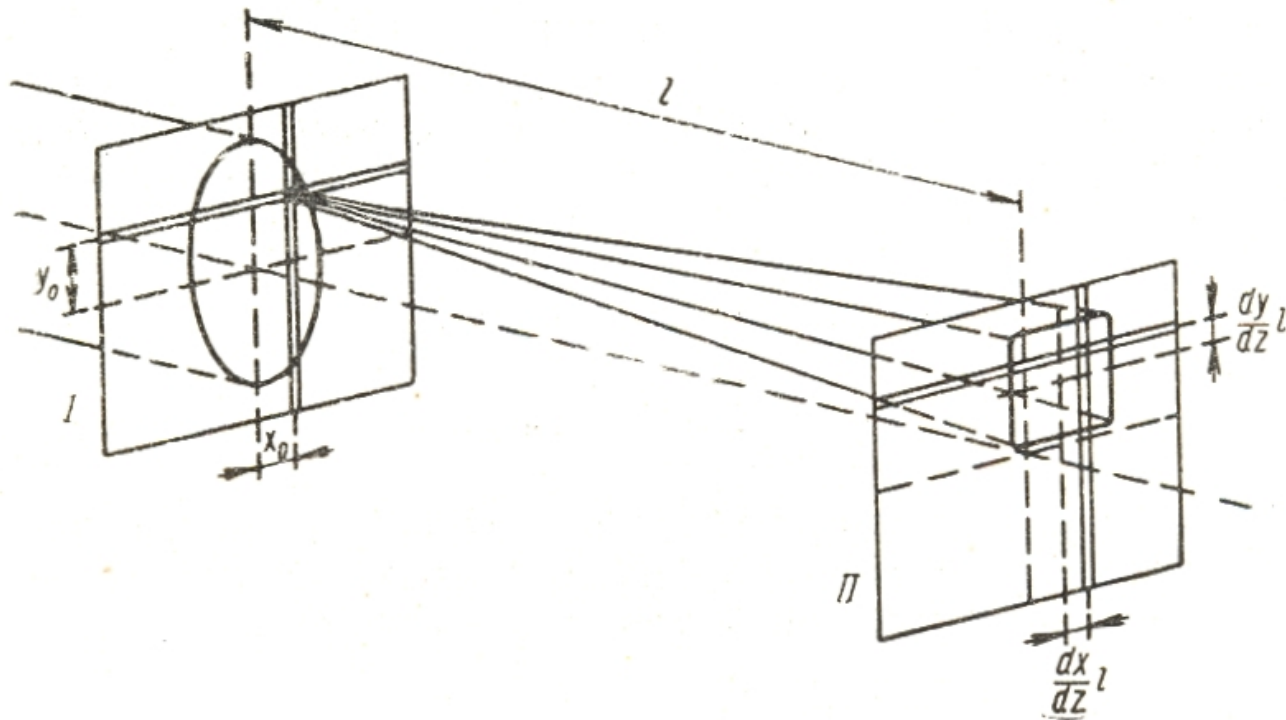


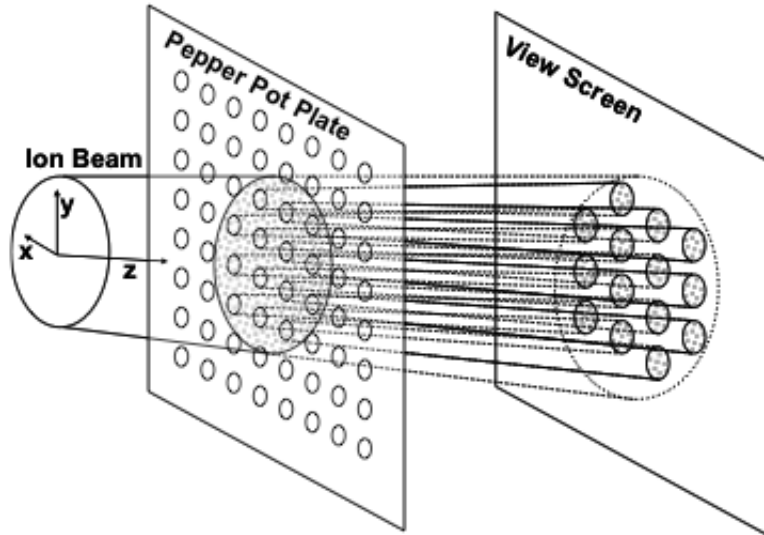
Figure 1: Schematic of SNS Allison Emittance Scanner.

Four Slits Method for 4D Phase Space Distribution

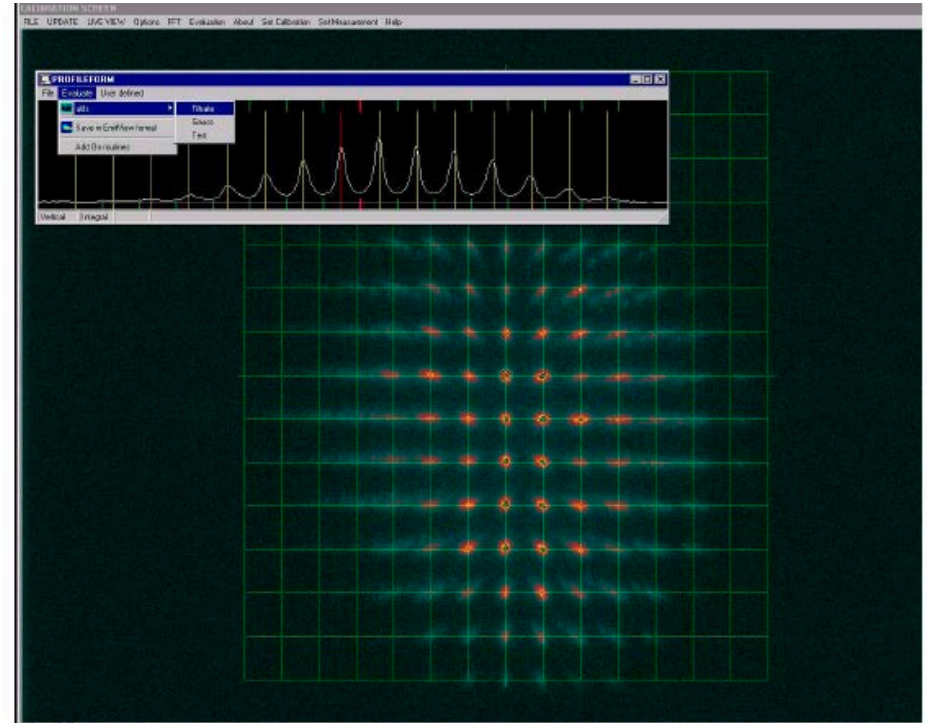
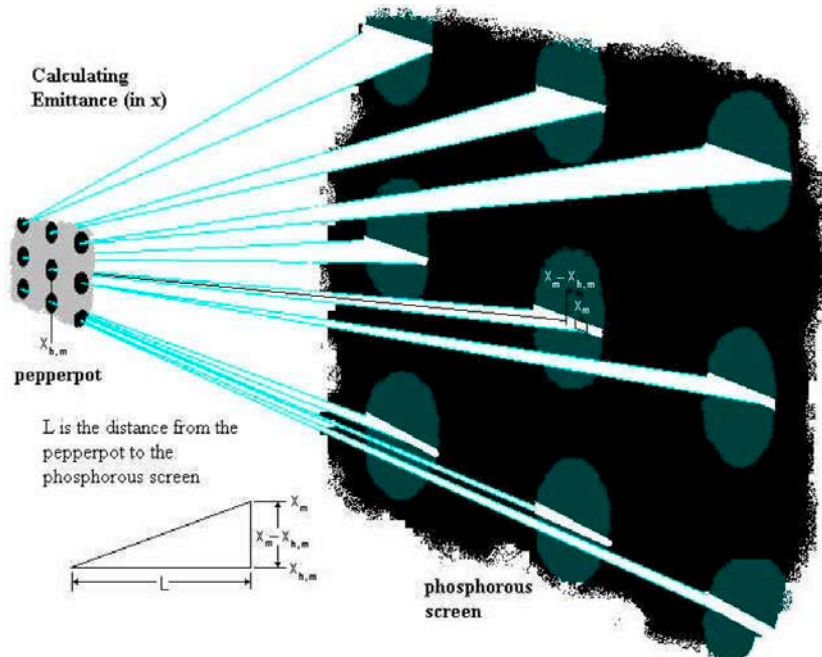


First pair of slits selects particles with coordinates x_0 , y_0 . Second pair of slits selects particles with certain angles dx/dz , dy/dz .

Pepper-Pot Method



Layout of pepper-pot method



1.4 MeV/u Ar+1 ion beam projection (P. Forck, LINAC 2000)

MEASURING THE FULL 4D TRANSVERSE BEAM MATRIX OF ION BEAMS”, M.Maier (IPAC16)

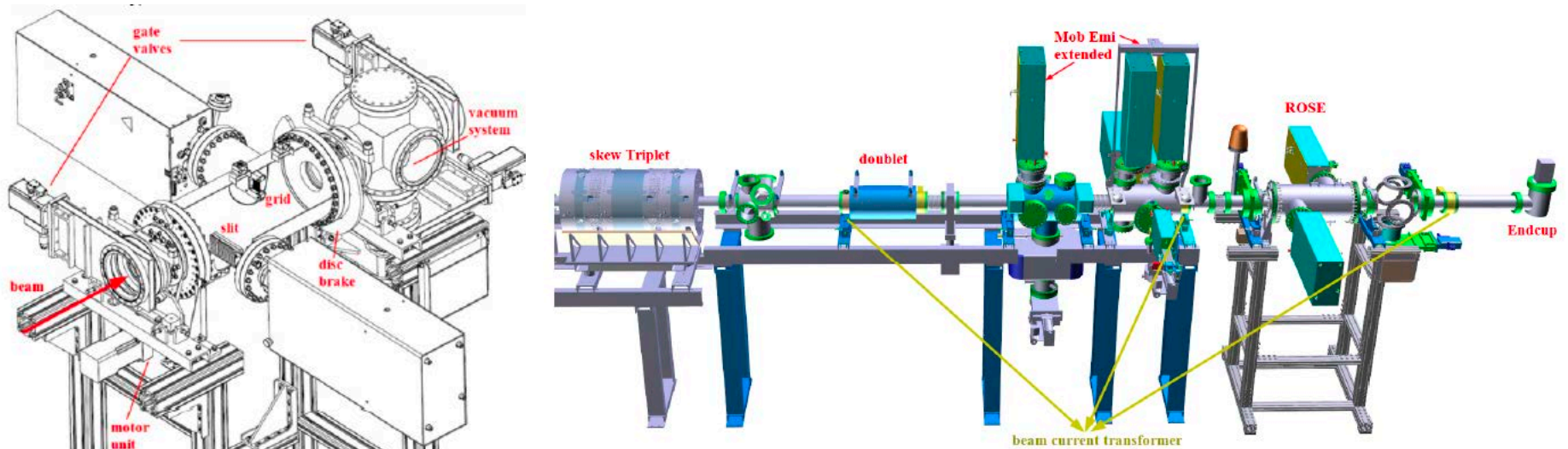


Figure 8: Experimental setup used for the ROSE commissioning.

$$C = \begin{bmatrix} XX & XX' & XY & XY' \\ X'X & X'X' & X'Y & X'Y' \\ YX & YX' & YY & YY' \\ Y'X & Y'X' & Y'Y & Y'Y' \end{bmatrix} \quad (1)$$

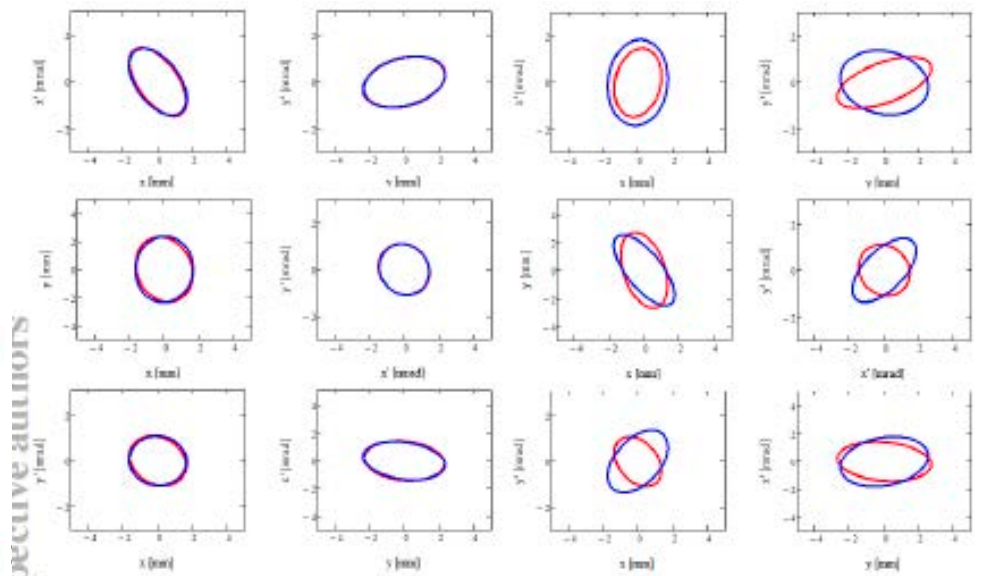
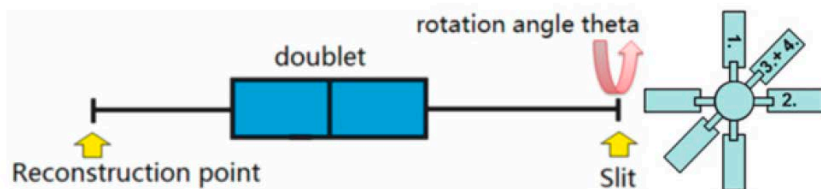
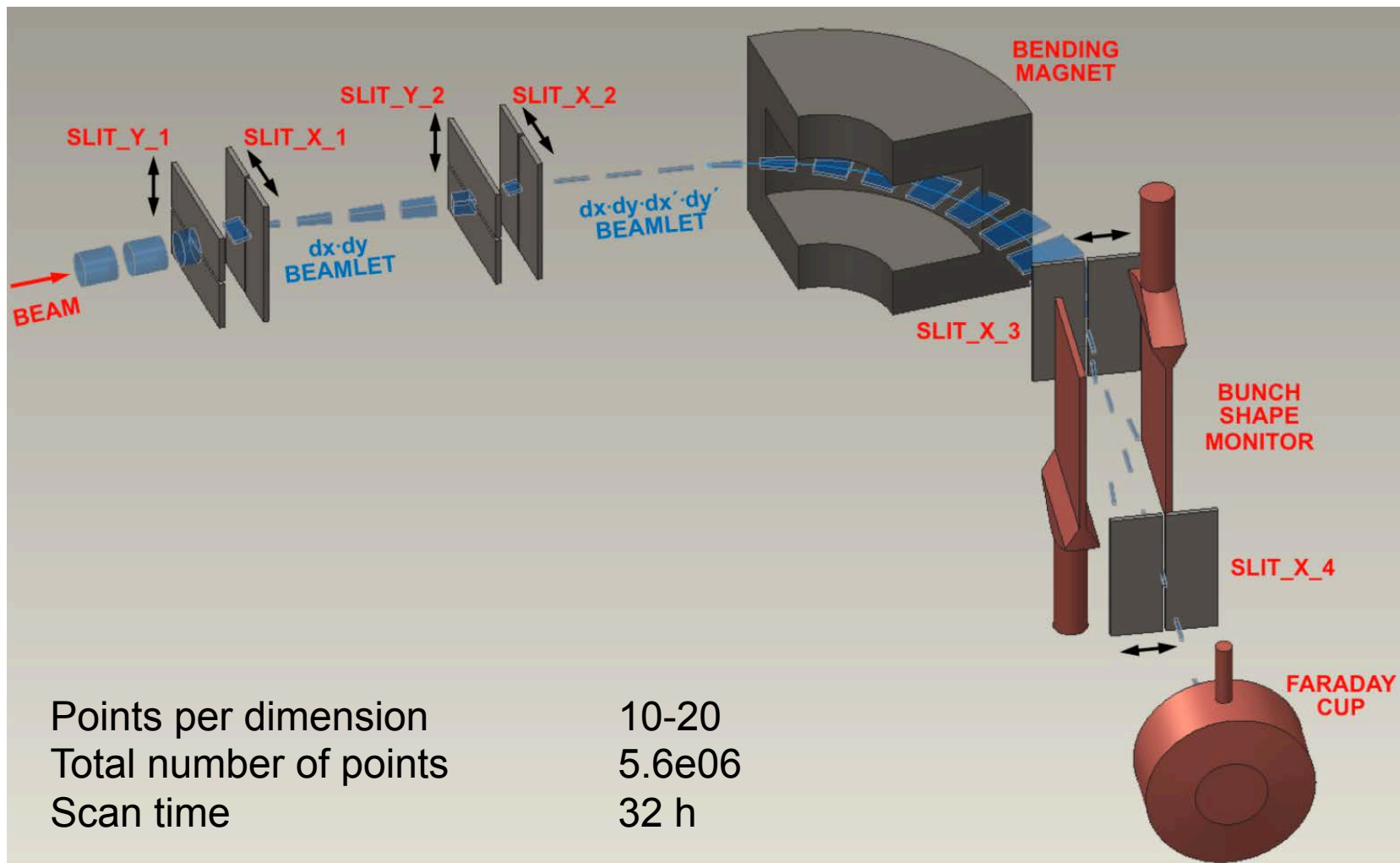


Figure 9: Experimental proof for ROSE capability to measure the 4d beam matrix.

MEASURING THE 6D BEAM DISTRIBUTION



Six-dimensional phase space measurement
(B.Cathey et al, PRL 121, 064804, 2018).

MEASURING THE 6D BEAM DISTRIBUTION (cont.)

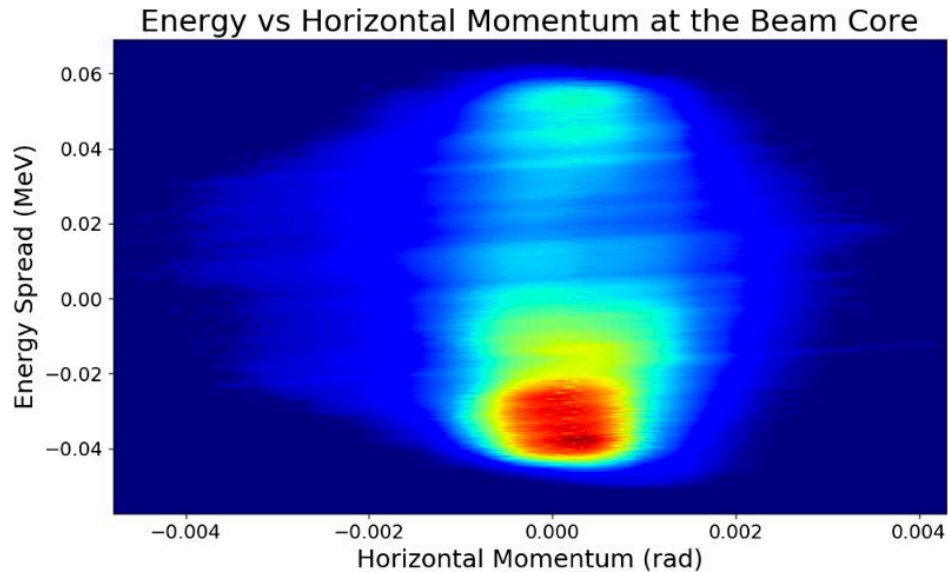


FIG. 3. A partial projection plot of the energy spread w against the horizontal momentum x' .

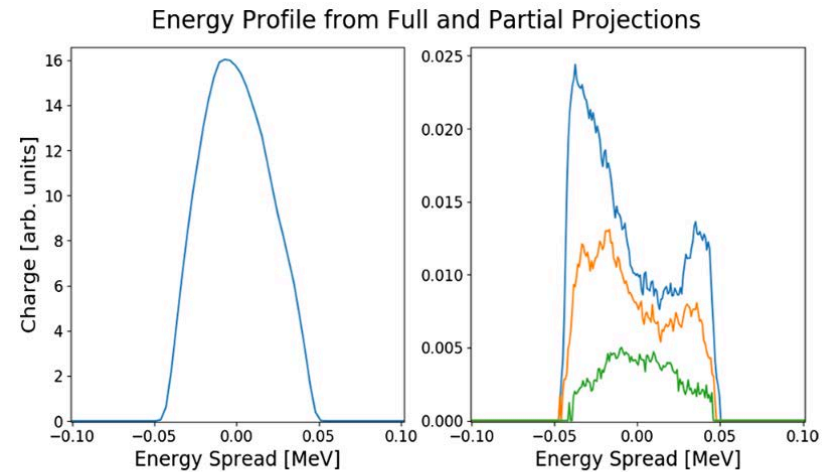
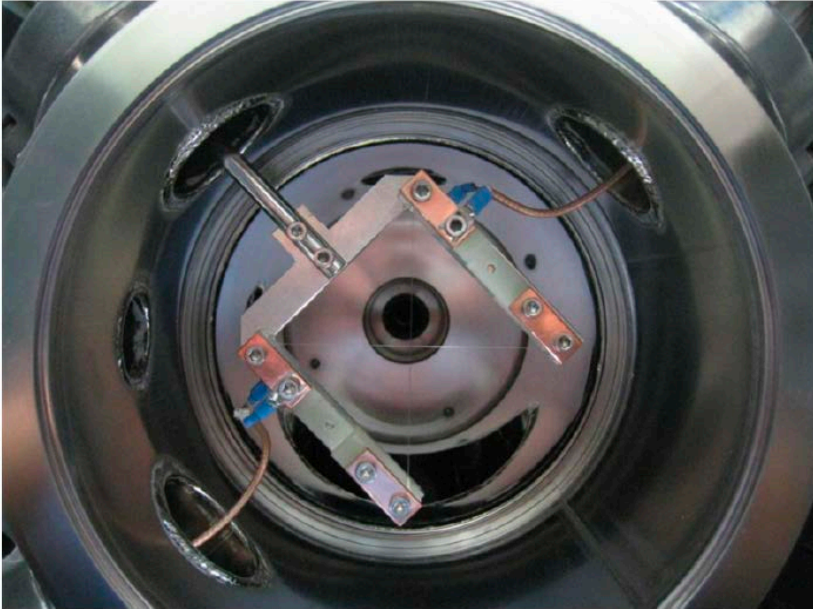


FIG. 4. Results from a 5D scan. The left plot shows the total projection of the energy spectrum. The right shows different 1D partial projections of energy with three different horizontal momenta. The blue curve's x' is about 0.2 mrad, the yellow's is about 0.7 mrad, and the green's is about 1 mrad.

Indirect Emittance Measurement: Wire Scans

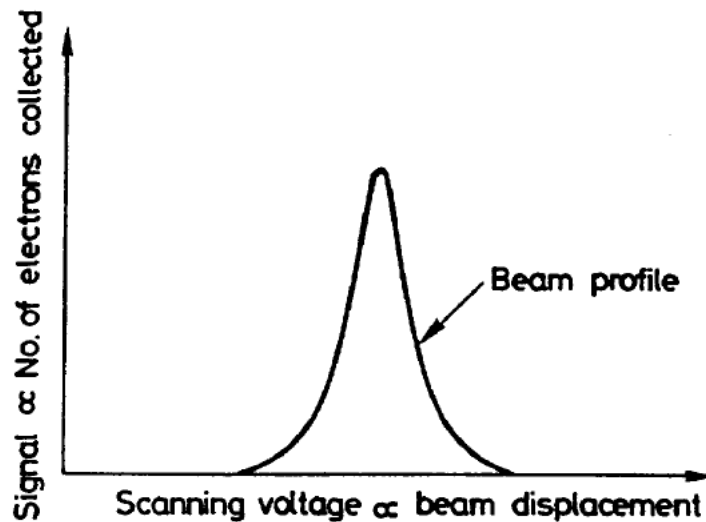


Single –particle transformation matrix

$$\begin{pmatrix} y \\ y' \end{pmatrix} = \begin{pmatrix} C & S \\ C' & S' \end{pmatrix} \begin{pmatrix} y_0 \\ y'_0 \end{pmatrix}$$

Evolution of an ellipse

$$\begin{pmatrix} \beta_1 \\ \alpha_1 \\ \gamma_1 \end{pmatrix} = \begin{pmatrix} C^2 & -2SC & S^2 \\ -CC' & SC' + S'C & -SS' \\ C'^2 & -2S'C' & S'^2 \end{pmatrix} \begin{pmatrix} \beta_0 \\ \alpha_0 \\ \gamma_0 \end{pmatrix}$$



System of equation to determine unknown values of $\alpha_0, \beta_0, \gamma_0$

$$\begin{pmatrix} R_1^2 / \vartheta \\ R_2^2 / \vartheta \\ R_3^2 / \vartheta \end{pmatrix} = \begin{pmatrix} C_1^2 & -2C_1S_1 & S_1^2 \\ C_2^2 & -2C_2S_2 & S_2^2 \\ C_3^2 & -2C_3S_3 & S_3^2 \end{pmatrix} \begin{pmatrix} \beta_0 \\ \alpha_0 \\ \gamma_0 \end{pmatrix}$$

Indirect Emittance Measurement: Wire Scans (cont.)

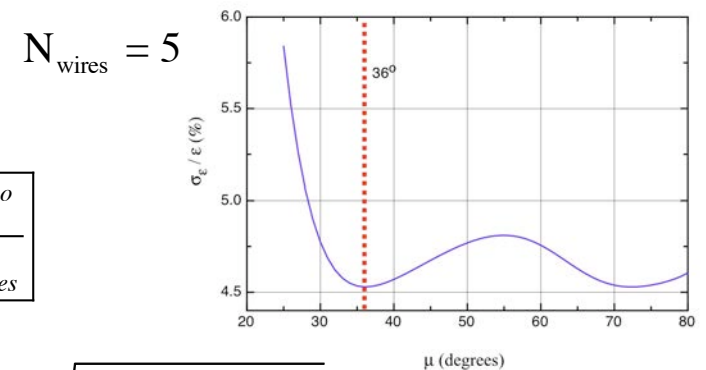
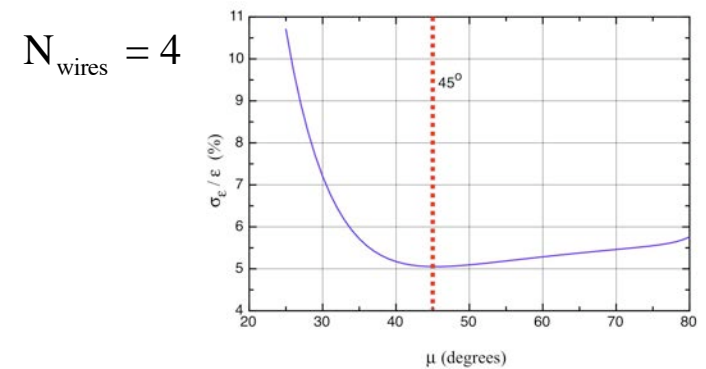
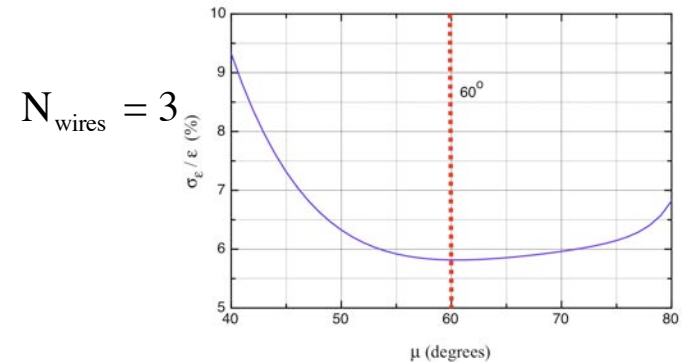
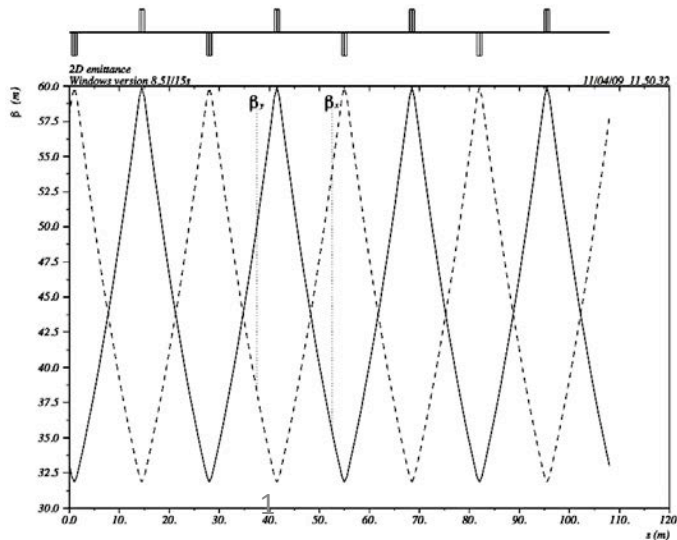
Emittance: $\epsilon = \sqrt{(\beta_o \epsilon)(\gamma_o \epsilon) - (\alpha_o \epsilon)^2}$

$$\alpha_o \epsilon = [C_3^2(R_2^2 S_1^2 - R_1^2 S_2^2) + C_1^2(R_3^2 S_2^2 - R_2^2 S_3^2) + C_2^2(R_1^2 S_3^2 - R_3^2 S_1^2)] / 2d,$$

$$\beta_o \epsilon = [-R_3^2 S_1 S_2 (C_2 S_1 - C_1 S_2) + C_3 S_3 (R_2^2 S_1^2 - R_1^2 S_2^2) - C_3^2 (C_1 S_1 R_2^2 - C_2 S_2 R_1^2)] / d,$$

$$\gamma_o \epsilon = [R_1^2 C_2 S_3 (C_2 S_3 - C_3 S_2) + C_1 S_1 (R_2^2 C_3^2 - R_3^2 C_2^2) + C_1^2 (C_2 S_2 R_3^2 - C_3 S_3 R_2^2)] / d,$$

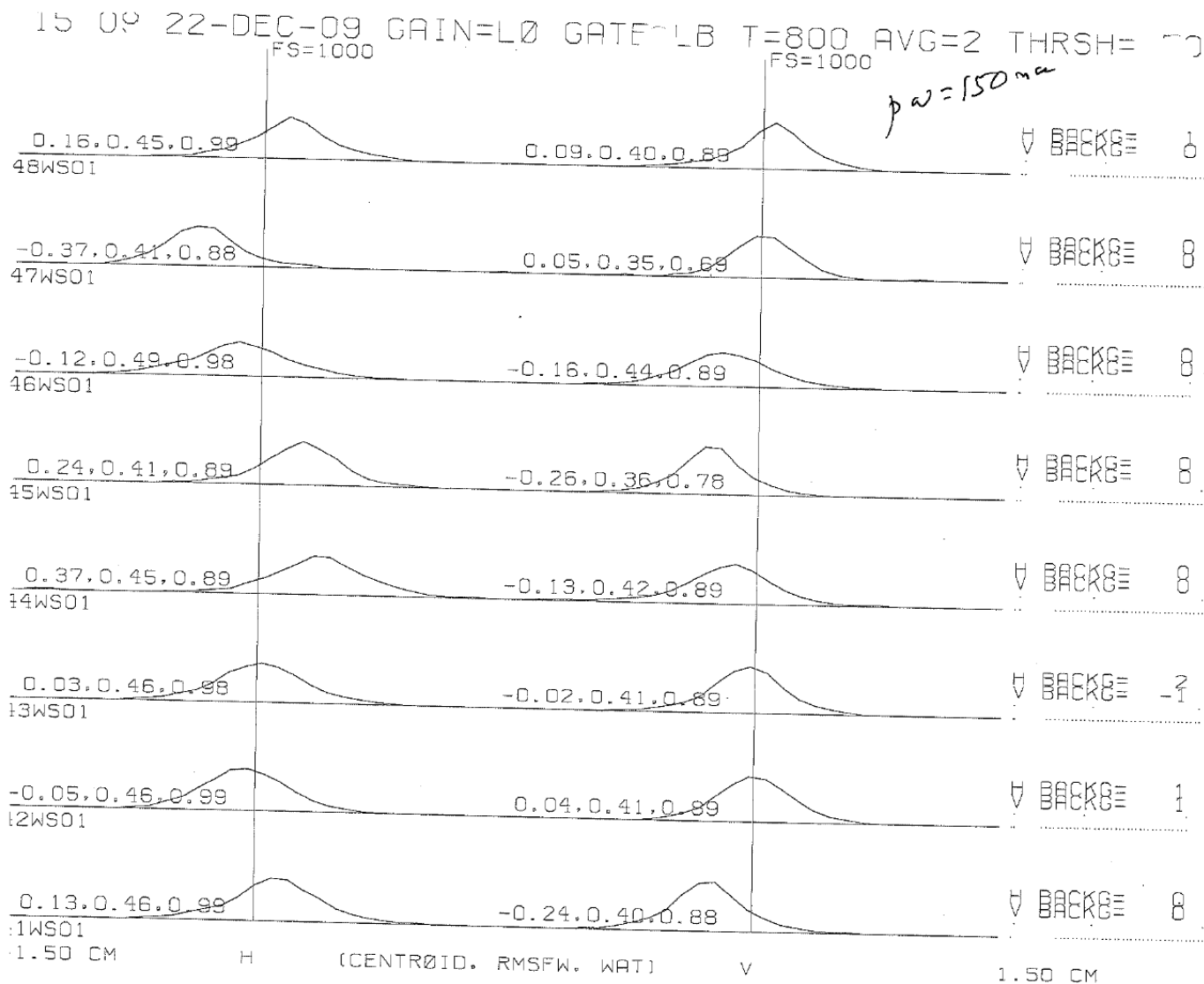
$$d = (C_2 S_1 - C_1 S_2)(C_3 S_1 - C_1 S_3)(C_2 S_3 - C_3 S_2)$$



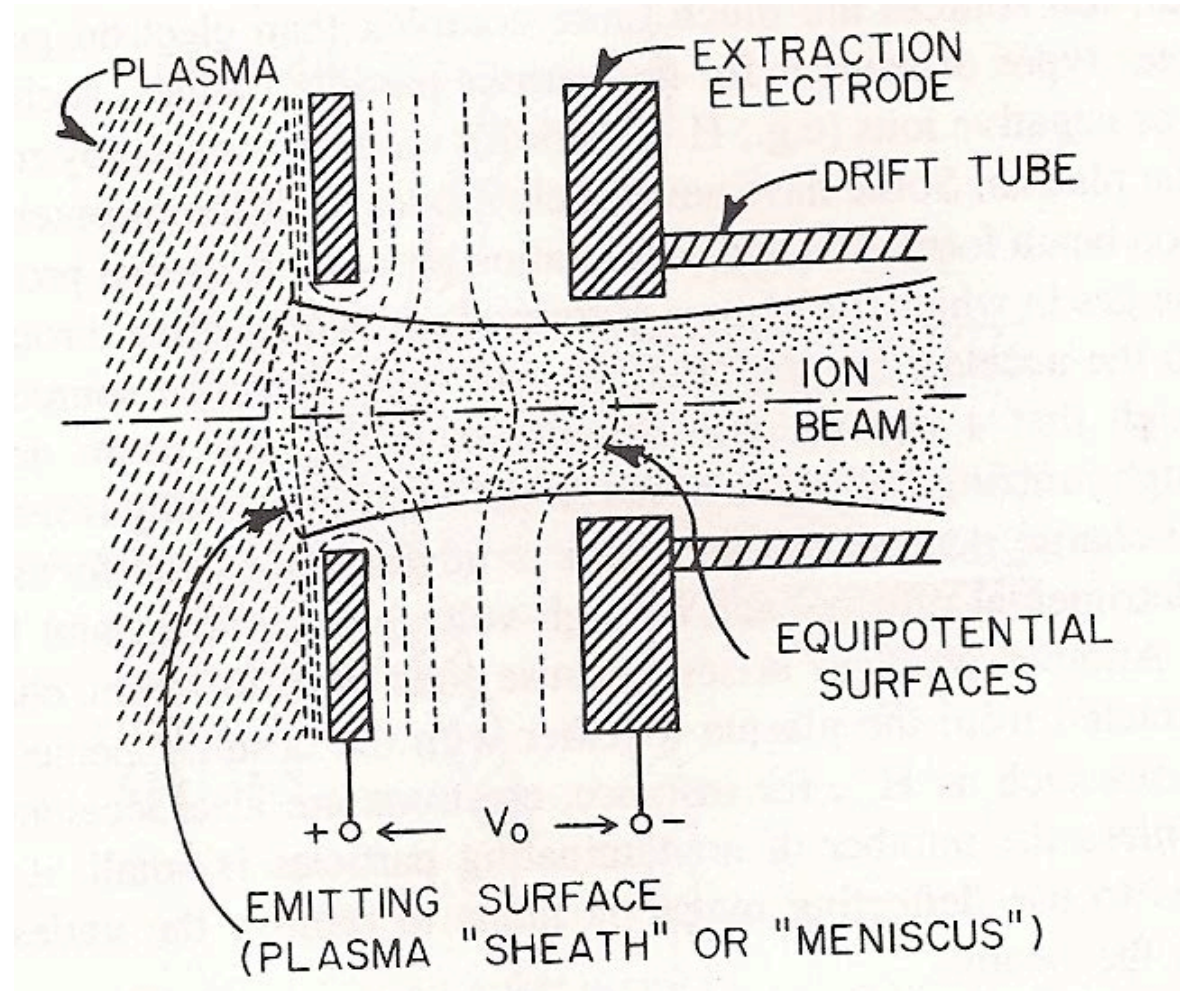
$$\mu_{\text{opt}} = \frac{180^\circ}{N_{\text{wires}}}$$

Error $\frac{\sigma_\epsilon}{\epsilon} = \frac{1}{\epsilon} \sqrt{\frac{1}{(N-1)} \sum_{i=1}^N (\epsilon_i - \bar{\epsilon})^2}$ in beam emittance determination as a function of phase advance for different numbers of wire scanners

Wire Scans of LANL Linac Modules 41 - 48



Emittance of the Beam Extracted from Ion Sources



Schematics of a plasma ion source (from M.Reiser, 1994).

Thermal Beam Emittance in Particles Sources

The ultimate goal of accelerator designers is to minimize emittance. An intrinsic limitation of beam emittance in particle sources comes from the finite value of plasma temperature in an ion source, or the finite value of cathode temperature in an electron source. Equilibrium thermal particle momentum distribution in these sources is in fact, close to the Maxwell distribution:

$$f(p) = n \left(\frac{m}{2\pi k_B T} \right)^{3/2} \exp\left(-\frac{p^2}{2mk_B T}\right)$$

Rms value of mechanical momentum is

$$\langle p_x^2 \rangle = mk_B T$$

Beam radius is usually adopted to be double the root-mean-square beam size, $R = 2 \sqrt{\langle x^2 \rangle}$. Fortunately, for particle sources, one can assume that $\langle x P_x \rangle = 0$ because there is no correlation between particle position and particle momentum. Therefore, the normalized emittance of a beam, extracted from a particle source, is

$$\varepsilon = 2R \sqrt{\frac{k_B T}{mc^2}}$$

Thermal Beam Emittance in Particles Sources (cont.)

Some sources can be operated only in presence of a longitudinal magnetic field, which produces an additional limitation on the value of the beam emittance. For instance, in an electron-cyclotron-resonance (ECR) ion source, charged particles are born in a longitudinal magnetic field B_z , fulfilling the ECR resonance condition $2\omega_L = \omega_{RF}$, where ω_L is the Larmor frequency of electrons and ω_{RF} is the microwave frequency. Canonical momentum of an ion, $P_x = p_x - qA_x$, in a longitudinal magnetic field B_z is:

$$P_x = p_x - q \frac{B_z y}{2}$$

The rms value of canonical momentum is given by:

$$\langle P_x^2 \rangle = \langle p_x^2 \rangle - q B_z \langle p_x y \rangle + \frac{q^2 B_z^2}{4} \langle y^2 \rangle$$

The first term describes the thermal spread of mechanical momentum of ions in plasma, and is given by $\langle p_x^2 \rangle = mkT$. The middle term equals zero because there is no correlation between p_x and y inside the source. The last term is proportional to the rms value of the transverse coordinate $\langle y^2 \rangle = R^2/4$. As a result, we can rewrite $\langle P_x^2 \rangle$ as follows:

$$\langle P_x^2 \rangle = \langle p_x^2 \rangle + \left(\frac{q B_z R}{2} \right)^2$$

Thermal Beam Emittance in Particles Sources (cont.)

The normalized beam emittance ε , extracted from the source is

$$\varepsilon = 2R \sqrt{\frac{k_B T}{mc^2} + \left(\frac{qB_z R}{4mc}\right)^2}$$

Therefore, the presence of a longitudinal magnetic field at the source acts to increase the value of the beam emittance.

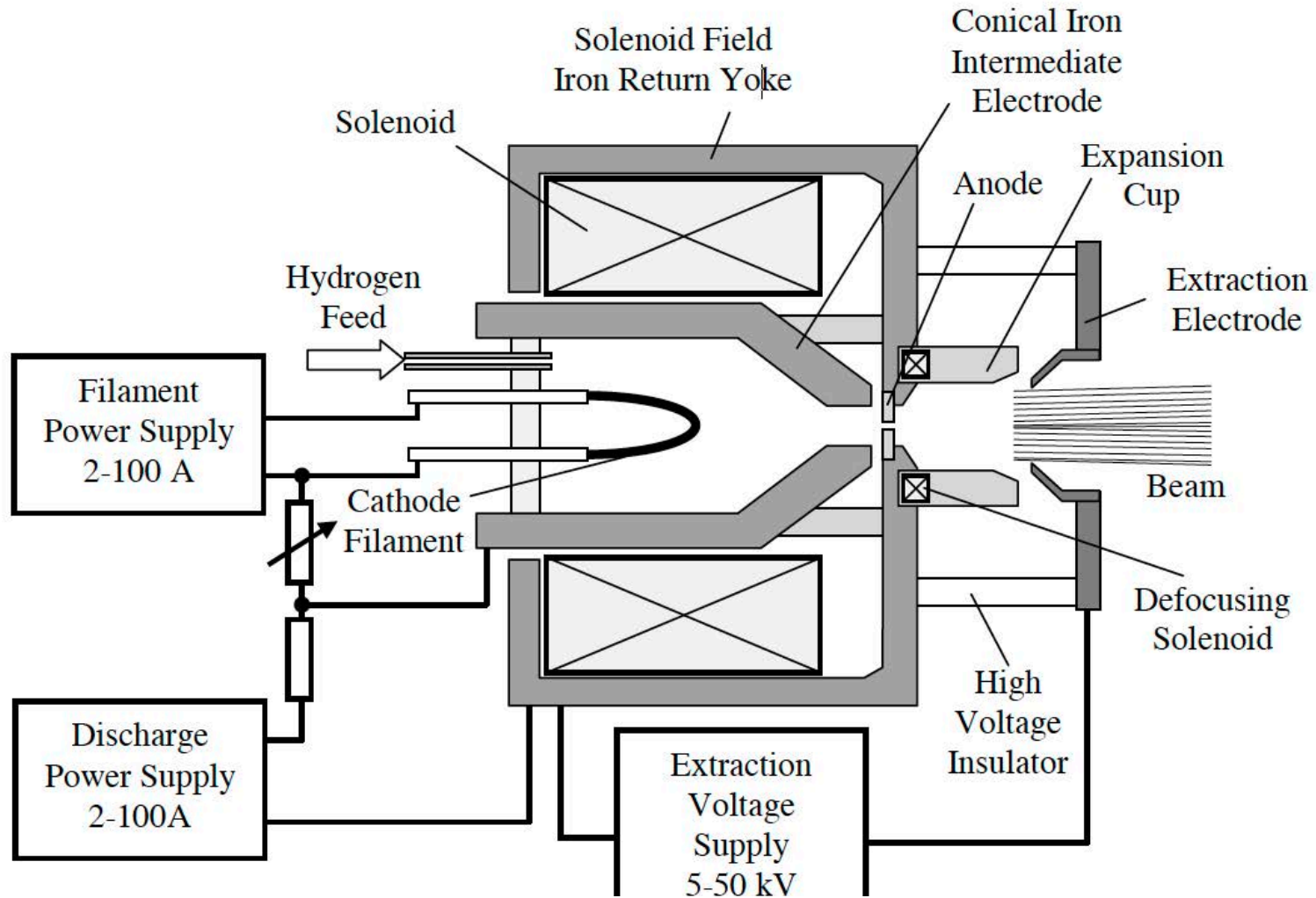
Example: Normalized beam emittance due to thermal spread of particles in plasma ($kT = 0.1$ eV, $R = 3$ mm, $mc^2 = 938$ MeV):

$$\varepsilon_{rms} = \frac{R}{2} \sqrt{\frac{kT}{mc^2}} = 1.5 \cdot 10^{-3} \pi \text{ cm mrad}$$

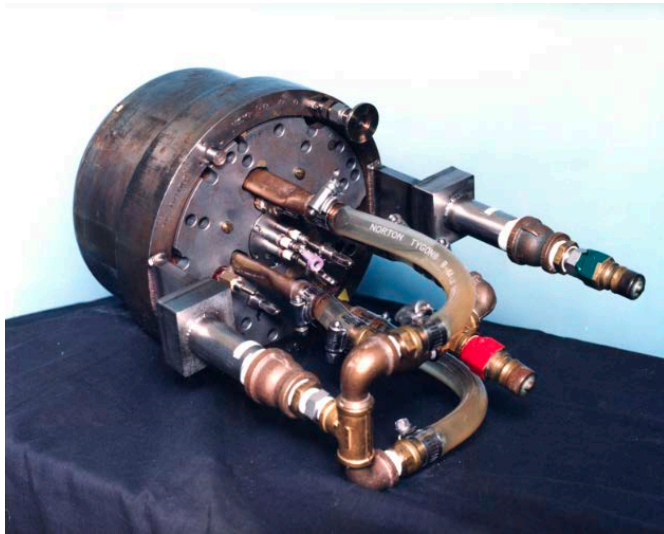
Additional sources contributing to beam emittance :

- irregularities in the plasma meniscus extraction surface
- aberrations due to ion-source extraction optics
- optical aberrations of the focusing elements of the LEBT
- non-linearity of the electric field created by the beam space charge
- beam fluctuations due to ion-source instability or power regulation

Duoplasmatron



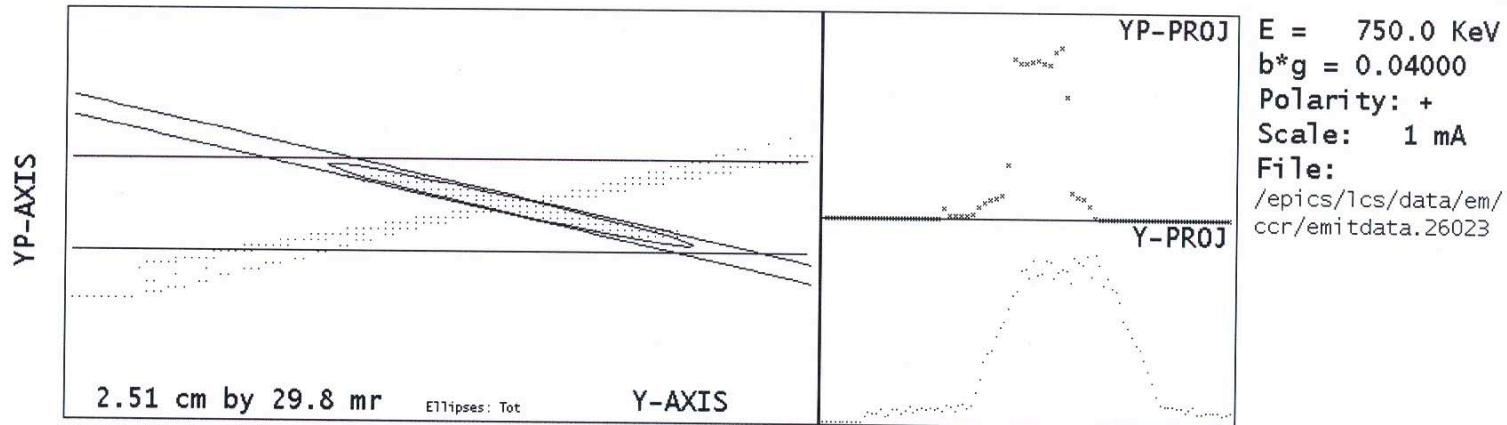
LANSCCE Duoplasmatron



Side view of assembled LANSCE duoplasmatron ion source with Pierce electrode.

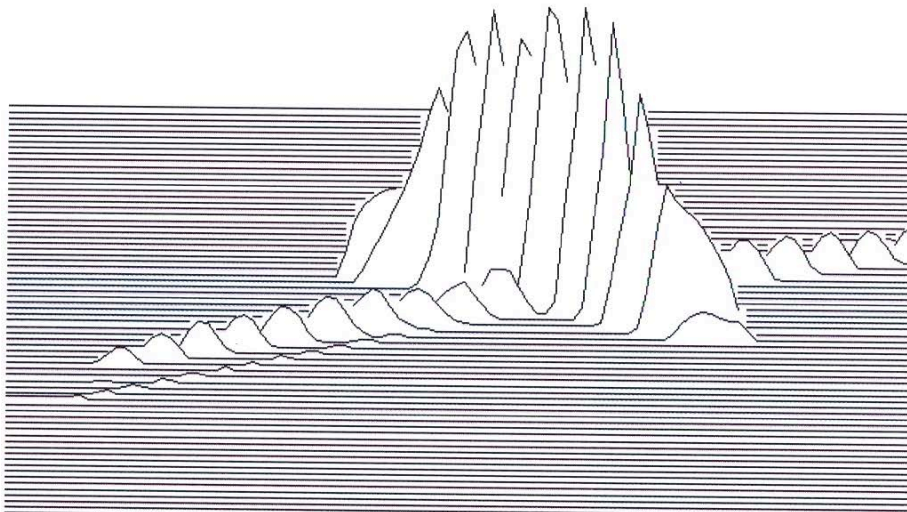
Pulse Rate (Hz)	Pulse Length (μs)	Beam Current (mA)	Normalized rms emittance (π cm mrad)
40	830	14	0.003

Emittance of LANSCE Proton Beam



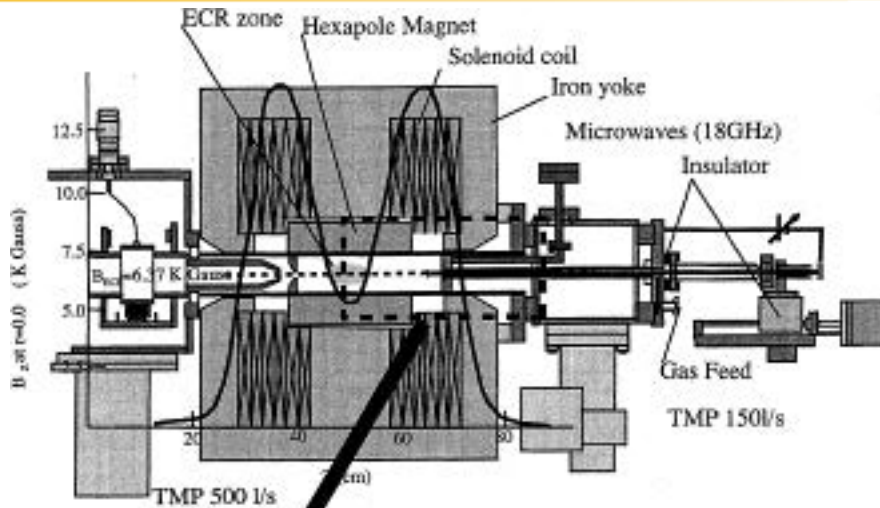
```

Run:26023    Stn: TAEM01-V
21:27:38    18-Jul-2015
Beam: H+    Meas, Norm
E(total)= 0.370, 0.015 pi
E(edge) = 0.282 pi
E(rms) = 0.063, 0.003 pi
Etot/rms= 5.90
Alpha = 4.882
Beta = 1.040
4*E(rms) = 0.251 pi
Cent = 0.232 cm
CentP = 0.786 mr
X Sigma = 0.2555 cm
XP Sigma= 1.2244 mr
Thold = 2.0 %, 24 cnts
Maximum Counts = 1214
Beam thru thresh= 44049
Total Beam = 44177
Slit Pos = 1294 1851
Clctr Pos= 1370 1911
Slit Rate = 237, Nom.= 225
Clctr Rate= 229, Nom.= 219
E(ea) = 0.651, 0.026 pi
E(ea)/E(rms) = 10.367
    
```

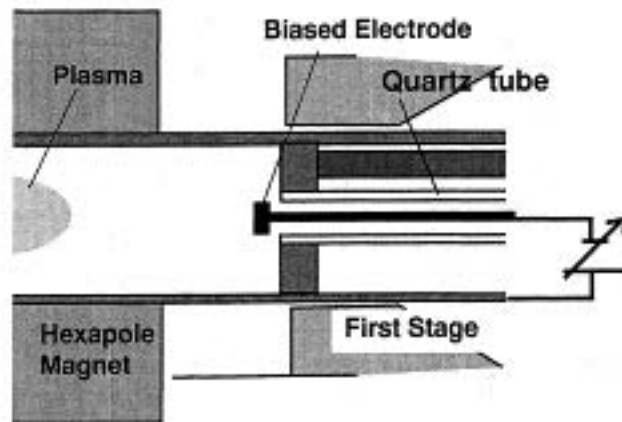
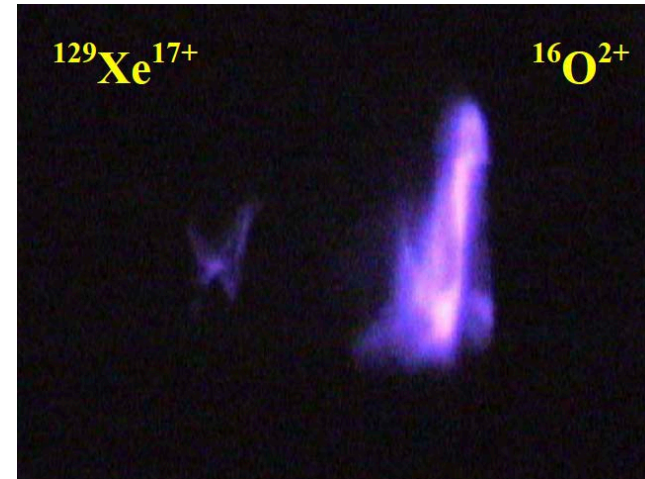


Emittance of proton beam extracted from LANSCE proton ion source. Additional component contains H_2^+/H_3^+ particles.

Electron-Cyclotron Resonance (ECR) Ion Source



ECR resonance condition: $\omega_c = \omega_{RF}$



2D image of the $^{129}\text{Xe}^{17+}$ ion beam of the energy of 255 keV and current of 12 μA extracted from the mVINIS Ion Source, together with the image of the $^{16}\text{O}^{2+}$ beam.

Cross sectional view of RIKEN 18 GHz ECRIS
(T.Nakagawa et al, NIM-A 396, p.9 (1997))

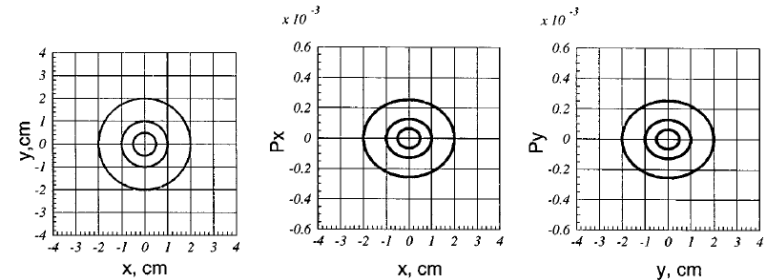
Electron-Cyclotron Resonance (ECR) Ion Source Beam Profile

In the electron cyclotron resonance ion source (ECRIS) plasma is confined in a minimum B magnetic mirror configuration created by solenoid coils and multipole lens. In many sources a sextupole lens is used to confine particles in a radial direction, while longitudinal confinement is provided by the solenoid field. The ECR surface, where electrons are heated, is defined by $2\omega_L = \omega_{RF}$, where ω_L is the electron Larmor's frequency and ω_{RF} is a frequency of microwave power. At this surface the absolute value of the vector of the magnetic field is equal to the resonance value B_{res} , which defines the ECR condition:

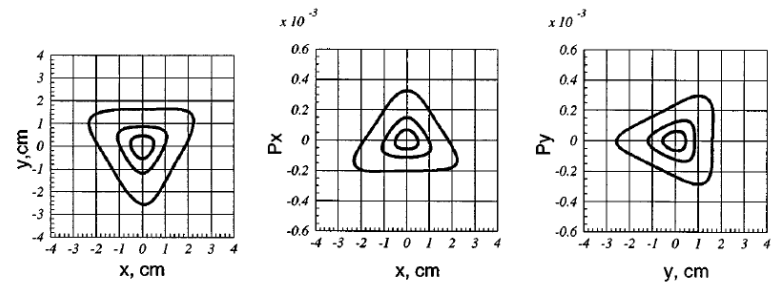
$$B_{res} = \sqrt{B_z^2 + B_r^2 + \frac{B_0^2}{R_0^4} r^4} = \frac{m_e}{e} \omega_{rf}$$

The extracted beam can have an axial-nonuniform shape due to the topology of the magnetic mirror field.

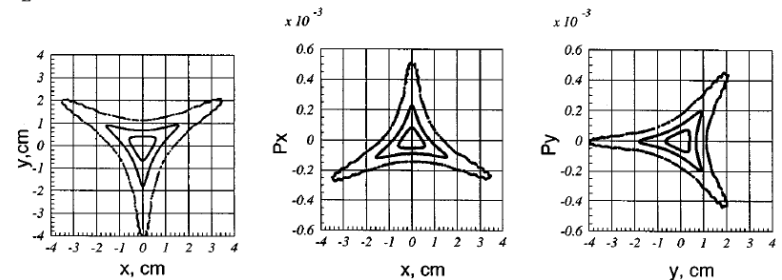
$\omega_L t = 0$



$\omega_L t = 8.96$



$\omega_L t = 26.88$



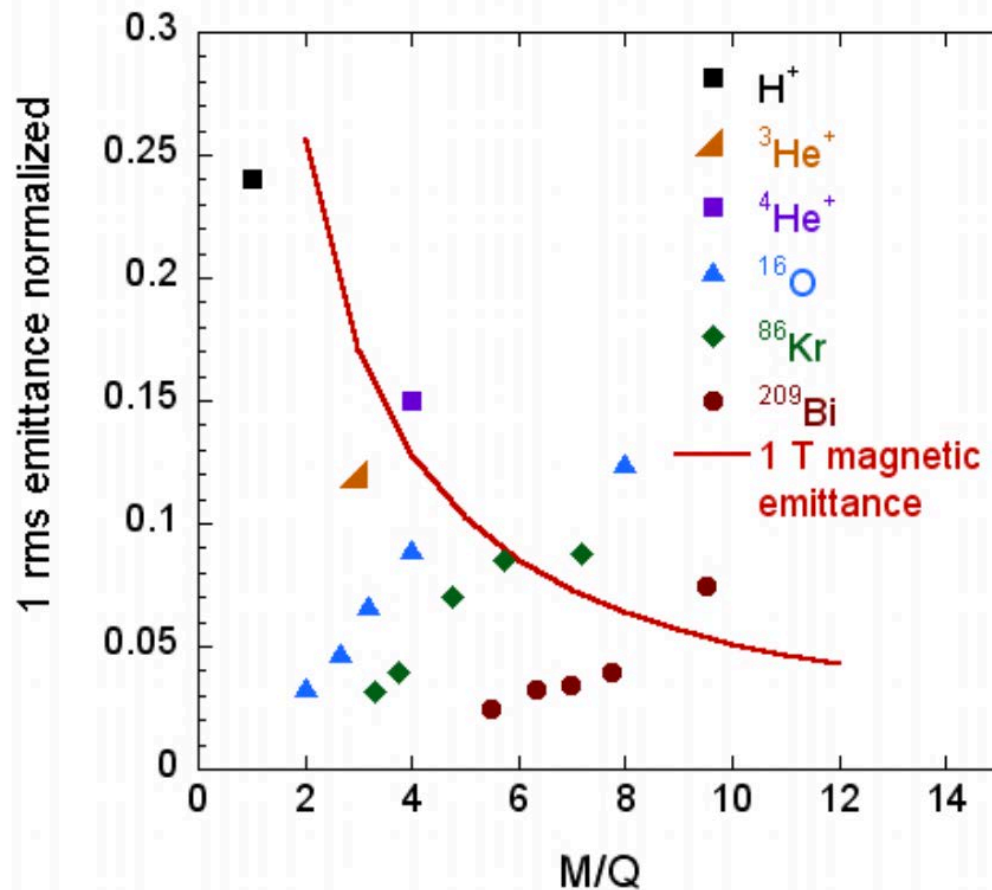
Ar+5 particle trajectories in combination with the solenoid field and the sextupole field (Y.B., Journal Appl. Phys., Vol. 83, No. 2, 1998).

Electron-Cyclotron Resonance (ECR) Ion Source Beam Profile



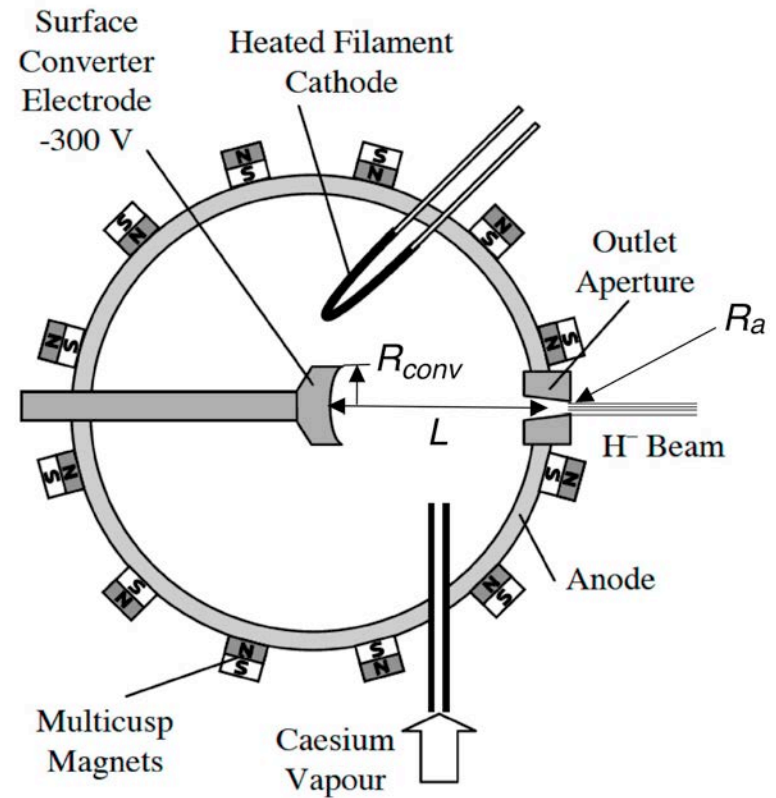
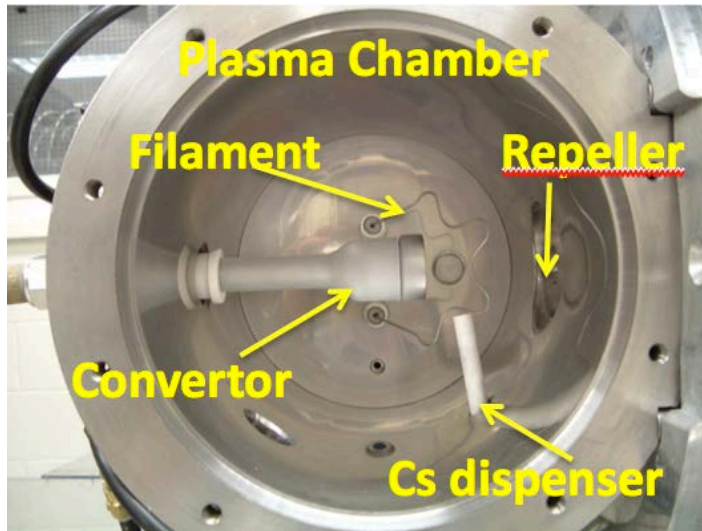
Image of a triangular He⁺ beam 80 cm after extraction.
(D.Winklehner et al, 2010 JINST 5, P1 2001)

Electron-Cyclotron Resonance (ECR) Ion Source

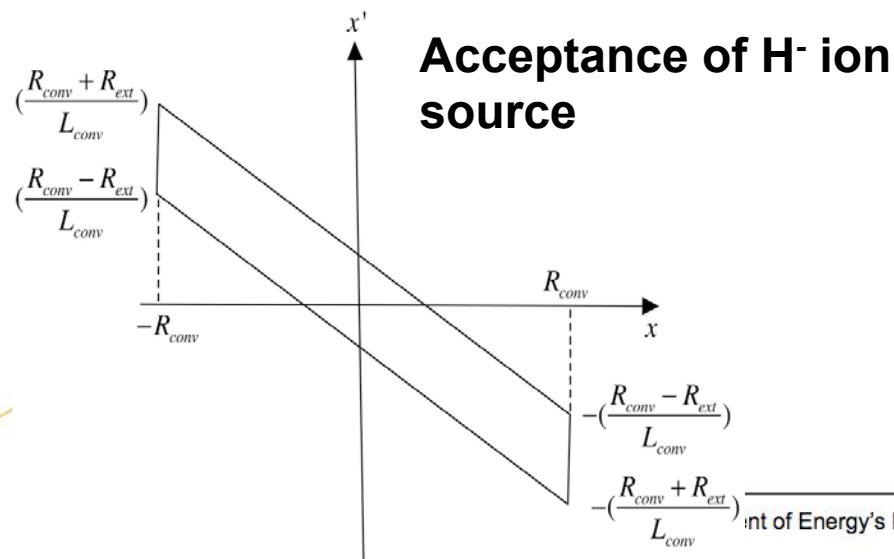


Emittance measurements on the AECR-U for various masses in comparison with predicted emittances for an extraction magnetic field of 1 T (D. Leitner et al, 2011 JINST 6 P07010)

H⁻ Ion Source

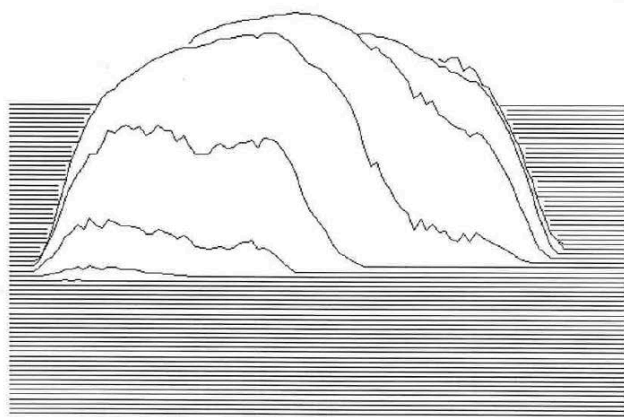
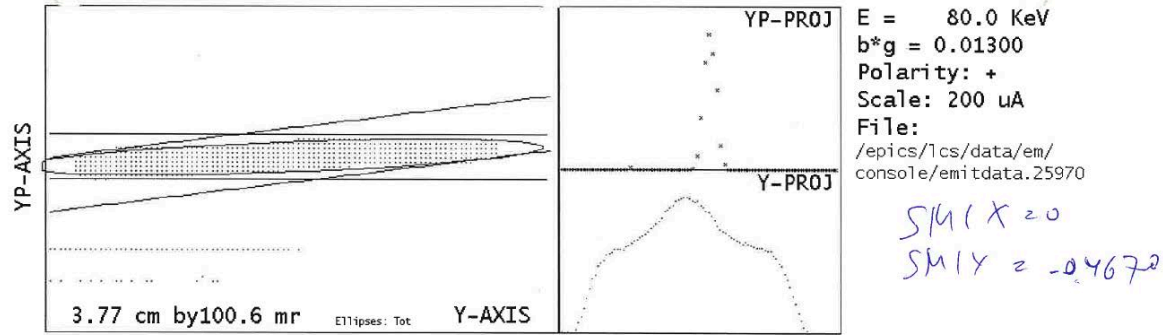


Sectional schematic of a multicusp surface converter ion source.



$$A = \frac{4}{\pi} \frac{R_{conv} R_a}{L}$$

LANSCCE H- Beam Emittance



```

Run:25970 Stn: IBEM01-V
12:26:47 10-Feb-2015
Beam: H- Meas Norm
Emittance (total)= 9.283, 0.121 pi
Emittance (edge) = 8.440 pi
Emittance (rms) = 1.348, 0.018 pi
Emittance tot/rms= 6.89
Alpha = -0.687
Beta = 0.411
4*E(rms)= 5.392 pi
Cent = -0.130 cm
CentP = 3.946 mr
X Sigma = 0.7447 cm
XP Sigma= 2.1964 mr
Thold = 2.0 %, 8 cnts
Maximum Counts = 423
Beam thru thresh= 91723
Total Beam = 92250
Slit Pos = 1167 1724
Cctr Pos= 840 1399
Slit Rate = 148, Nom.= 145
Cctr Rate= 148, Nom.= 146
E(ea)=16.515, 0.215 pi
E(ea)/E(rms)=12.252
    
```

Normalized beam emittance:

$$\epsilon = \frac{4}{\pi} \sqrt{\frac{2qU_{conv}}{mc^2} \frac{R_{conv}R_a}{L}}$$

Analytical beam emittance (π cm mrad)	Experimental $4\epsilon_{rms}$ beam emittance (π cm mrad)
0.076	0.072

H⁻ Ion Source Parameters

TABLE I

LIST OF ACCELERATOR H⁻ ION SOURCES ALONG WITH THE RELEVANT PARAMETER SPACE DISCUSSED WITHIN THIS REVIEW. TYPICAL I_{H^-} CURRENTS ARE GIVEN WITH AN ASSOCIATED EMITTANCE. [13], [14] WERE USED TO FILL IN VALUES NOT PREVIOUSLY CITED. UNDERLINED PARAMETERS ARE FROM [13] AND BRACKETED PARAMETERS ARE FROM [14]

Source Type (drive)	Source Location	I_{H^-} (ma)	Beam df (%)	Rep. Rate (Hz)	ϵ_{rms} x/y (π mm-mrad)	P_d (kW)	e/H ⁻	Life-time (month)
Multicusp Volume, H₂								
RF	DESY (HERA)	40	0.12	8	0.25	~20	26	> 12
LaB ₆ fil.	J-PARC (KEK)	38	0.9	25		35		
Multicusp Volume, Cs+H₂								
RF	SNS	33	6.0	60	0.22/0.18	~40		
W fil.	TRIUMF	20	100	dc	0.022	~5	4-5	~?
W fil.	J-PARC (JAERI)	72	5.0	50	0.13/0.15			
SPS								
Magnetron	BNL	100	0.5	7.5	0.4	~2	0.5	~6
	Fermilab	60	0.1	15	0.2/0.3	~7		~6
	DESY	50	<u>0.05</u>	<u>6</u>	0.46/0.31	{~5}		<u>~9</u>
Penning	ISIS	45	1.0	50	0.6/0.7	<u>4</u>		~2
	INR	50	2.0	100	0.4/0.7 ($\epsilon_{n,F7}$)	{~10}		<u>~0.5</u>
Hollow cath.	BINP	8	100	dc	0.2/0.3	0.4		<u>~0.2</u>
Converter (W fil.)	LANSCE	17	12.0	120	0.13	~6	2.5	~1
(LaB ₆ fil.)	KEK	20	0.5	20	0.33	~4	4.5	3-4